https://www.sciltp.com/journals/gefr
Online ISSN: 2982-2106
Volume 1, Issue 1

Green Energy and Fuel Research

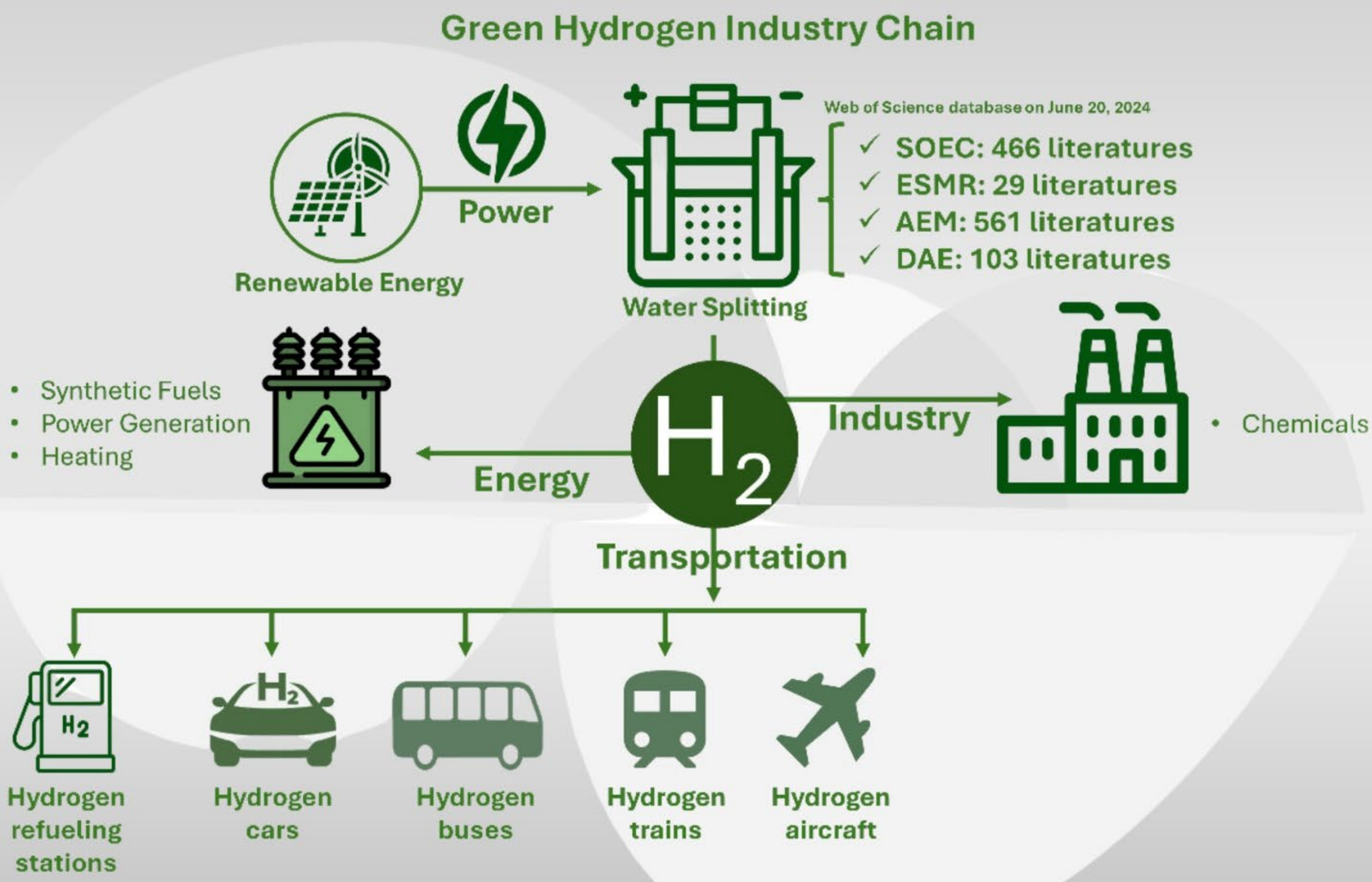

A Brief Overview of Green Hydrogen on Production, Regulations, and Commercialization

Scilight

Editorial Board Members

Aims & Scope

Green Energy and Fuel Research is a new journal with the aim to provide a forum for scientists, engineers, chemists, physicists, policymakers, and other researchers related to the field to exchange new conceptual thinking and scientific findings in green energy and fuel science and engineering. This journal also provides a platform for sharing information on innovation, research, development, and demonstration in green energy conversion, green fuel production, clever energy resource use, and energy process and system analysis and optimization for net zero and sustainability. It is published quarterly online by Scilight Press.

This journal disseminates high-quality papers to showcase novel results and approaches to innovative green energy and fuel research. It emphasizes interdisciplinary and innovative energy and fuel research to address the key issues and challenges in the field of green energy and fuel science. This journal welcomes contributions supporting and advancing the UN's sustainable development goals, particularly SDG 7: Affordable and Clean Energy.

Contact
Add: Level 19, 15 William Street, Melbourne, Victoria 3000, Australia
Web: https://www.sciltp.com/
General Inquiries: info@sciltp.com

Contents

Vol.1 No.1 November 2024

Editorial

Editorial for First Issue of Green Energy and Fuel Research

Wei-Hsin Chen [1,2,3]

1 Department of Aeronautics and Astronautics, National Cheng Kung University, Tainan 701, Taiwan
2 Research Center for Smart Sustainable Circular Economy, Tunghai University, Taichung 407, Taiwan
3 Department of Mechanical Engineering, National Chin-Yi University of Technology, Taichung 411, Taiwan
Correspondence: weihsinchen@gmail.com; chenwh@mail.ncku.edu.tw
Received: 29 April 2024; Revised: 18 May 2024; Accepted: 22 May 2024; Published: 22 May 2024

On behalf of the editors, I am thrilled to introduce the journal *Green Energy and Fuel Research* (GEFR), addressing the state-of-the-art development and application of green energy and fuel research. Our enthusiasm for this inaugural issue stemmed from today's unprecedented opportunity to develop novel and cutting-edge technology for green energy and fuel due to the remarkable concern and urgent problem for resource and environmental stainability [1]. This publication marks the commencement of a series of direct submissions, establishing GEFR as an exceptional platform for disseminating high-quality research contributions from scientists worldwide. GEFR, as a gold open-access journal, is dedicated to advancing knowledge in the domains of green energy and fuel research, with a shared emphasis on green energy systems, green energy materials, green fuel production, catalyst preparation, system process optimization, etc., which underpin the fundamental understanding and sustainable development in the fields of green energy and fuel science, technology, and engineering [2–5].

The *Global Energy and Fuel Reports* (GEFR) has an intentionally broad scope, aiming to embrace original and pioneering fundamental research. We acknowledge the complex challenges of green energy and fuel production, conversion, storage, life cycle assessment, and environmental impact. Therefore, any submitted work should directly relate to the dynamic interplay between green energy and fuel and be of significant interest to our diverse readership. Our scope encompasses a wide range of research, from groundbreaking discoveries to interdisciplinary studies, spanning mechanical, chemical, physical, and environmental science and engineering disciplines.

GEFR publishes articles that focus on, but are not limited to, the following areas:

Renewable energy (bioenergy, solar energy, wind energy, marine energy, hydropower, geothermal energy, etc.

- Hydrogen energy
- Biofuel
- Carbon capture and utilization
- Circular economy of green energy and fuel
- Materials for energy and fuel
- Catalysis for energy and fuel
- Energy saving
- Energy storage
- Energy and fuel for sustainability

In March 2024, I extended invitations to outstanding scientists to join our editorial board, and I am profoundly grateful for their enthusiastic support in embarking on this meaningful and demanding endeavor. While we anticipate the growth of our editorial board to meet emerging challenges, it is my privilege to introduce our current partners: JS Chang, Tunghai University, Taiwan; LW Jin, Xi'an Jiaotong University, China; YK Park, University of Seoul, Republic of Korea; YS Shen, University of New South Wales, Australia; KS Khoo, Yuan Ze University, Taiwan; KT Lee, Tunghai University, Taiwan; SL Lin, National Cheng Kung University, Taiwan; TB Nguyen, National Kaohsiung University of Science and Technology, Taiwan; AK Sharma, University of Petroleum & Energy Studies, India; HC Ong, Sunway University, Malaysia; A Pétrissans, Université de Lorraine, France; A Saravanakumar, SRM Institute of Science and Technology, India; KQ Tran, Norwegian University of Science and Technology, Norway; CY Zhang, Northeast Agricultural University, China; RL Quirino, Georgia Southern University, USA; YK Chih, National University of Tainan, Taiwan; YP Wang, Xi'an Jiaotong University, Xi'an, China.

In conclusion, I am confident that our authors, editorial board members, reviewers, the Scilight Press team, and our young editorial board members worldwide will position *Green Energy and Fuel Research* (GEFR) at the forefront of scientific research.

Funding: This research received no external funding

Institutional Review Board Statement: Not applicable.

Informed Consent Statement: Not applicable.

Data Availability Statement: Not applicable.

Conflicts of Interest: The authors declare no conflict of interest.

Reference

1. van Soest, H.L.; den Elzen, M.G.; van Vuuren, D.P. Net-zero emission targets for major emitting countries consistent with the Paris Agreement. *Nature Commun.* **2021**, *12*, 2140
2. Pourasl, H.H.; Barenji, R.V.; Khojastehnezhad, V.M. Solar energy status in the world: A comprehensive review. *Energy Rep.* **2023**, *10*, 3474–393
3. Chen, W.-H.; Lin, B.-J.; Lin, Y.-Y.; et al. Progress in biomass torrefaction: Principles, applications and challenges. *Prog. Energy Combust. Sci.* **2021**, *82*, 100887.
4. Lund, J.W.; Toth, A.N. Direct utilization of geothermal energy 2020 worldwide review. *Geothermics* **2021**, *90*, 101915
5. Bhuiyan, M.A.; Hu, P.; Khare, V.; et al. Economic feasibility of marine renewable energy. *Front. Mar. Sci.* **2022**, *9*, 988513
6. Ubando, A.T.; Felix, C.B.; Chen, W.-H. Biorefineries in circular bioeconomy: A comprehensive review. *Bioresour. Technol.* **2020**, *299*, 122585

Review

A Brief Overview of Green Hydrogen on Production, Regulations, and Commercialization

Kuan-Ting Lee *, Yuan-Shao Cai, Qian-Yi Hou, Ting-Jung Hsu, and Wei-Hao Hsu

Department of Chemical and Materials Engineering, Tunghai University, Taichung 407, Taiwan
* Correspondence: s9832806@gmail.com or ktlee@thu.edu.tw

Received: 1 July 2024; Revised: 19 July 2024; Accepted: 22 July 2024; Published: 15 August 2024

Abstract: With the deadline for meeting the net-zero emissions target by 2050 fast approaching, developing low-carbon energy sources has become a priority for governments worldwide. Green hydrogen is considered a promising low-carbon energy in response to the urgent need for net-zero energy. In this minor review, we have provided an overview of the progress made in the commercialization of green hydrogen, focusing on aspects such as manufacturing, regulations, and patent analysis for achieving environmental sustainability and net-zero emissions. In addition, the developemental progress achieved in green hydrogen by various countries such as Europe, United States, Japan, and South Korea is also highlighted, emphasizing their determination and commitment to exploit and incorporate hydrogen energy industry into existing energy policy. Key challenges identified include the difficulty of ensuring a stable supply source, optimizing transportation and storage infrastructure, and reducing energy consumption costs. The international regulations and patents related to green hydrogen are also discussed. This review provides insights into the current state of green hydrogen industries of various countries as we aim to achieve net zero emmissions and improve sustainability.

Keywords: green hydrogen; hydrogen energy; net zero; commercialization; regulations; environmental sustainability

1. Green Hydrogen Production

According to EN ISO 14067, green hydrogen is defined as hydrogen produced through green power, while green power is produced from the electrolysis of water using renewable energy power. The mature renewable energy infrastructure is crucial for developing the green hydrogen industry [1]. According to the data from the International Energy Agency, over 90% of the global hydrogen supply came from grey hydrogen in 2020, while the supply of green hydrogen accounted for less than 10% of the total [2]. The lack of stable green electricity is one of the main reasons for this issue. Currently, green hydrogen production can be categorized into four types, namely Solid Oxide Electrolyser Cells (SOEC), Electrified Steam Methane Reforming (ESMR), Anion Exchange Membranes (AEMs), and Direct Air Electrolysis (DAE) [1]. Among these, SOEC exhibits the highest hydrogen production efficiency, approximately 90% [1]. In 2024, three internationally renowned companies Topsoe (Denmark), ABB (Switzerland), and Fluor (United States) announced that they would develop SOEC technology jointly. Topsoe is distinguished for its technologies that reduce carbon emissions. ABB is a pioneer in the facilities of electrification and automation. Fluor is a frontrunner in engineering, procurement, and construction services. Topsoe is building its first SOEC factory in Herning, Denmark, which is expected to start operating by 2025 [3]. A search conducted on the database of Web of Science on 26 June 2024, identified 466 literatures related to SOEC and hydrogen production, 29 literatures related to ESMR, 561 literatures related to AEMs, and 103 literatures related to DAE. These indirectly indicate that the production technology of green hydrogen is still in the germination stage. Figure 1 shows the distribution map of green hydrogen literature using VOSviewer.

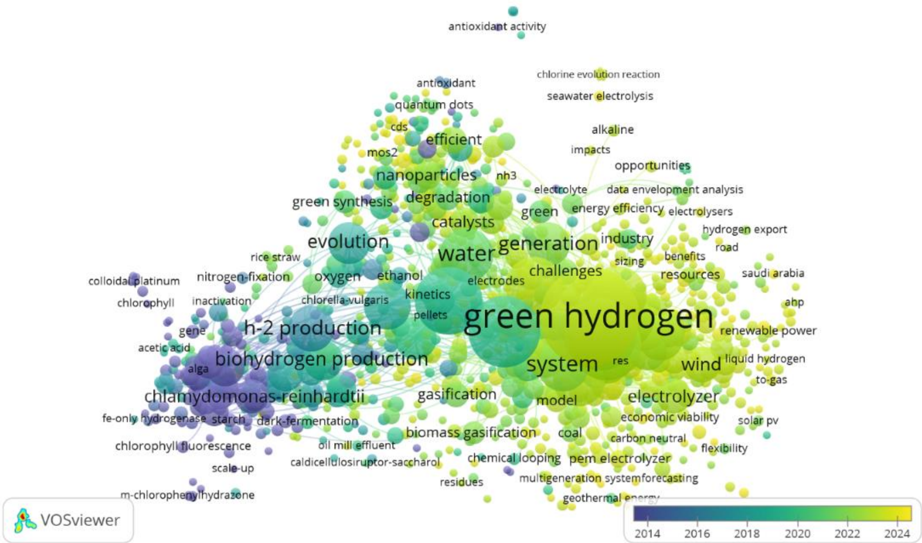

Figure 1. Distribution map of green hydrogen literature.

By examining the evolution of the global hydrogen energy industry chain, we identify three mainstream fields of energy, industry, and transportation as the current application fields of hydrogen energy [4]. The transportation field includes hydrogen refueling stations, hydrogen-powered cars, hydrogen buses, hydrogen trains, hydrogen aircraft, and others [5–9]. Synthetic fuel, power generation, and heating are the three applications of hydrogen in the energy field. While in the industrial field, hydrogen can be applied to industrial raw materials, ammonia production, refining, etc. [10]. Figure 2 shows the applications of green hydrogen in Power-to-X (PtX) mode. PtX is currently the primary model that is adopted by countries worldwide for the diversified application of hydrogen energy [11,12]. This model uses power generated from renewable energy to electrolyze water into hydrogen and oxygen. The produced green hydrogen is then stored or further utilized as a crucial resource in gaseous energy [13], hydrogen fuel cell vehicles [14], and the industry of using hydrogen to produce ammonia [15,16]. This PtX mode approach reflects the global trend towards the sustainable use of hydrogen energy. Under the PtX model framework, the Australian government has actively promoted projects such as Power to Gas, Power to Mobility, and Power to Ammonia in recent years. In 2021, the Danish Energy Agency projected the potential of the global PtX hydrogen market by 2035. They proposed that green hydrogen production is a mainstream potential market worth approximately 141.1 billion euros [17].

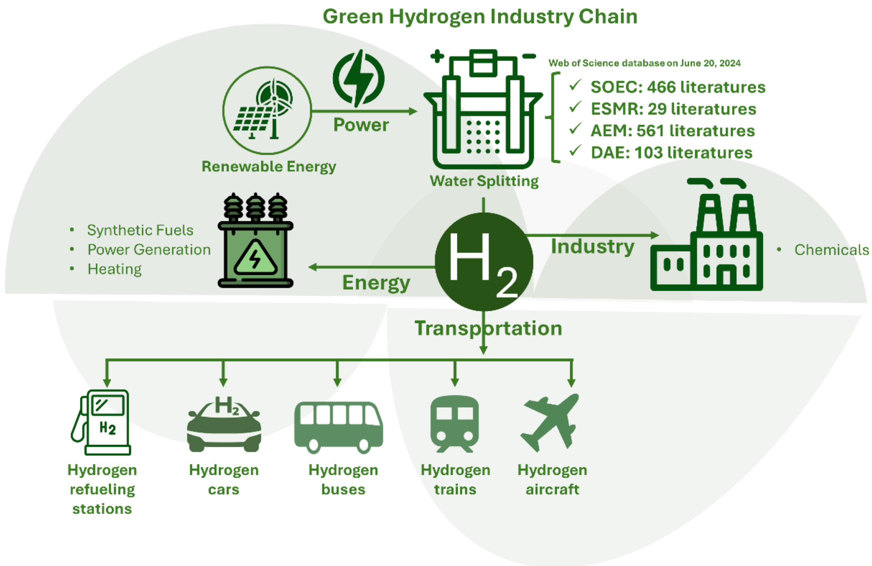

Figure 2. Applications of green hydrogen in PtX mode.

2. Regulations

Hydrogen is a colorless, odorless, non-toxic flammable gas [18]. Hydrogen comprises two hydrogen atoms, with a density of about 0.09 kg·m^{-3} under standard conditions (0 °C and 1 atm) [19]. Since its density is lower than air, which is 1.225 kg·m^{-3} [20], hydrogen disperses more readily than air. When using hydrogen, special attention should be paid to the possibility that combustion reactions can easily occur when the concentration of hydrogen in the air falls within the range of 4% to 75% [21]. Furthermore, hydrogen has an autoignition temperature of 576 °C in air [22]. These observations highlight the importance of safety in manufacturing, transportation, storage, supply, and end-use, with the aim of preventing potential fire or explosion.

Before investing in and developing the hydrogen energy industry, governments and enterprises worldwide consider risk assessment and safety levels as primary evaluation items. One crucial consideration is the selection of appropriate container materials to prevent hydrogen leakage caused by hydrogen embrittlement, thereby triggering potential safety hazards. In the past, many explosion accidents caused by hydrogen leaks have occurred. For example, in May 2019, a venture firm located in Gangwon Technopark, South Korea, experienced a hydrogen tank explosion, resulting in two fatalities and six injuries. The explosive force was potent enough to damage buildings located 100 m away from the site. The hydrogen in the tank was produced by water splitting. The primary cause of the explosion was the inadvertent infiltration of oxygen into the hydrogen storage tank. Typically, the storage tank for hydrogen, made of steel, had a capacity of 400 L and operated at a pressure of 1 MPa [23,24]. In June 2019, a hydrogen tank truck explosion occurred in Santa Clara, United States. The hydrogen tank truck was owned by Air Products and Chemicals, Inc. The explosion primarily resulted from a leak during the refueling of a hydrogen tank truck at a gas station. A subsequent fire was induced by this explosion. Fortunately, no casualties were reported. Following the occurrence of the event, to prevent the Butterfly Effect, firefighters conducted air sampling and thermal imaging to ensure the concentration of hydrogen in the air is outside the range of 4~75%. [25,26]. In the same month, a hydrogen equipment manufacturer in Norway encountered a hydrogen leakage issue at the Kjorbo hydrogen refueling station. This is caused by incorrect assembly of the plug in the hydrogen tank. Although the incident did not result in any disasters, the company was still fined $2.96 million by the local government. The above incidents have highlighted the importance of risk consideration and safety assessment in the hydrogen energy industry chain [27,28].

Figure 3 illustrates 65 international hydrogen energy standards. These standards cover different stages of the hydrogen energy industry chain. The stages include hydrogen manufacturing, quality, transportation, storage, supply, and end-use. These standards provide important guidance for the hydrogen energy industry chain. Among these standards, approximately 7% pertain to hydrogen manufacturing, including the currently relatively mature technologies, water splitting for hydrogen production, natural gas reforming for hydrogen production, and methane pyrolysis for hydrogen production. Purification is a crucial step in determining the quality of hydrogen, and the regulations listed include pressure swing adsorption systems, hydrogen composition, and analysis methods. Storage is a key factor that determines the developmental speed of hydrogen energy industry chain. The listed regulations are designed to prevent a decrease in the hydrogen storage capacity of vessels, which can occur due to hydrogen embrittlement. Finally, most regulations on hydrogen energy applications emphasize its use in power generation and transportation.

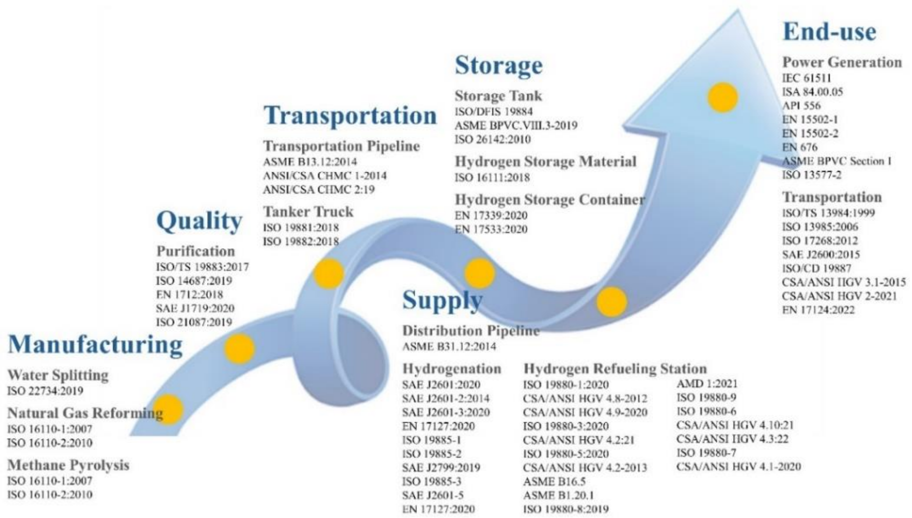

Figure 3. Hydrogen energy standards.

According to the Innography database, there is a total of 148,364 patents related to green hydrogen worldwide. These patents cover various aspects of green hydrogen technology, reflecting the widespread attention and investment in green hydrogen technology globally, as shown in Figure 4a. Among these patents, utility model patents account for more than 99%, design patents make up less than 0.1%, and even fewer are invention patents. This indicates that the number of utility model patents far exceeds that of other patents. Of all 148,364 patents, 99,266 have expired and approximately 33% are still valid. Figure 4b collects the number of green hydrogen patents over the past 20 years. Notably, the annual growth rate of applied patents has gradually increased since 2020. Before 2020, the annual growth rate of patents is just approximately 10–15%. China holds the most patents worldwide, with approximately 19,000. The United States follows with around 11,000 patents, South Korea with about 4600, Japan with around 4500, and Germany with about 1400. The rest of the countries all have fewer than 1000. This distribution of active patents suggests a concentrated development of green hydrogen technology in specific countries, such as China and the United States. Although China has the largest number of green hydrogen-related patents, most patents do not belong to industry but to universities.

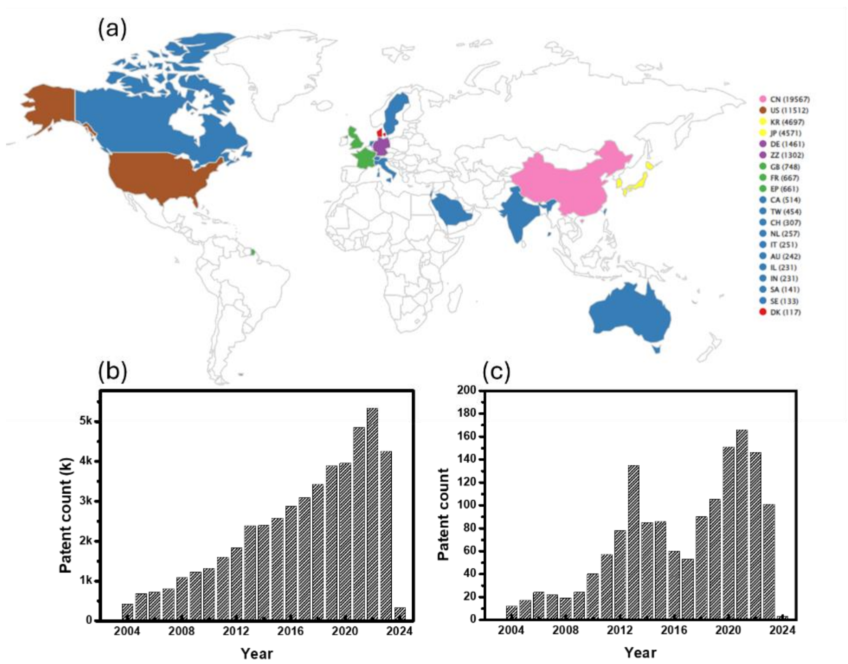

Figure 4. (**a**) Distribution map and the number of green hydrogen patents over the past 20 years (**b**) Global, (**c**) Samsung Electronics Co., Ltd. (Suwon, South Korea).

To understand the correlation between applied patents and industries, further discussion is needed to understand the implications of this distribution for the global green hydrogen industry. Samsung Electronics Co., Ltd. in South Korea currently holds the most patents about green hydrogen globally, with over 1400 patents. Following Samsung, the companies with the most patents are Universal Display Corporation with 855 patents, Sumitomo Chemical Company, Limited with 666 patents, LG Display Co Ltd. with 532 patents, and FUJIFILM Holdings Corp with 509 patents. An analysis of the patent portfolio of Samsung reveals that over 80% of the patent portfolio is related to the field of hydrogen separation membranes. Hydrogen separation membranes can effectively separate hydrogen from other gases during hydrogen production, to ensure the purity of the hydrogen produced, making it suitable for further use or storage. Figure 4c shows the number of patents about green hydrogen on Samsung Electronics Co., Ltd. over the past 20 years.

3. Commercialization

With the rapid development of the global hydrogen energy industry in recent years, hydrogen has become an important energy carrier. It has gradually expanded into many fields such as electric energy and kinetic energy conversion. Green hydrogen costs an estimated US$3.7 to 5.3 per kilogram, while gray hydrogen costs only US $1.6 per kilogram [29]. To accelerate the sustainable development of the hydrogen energy industry, the proportion of green hydrogen supply is expected to increase significantly to 25% in the next ten years [30]. By 2050, it is projected that the proportion of green hydrogen supply will exceed 62% and become the main source of global hydrogen supply [31]. According to the International Energy Agency, global hydrogen demand is expected to surge to 520 million tons by 2070 [32].

Governments worldwide have begun to formulate strategies for the green hydrogen industry and have made related announcements. For instance, the china government has initiated over 100 green hydrogen projects [33]. By 2050, the Canadian government anticipates hydrogen to account for 30% of its total energy use [34]. Australia has set a goal to become one of the top three hydrogen exporters in Asia by 2030 [35]. Japan is projecting an annual green hydrogen production of 3 million tons by 2030 [36]. The United States has set a goal to reach an annual production of 50 million tons by 2050 [37]. By 2030, Germany and the United Kingdom aim to achieve a green hydrogen electrolysis capacity of 10GW. Meanwhile, the European Union has set a target of 40 GW [38,39].

Numerous prominent companies significantly shape the green hydrogen production sector. Key players include Air Products and Chemicals (Allentown, PA, USA), H&R Olwerke Schindler (Hamburg, Germany), Siemens Energy (Taipei, Taiwan), Linde Gas (Munich, Germany), Toshiba Energy Systems & Solutions (Kawasaki-shi, Japan), Nel ASA (Oslo, Norway), Guangdong Nation-Synergy Hydrogen Power Technology (Yunfu, China), and Cummins (Columbus, IN, USA). These companies are making significant strides in advancing green hydrogen technologies and shaping the future of sustainable energy [40].

3.1. Europe

Since 2021, Europe has been the host to over half of the 131 hydrogen projects initiated worldwide, as per the International Hydrogen Energy Committee and McKinsey & Company's (Brussels, Belgium) data [41,42]. These projects cover multiple industrial applications such as hydrogen production, supply, and transportation. Upon commercialization of all hydrogen projects, the International Hydrogen Energy Committee estimates a total investment of 500 billion US dollars in the global hydrogen energy field by 2030, with Europe contributing about 45% of this investment [43].

Figure 5 shows an illustration of European investment in the hydrogen energy industry chain. The Green Energy Initiative agreement, signed by Chile and the Netherlands, paves the way for future exports of green hydrogen from Chile to the Netherlands and the rest of Europe [44]. The UAE, having signed a letter of intent with German and Japanese companies, is planning to set up a green hydrogen production demonstration plant in Masdar [45]. Germany has currently built 105 hydrogenation stations and plans to increase the number annually to reach the goal of 1,000 hydrogenation stations [46,47]. Germany and Saudi Arabia are set to collaborate closely on the production, processing, application, and transportation of green hydrogen. In terms of pipeline hydrogen transmission, the European GET H_2 plan has established a cross-border long-distance pipeline network. This initiative will enable the transportation of green hydrogen through pipelines by refineries, steel mills, and other factories by 2030, resulting in an estimated reduction of around 16 million tons in CO_2 emissions [48]. The UK has been invested 28 million pounds to the HyNet hydrogen energy project in 2020, with the hydrogen production capacity expected to hit 5GW by 2030 [49]. By 2050, hydrogen energy is expected to make up 20% to 35% of the UK's total energy consumption [50]. Italy initiated the SNAMTEC plan in 2019, targeting the deployment of 25,000 fuel cell vehicles by 2025 [51,52]. Concurrently, France has formulated a plan to establish an electrolyzer capacity of 6.5GW by 2030, aiming to produce 700,000 tons of renewable or low-carbon hydrogen and reduce CO_2 emissions by 6 million tons [53,54]. These initiatives reflect the global commitment to sustainable energy and carbon reduction.

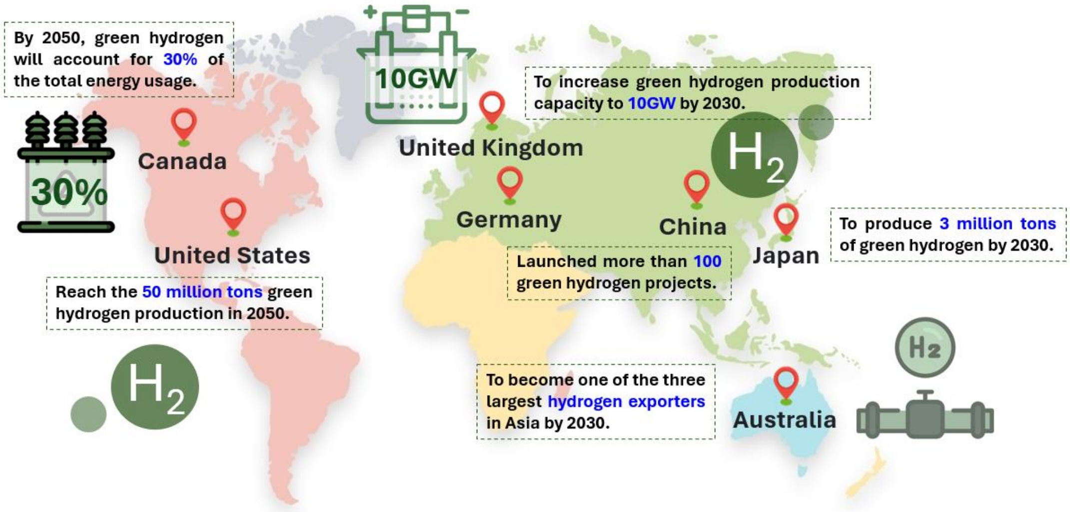

Figure 5. Illustration of European investment in the hydrogen energy industry chain [55–58].

3.2. United States

Since 1990, the U.S. government has formulated a series of policies to promote the development of the hydrogen energy industry [59,60]. In 2002, the U.S. Department of Energy released a document of "National Hydrogen Energy Roadmap" [61]. The main goal of this is to establish a systematic hydrogen energy system, thereby maintaining a leading position in the field of global energy technology in the long term. This reflects the strategic foresight of the U.S. in recognizing the potential of hydrogen energy and its commitment to leading the development of this technology on a global scale. In 2020, the U.S. Department of Energy released a report titled "Hydrogen Strategy - Enabling a Low-Carbon Economy" [62]. The report emphasizes the importance of advancing the technical research and application of integrating hydrogen into the fossil fuel. The report suggests that efforts to support hydrogen energy should be focused on areas such as power generation, transportation, heating, and industrial raw materials [62]. This reflects the strategic direction of the U.S. in promoting the development and application of hydrogen energy in various sectors. According to the "U.S. Hydrogen Energy Economic Roadmap Executive Summary Report" published by the Fuel Cell and Hydrogen Energy Association (FCHEA) [63], the U.S. Department of Energy provided annual funding of approximately 100 million to 280 million U.S. dollars for the field of hydrogen energy and fuel cells from 2010 to 2019. This demonstrates the U.S. government's emphasis on hydrogen energy and fuel cell technology, and its active investment of resources to promote the development of related technologies. By 2030, the US expects total hydrogen demand across various applications to exceed 17 million tons. By 2050, the US expects hydrogen to account for 14% of energy needs. The United States currently operates 17 MW of electrolytic hydrogen production projects and maintains a hydrogen pipeline capacity of 1.4 GW [63].

3.3. Japan

Since 1978, Japan established the Hydrogen Energy Association, which is dedicated to developing hydrogen-related technologies. This demonstrates Japan's long-term commitment in hydrogen technology. In 1981, Japan launched the Moonlight Project to develop fuel cells [64,65]. In 2002, the Japan government cooperated with Toyota and Honda car manufacturers to develop a fuel cell demonstration vehicle [66–69]. This means the beginning of the upcoming application of large-scale fuel cells. In 2013, Japan formally established hydrogen energy development as a national policy and began preliminary work on the construction of hydrogen refueling stations [70]. In 2015, Japan released the Hydrogen Energy White Paper and set hydrogen energy as the third main source of domestic power generation. In 2017, the Japanese Ministry of Transport and the Australian Maritime Safety Authority signed a hydrogen energy transportation safety standards agreement. These policies and agreements demonstrate Japan's proactive attitude and actions in developing hydrogen energy [71,72]. In 2019, the Japan government established the world's largest renewable energy water splitting hydrogen production base in Fukushima Prefecture. This base primarily uses solar panels and electrolyzers to produce hydrogen, which is then used to supply the energy needs of households and fuel cell vehicles [73,74]. Green hydrogen installations in Japan currently cost about 200,000 yen per kilowatt, with projections for a decrease to 50,000 yen per kilowatt by 2030. Concurrently, hydrogen production efficiency from water splitting is set to improve from the present 5 kilowatt-hours per cubic meter to 4.3 kilowatt-hours [75]. By 2030, Japan aims to mix 30% hydrogen into methane gas power plants and achieve an annual supply of hydrogen energy reaching 3 million tons [70,76,77]. By 2050, the annual supply of hydrogen energy is expected to reach 20 million tons [78–80]. The Japanese government is actively advancing hydrogen steelmaking and water-splitting hydrogen production technologies. They are also popularizing mixed hydrogen combustion power generation, all aiming to realize pure hydrogen power generation [75].

3.4. South Korea

Since 2012, the South Korean government has implemented a policy encouraging both public and private power companies to utilize renewable energy [81]. This policy aims to promote energy transition and reduce reliance on traditional fossil fuels. In 2018, the hydrogen economy was listed as one of South Korea's three strategic investment areas. In 2019, the South Korean government unveiled a national hydrogen economy roadmap, with the development of hydrogen-powered vehicles and fuel cells as the primary strategy [82]. In 2020, the South Korean government formulated the "Hydrogen Economy Promotion and Hydrogen Safety Management Act" to promote the hydrogen economy and safety management [83]. In 2021, the South Korean government announced a policy named 'Hydrogen Leading Country Vision', to dominate the global hydrogen energy market by 2030 [84]. South Korean plans to increase its annual production capacity of hydrogen fuel cell passenger cars to 100,000 units in 2025 and produce 6.2 million hydrogen vehicles by 2040 [85,86]. For the hydrogen production part, it is expected to produce 250,000 tons of hydrogen in 2030, with the cost per kilogram falling to 3500 won [87]. Further, hydrogen production is expected to reach 3 million tons in 2050 and the cost will be reduced to 2500 won [87]. To increase the production capacity of hydrogen vehicles, the South Korean government plans to establish more than 2000 hydrogen refueling stations nationwide [85].

3.5. Conclusions and Challenges

The accelerating impacts of global climate change have necessitated a worldwide shift towards sustainable energy sources. Hydrogen energy stands out among various low-carbon energy transition strategies. Not only is it a technical solution eagerly awaited by all stakeholders, but it also represents a green resource that can be used to compete on a global scale in the future. Independent hydrogen supply system using green electricity is a key link in the green hydrogen industry chain. In recent years, governments across the world have intensified efforts to construct renewable energy infrastructure to provide a stable source of green electricity for the future green hydrogen industry. Therefore, countries should incorporate hydrogen infrastructure and transmission backbone into the national infrastructure. Priority should be given to retrofitting existing gas supply networks in industrial or transport settlements to accommodate future hydrogen delivery needs. To establish a sustainable hydrogen energy ecosystem, three primary challenges must be addressed: securing a reliable supply, optimizing transportation and storage infrastructure, and reducing production costs.

Author Contributions: K.T.L.: Conceptualization, Formal analysis, Funding acquisition, Investigation, Project administration, Resources, Supervision, Writing – review & editing. Y.S.C.: Investigation, Methodology, Validation, Formal analysis, Writing – original draft. Q.Y.H.: Data collection, Methodology, Writing – original draft. T.J.H.: Investigation, Formal analysis, Writing – review & editing. W.H.H.: Investigation, Writing – review & editing.

Funding: This research received the financial support from the National Science and Technology Council, Taiwan, under the contracts NSTC 113-2218-E-006-012-, NSTC 113-2515-S-029-002-, and NSTC 113-2221-E-029-001-MY3. This research is also supported in part by the NSTC 112-2218-E-006-025-, NSTC 112-2218-E-002-052-.

Institutional Review Board Statement: Not applicable.

Informed Consent Statement: Not applicable.

Data Availability Statement: Not applicable.

Conflicts of Interest: The author declares no conflict of interest.

References

1. Zainal, B.S.; Ker, P.J.; Mohamed, H.; et al. Recent advancement and assessment of green hydrogen production technologies. *Renewable Sustainable Energy Rev.* **2024**, *189*, 113941.
2. IEA, Renewables 2020. Available online: https://www.iea.org/reports/renewables-2020 (access on 1 July 2024).
3. Topsoe, ABB and Fluor form Alliance to Develop Standardized Concept for SOEC Electrolyzer Factory. Available online: https://new.abb.com/news/detail/116827/topsoe-abb-and-fluor-form-alliance-to-develop-standardized-concept-for-soec-electrolyzer-factory (access on 1 July 2024).
4. Widera, B. Renewable hydrogen implementations for combined energy storage, transportation and stationary applications. *Therm. Sci. Eng. Prog.* **2020**, *16*, 100460.
5. Genovese, M.; Fragiacomo, P. Hydrogen refueling station: Overview of the technological status and research enhancement. *J. Energy Storage* **2023**, *61*, 106758.
6. Hosseini, S.E.; Butler, B. An overview of development and challenges in hydrogen powered vehicles. *Int. J. Green Energy* **2020**, *17*, 13–37.
7. Logan, K.G.; Nelson, J.D.; Hastings, A. Environment. Electric and hydrogen buses: Shifting from conventionally fuelled cars in the UK. Transp. *Res. Transp. Environ.* **2020**, *85*, 102350.
8. Haseli, Y.; Naterer, G.; Dincer, I. Comparative assessment of greenhouse gas mitigation of hydrogen passenger trains. *Int. J. Hydrogen Energy* **2008**, *33*, 1788–96.
9. Brewer, G.D. *Hydrogen Aircraft Technology*; Routledge: New York, NY, USA, 2017.
10. Filippov, S.P.; Yaroslavtsev, A. Hydrogen energy: Development prospects and materials. *Russ. Chem. Rev.* **2021**, *90*, 627.
11. Incer-Valverde, J.; Patiño-Arévalo, L.J.; Tsatsaronis, G.; et al. Hydrogen-driven Power-to-X: State of the art and multicriteria evaluation of a study case. *Energy Convers. Manage.* **2022**, *266*, 115814.
12. Ince, A.C.; Colpan, C.O.; Hagen, A.; et al. Modeling and simulation of Power-to-X systems: A review. *Fuel* **2021**, *304*, 121354.
13. Hosseini, S.E.; Wahid, M. Hydrogen production from renewable and sustainable energy resources: Promising green energy carrier for clean development. *Renewable Sustainable Energy Rev.* **2016**, *57*, 850–866.
14. Manoharan, Y.; Hosseini, S.E.; Butler, B.; et al. Hydrogen fuel cell vehicles; current status and future prospect. *Appl. Sci.* **2019**, *9*, 2296.
15. Crolius, S.H. On the Ground in Australia: Two Key Mentions for Ammonia Energy. Available online: https://ammoniaenergy.org/articles/on-the-ground-in-australia-two-key-mentions-for-ammonia-energy/ (access on 1 July 2024).
16. Asif, M.; Bibi, S.S.; Ahmed, S.; et al. Recent advances in green hydrogen production, storage and commercial-scale use via catalytic ammonia cracking. *Chem. Eng. J.* **2023**, *473*, 145381.
17. Danish Energy Agency. Export Potential Ccus & Ptx Technology. Available online: https://ens.dk/sites/ens.dk/files/ptx/ptx_and_ccus_technology_export_potential.pdf (access on 1 July 2024).
18. Foorginezhad, S.; Mohseni-Dargah, M.; Falahati, Z.; et al. Sensing advancement towards safety assessment of hydrogen fuel cell vehicles. *J. Power Sources* **2021**, *489*, 229450.
19. Züttel, A. Hydrogen storage and distribution systems. *Mitigation Adapt. Strategies Global Change* **2007**, *12*, 343–365.
20. Rajeshwar, K.; McConnell, R.; Harrison, K.; et al. *Renewable Energy and the Hydrogen Economy*; Springer: New York, NY, USA, 2008; pp. 1–18.
21. Fayaz, H.; Saidur, R.; Razali, N.; et al. An overview of hydrogen as a vehicle fuel. *Renewable Sustainable Energy Rev.* **2012**, *16*, 5511–5528.
22. Kahraman, E.; Ozcanlı, S.C.; Ozerdem, B. An experimental study on performance and emission characteristics of a hydrogen fuelled spark ignition engine. *Int. J. Hydrogen Energy* **2007**, *32*, 2066–2072.
23. Guo, L.; Su, J.; Wang, Z.; et al. Hydrogen safety: An obstacle that must be overcome on the road towards future hydrogen economy. *Int. J. Hydrogen Energy* **2024**, *51*, 1055–1078.
24. Yonhap News Agency. Hydrogen Tank Explosion Kills 2 in Gangneung. Available online: https://en.yna.co.kr/view/PYH20190524054600315 (access on 1 July 2024).
25. Genovese, M.; Blekhman, D.; Dray, M.; et al. Hydrogen losses in fueling station operation. *J. Cleaner Prod.* **2020**, *248*, 119266.
26. Santa Clara Weekly. Hydrogen Gas Explosion And Fire at Air Products And Chemicals. Available online: https://www.svvoice.com/hydrogen-gas-explosion-and-fire-at-air-products-and-chemicals-inc-in-santa-clara/ (access on 1 July 2024).
27. Ustolin, F.; Paltrinieri, N.; Berto, F. Loss of integrity of hydrogen technologies: A critical review. *Int. J. Hydrogen Energy* **2020**, *45*, 23809–23840.
28. Edwardes-Evans, H. Norway's Nel Notified of Fines for Hydrogen Fueling Station Incident. Available online: https://www.spglobal.com/commodityinsights/en/market-insights/latest-news/electric-power/021621-norways-nel-notified-of-fines-for-hydrogen-fueling-station-incident (access on 1 July 2024).
29. Taibi, E.; Miranda, R.; Carmo, M.; et al. Green Hydrogen Cost Reduction. Available online: https://www.h2knowledgecentre.com/content/researchpaper1613 (access on 1 July 2024).
30. Capurso, T.; Stefanizzi, M.; Torresi, M.; et al. Perspective of the role of hydrogen in the 21st century energy transition. *Energy Convers. Manage.* **2022**, *251*, 114898.
31. Yakubson, K.I. Prospects for Using Hydrogen in Various Branches of the World Economy as One of the Directions of Its Decarbonization. *Russ. J. Appl. Chem.* **2022**, *95*, 309–340.
32. Energy Bo. *2021 Energy Supply Statistics*; Ministry of Economic Affairs: Taiwan, China, 2022.

33. Brown, A.; Grünberg, N. CHINA'S NASCENT GREEN HYDROEN SECTOR: How policy, research and business are forging. *Mercato Inst. China Stud.* **2022**, 1–24
34. Beauchemin, A. What can we expect from clean hydrogen in Canada? Available online: https://www.cbc.ca/news/science/clean-hydrogen-canada-1.6856584 (access on 1 July 2024).
35. "Green" Hydrogen—Australia's Race to be a Global Player. Available online: https://www.gtlaw.com.au/knowledge/green-hydrogen-australias-race-be-global-player (access on 12 August 2021).
36. James, W. Japan's Hydrogen Ambitions May Do More Harm than Good. Available online: https://eastasiaforum.org/2024/01/23/japans-hydrogen-ambitions-may-do-more-harm-than-good/#:~:text=In%20Brief,aviation%20fuels%20and%20heavy%20industry (access on 23 January 2024).
37. Nilsen, E. The Biden Administration Sees Hydrogen as a Game-Changing Climate Technology. The Reality Is Far More Complicated. 2023. Available online: https://edition.cnn.com/2023/06/05/politics/hydrogen-goal-biden-administration-energy-climate/index.html (access on 5 June 2023).
38. Collins, L. Germany doubles its green hydrogen production target for 2030 in new update of national strategy. 2023. Available online: https://www.hydrogeninsight.com/policy/germany-doubles-its-green-hydrogen-production-target-for-2030-in-new-update-of-national-strategy/2-1-1491715 (access on 26 June 2023).
39. Chang, A. Wind energy to fuel EU in achieving 40 GW hydrogen by 2030. Available online: https://www.infolink-group.com/energy-article/wind-to-play-vital-role-in-achieving-EUs-40-GW-of-electrolysis-capacity-by-2030 (access on 24 October 2022).
40. Patil, R. UAE Green Hydrogen Market Competition Strategy, Key Players, Development Plans, Strategies Business Growth and Demand By 2030. 2024. Available online: https://isig.ac.cd/alumni/blogs/20276/UAE-Green-Hydrogen-Market-Competition-Strategy-Key-Players-Development-Plans?lang=en_us (access on 22 March 2024).
41. Wouters, F. A Small Molecule with a Big Potential in MENA. Available online: https://foresightmedia.com/story/swp173746-aeRpzz76-20903 (access on 28 September 2021).
42. Council, H. Hydrogen Insights 2021. Available online: https://hydrogencouncil.com/en/hydrogen-insights-2021/ (access on 15 July 2021).
43. Council, H. Hydrogen Insights: A perspective on hydrogen investment, market development and cost competitiveness. Available online: https://hydrogencouncil.com/wp-content/uploads/2021/02/Hydrogen-Insights-2021.pdf (access on 1 February 2021).
44. REN21. Renewables 2023 Global Status Report Collection CHILE A Hidden Hydrogen Champion Is Awakening. Available online: https://www.ren21.net/wp-content/uploads/2019/05/GSR-2023_Energy-Supply-Module.pdf (access on 1 July 2024).
45. Infrastructure UMoEa. UAE signs MoU with German and Japanese firms for green hydrogen project in Masdar. Available online: https://www.reuters.com/business/sustainable-business/uae-masdar-signs-mou-with-dutch-companies-develop-green-hydrogen-supply-chain-2023-01-13/ (access on 18 July 2023).
46. Nazir, H.; Muthuswamy, N.; Louis, C.; et al. Is the H2 economy realizable in the foreseeable future? Part III: H2 usage technologies, applications, and challenges and opportunities. *Int. J. Hydrogen Energy* **2020**, *45*, 28217–28239.
47. Hydrogen R. Record 45 New Hydrogen Filling Stations Open in Europe in 2022. Available online: https://fuelcellsworks.com/news/record-45-new-hydrogen-filling-stations-open-in-europe-in-2022/#:~:text=A%20record%2045%20new%20public,%2C%20according%20to%20H2stations.org (access on 14 February 2023).
48. Burgess, J. Feature: Pipeline Network Crucial to Europe's Bold 2030 Hydrogen Plans. Available online: https://www.spglobal.com/commodityinsights/en/market-insights/latest-news/energy-transition/013024-pipeline-network-crucial-to-europes-bold-2030-hydrogen-plans (access on 4 February 2024).
49. Strategy UH. UK Hydrogen Strategy. Available online: https://www.gov.uk/government/publications/uk-hydrogen-strategy (access on 17 August 2021).
50. Department for Business EIS; The Rt Hon Kwasi Kwarteng; The Rt Hon Anne-Marie Trevelyan. UK Government Launches Plan for A World-Leading Hydrogen Economy. Available online: https://www.britishaviationgroup.co.uk/knowledge/uk-government-launches-plan-for-a-world-leading-hydrogen-economy/ (access on 23 August 2021).
51. Ciminelli, M. Hydrogen Law, Regulations & Strategy In Italy. Available online: https://cms.law/en/int/expert-guides/cms-expert-guide-to-hydrogen/italy (access on 24 November 2021).
52. Samsun, R.C.; Rex, M.; Antoni, L.; et al. Deployment of Fuel Cell Vehicles and Hydrogen Refueling Station Infrastructure: A Global Overview and Perspectives. *Energies* **2022**, *15*, 4975.
53. Boucly, P. France is ready to lead the battle against climate change. Available online: https://hydrogen.revolve.media/2022/case-studies/france-is-ready-to-lead-the-battle-against-climate-change/#:~:text=France%20is%20ready!,hydrogen%20in%20France%20by%202030 (access on 1 July 2024).
54. Vaid, M. Joint efforts within the ISA, Progress in Nuclear Energy, and Advancements in Green Hydrogen Highlight India and France's Mutual Commitment to Promoting Sustainability. Available online: https://www.orfonline.org/expert-speak/france-and-india-partners-for-a-green-future (access on 7 August 2023).
55. Kovač, A.; Paranos, M.; Marciuš, D. Hydrogen in energy transition: A review. *Int. J. Hydrogen Energy* **2021**, *46*, 10016–10035.
56. Citaristi, I. International energy agency—Iea. In *The Europa Directory of International Organizations 2022*; Routledge: London, UK, 2022; pp. 701–702.
57. Panchenko, V.; Daus, Y.V.; Kovalev, A.; et al. Prospects for the production of green hydrogen: Review of countries with high potential. *Int. J. Hydrogen Energy* **2023**, *48*, 4551–4571.
58. Hassan, Q.; Abdulateef, A.M.; Hafedh, S.A.; et al. Renewable energy-to-green hydrogen: A review of main resources routes, processes and evaluation. *Int. J. Hydrogen Energy* **2023**, *48*, 17383–17408.
59. Department of Energy, Biden-Harris Administration Releases First-Ever National Clean Hydrogen Strategy and Roadmap to Build a Clean Energy Future, Accelerate American Manufacturing Boom. Available online:

https://www.energy.gov/articles/biden-harris-administration-releases-first-ever-national-clean-hydrogen-strategy-and (access on 5 June 2023).
60. Cresko, J.; Rightor, E.; Carpenter, A.; et al. *DOE Industrial Decarbonization Roadmap*; USDOE Office of Energy Efficiency and Renewable Energy (EERE): Washington, DC, USA, 2022.
61. None, N. *National Hydrogen Energy Roadmap*; EERE Publication and Product Library: Washington, DC, USA, 2002.
62. Strategy, H. Enabling a Low-Carbon Economy. Available online: https://www.energy.gov/sites/default/files/2020/08/f77/Hydrogen%20Economy%20Strategy%20Fact%20Sheet.pdf (access on 1 July 2020).
63. Association FCHE. Road Map to a US Hydrogen Economy. Available online: https://h2fcp.org/sites/default/files/Road+Map+to+a+US+Hydrogen+Economy+Full+Report.pdf (access on 1 July 2024).
64. Suvorov, V.Y.; Pyankov, V.V. Improving the heat-resistance of parts of metallurgical equipment. *Metallurgist* **1983**, *27*, 379–81.
65. Hashimoto, N. Japan's efforts to realize a hydrogen society. Available online: https://www.eai.enea.it/archivio/pianeta-idrogeno/japan-s-efforts-to-realize-hydrogen-society.html (access on 1 July 2024).
66. Panov, V.P. Ultrasonic soldering heat exchanging equipment made of aluminum-alloys. *Weld. Prod.* **1985**, *32*, 21–22.
67. Kusov, V.I.; Shapovalov, A.P.; Gruznov, A.K.; et al. Mastering the heating equipment in the cold-rolling shop. *Metallurgist* **1982**, *26*, 342–345.
68. Honda. Honda FCX Fuel Cell Vehicle Earns Japanese Ministry of Land, Infrastructure and Transport Approval-Lease Marketing to CommenceDecember 2nd in Japan and the U.S.-. Available online: https://global.honda/en/newsroom/news/2002/4021122-fcx-eng.html (access on 22 November 2002).
69. Toyota Europe Newsroom. FCV-R Fuel Cell Concept—Revolution and reality. Available online: https://newsroom.toyota.eu/2016-fcv-r-fuel-cell-concept--revolution-and-reality/ (access on 1 July 2024)
70. Nakano, J. Japan's Hydrogen Industrial Strategy. Available online: https://www.csis.org/analysis/japans-hydrogen-industrial-strategy (access on 1 July 2024).
71. Satanovskii, L.G. Equipment for heat-treating long articles (from foreign technology). *Met. Sci. Heat Treat.* **1983**, *25*, 51–54.
72. Government of South Australia. A Hydrogen Roadmap forSouth Australia. Available online: https://www.energymining.sa.gov.au/industry/hydrogen-and-renewable-energy/hydrogen-in-south-australia/hydrogen-files/hydrogen-roadmap-11-sept-2017.pdf (access on 1 July 2024).
73. Satanovskii, L.G. Equipment for heat treating roller-bearings (from foreign technology). *Met. Sci. Heat Treat.* **1977**, *19*, 309–12.
74. NEDO Advanced Battery and Hydrogen Technology Department The World's Largest-Class Hydrogen Production, Fukushima Hydrogen Energy Research Field (FH2R) Now Is Completed at Namie town in Fukushima. Available online: https://www.nedo.go.jp/english/news/AA5en_100422.html (access on 7 October 2019).
75. Tatsuno, D.; Yoneyama, T.; Matsumoto, T. Local heat clamp bending of carbon fiber-reinforced thermoplastic sheet. *Int. J. Adv. Manuf. Technol.* **2020**, *111*, 1517–1533.
76. Gutman, M.B.; Shur, N.F. Seminar on modern electrothermal equipment for heat-treating metallic materials. *Met. Sci. Heat Treat.* **1979**, *21*, 561–563.
77. Chance, C. Focus on Hydrogen: Japan's Energy Strategy for Hydrogen and Ammonia. *Clifford Chance* **2022**, 1–10.
78. Kern, R.F. Heat treating carbon-manganese-boron steel parts for heavy equipment. *Metal Prog.* **1973**, *103*, 90–94.
79. Yun, M.R.S.; Kim, S.H.; Hsu, W.T.; et al. One-Dimensional Thermal Network for Prediction of Heat Transfer Performance of Flat Heat Pipe. *Trans. Korean Soc. Mech. Eng. B* **2023**, *47*, 225–34.
80. Kyodo News. Japan to invest 15 tril. yen in hydrogen supply for decarbonization. Available online: https://english.kyodonews.net/news/2023/06/c8162f931ea8-japan-to-invest-15-tril-yen-in-hydrogen-supply-for-decarbonization.html (access on 6 June 2023).
81. Kwon, T.-H. Renewable portfolio standard in South Korea: A short policy review. Proceedings of Meeting Asia's Energy Challenges. -the 5th IAEE Asian Conference, Perth, Australia, 14–17 February 2016. International Association for Energy Economics, 2016.
82. Ha, J.E. Hydrogen Economy Plan in Korea. *Neth. Enterp. Agency, January* **2019**, *18*, 2019.
83. South Korea. Hydrogen economy promotion and hydrogen safety management act. Available online: https://elaw.klri.re.kr/eng_mobile/viewer.do?hseq=60917&type=sogan&key=13 (access on 1 July 2024).
84. Min-hee, J. Hydrogen Expected to Become Biggest Energy Source in Korea in 2050. Available online: https://www.businesskorea.co.kr/news/articleView.html?idxno=82450#google_vignette (access on 29 November 2021).
85. Stangarone, T. South Korean efforts to transition to a hydrogen economy. *Clean Technol. Environ. Policy* **2021**, *23*, 509–516.
86. Chung-un, C. Korea to produce 6.2 million hydrogen cars by 2040. Available online: https://www.koreaherald.com/view.php?ud=20190117000468 (access on 1 July 2024).
87. Lee, C. S Korea to provide 27.9 mil mt/year of 'clean hydrogen' by 2050. Available online: https://www.spglobal.com/commodityinsights/en/market-insights/latest-news/energy-transition/112621-s-korea-to-provide-279-mil-mtyear-of-clean-hydrogen-by-2050 (access on 26 November 2021).

Review

Progress in Green Energy and Fuel for Sustainability

Wei-Hsin Chen [1,2,3]

[1] Department of Aeronautics and Astronautics, National Cheng Kung University, Tainan 701, Taiwan; weihsinchen@gmail.com or chenwh@mail.ncku.edu.tw
[2] Research Center for Smart Sustainable Circular Economy, Tunghai University, Taichung 407, Taiwan
[3] Department of Mechanical Engineering, National Chin-Yi University of Technology, Taichung 411, Taiwan

Received: 26 June 2024; Revised: 9 August 2024; Accepted: 9 August 2024; Published: 27 August 2024

Abstract: Developing green energy and sustainable fuels is crucial to overcoming the environmental and resource challenges posed by fossil fuel consumption and dependence. To provide a comprehensive insight into the progress in green energy and fuels, including solar, wind, bioenergy, hydropower, marine, and geothermal energy, this study explores significant advancements and ongoing challenges in various renewable energy sectors. This study also highlights the development of green fuels such as biofuels, hydrogen, ammonia, and synthetic fuels, emphasizing their potential to achieve carbon neutrality and integration into existing infrastructures. Key challenges are identified, such as improving the efficiency and performance of renewable technologies, addressing high initial investment costs, and overcoming policy and social acceptance barriers. The environmental impacts of renewable energy production and resource availability are also discussed. The research underscores the necessity of collaborative efforts, supportive policies, and public engagement to overcome these challenges and achieve a sustainable energy future. This comprehensive overview provides insights into the current state and future prospects of green energy and fuel research for sustainability.

Keywords: green energy and fuel; biofuel; biochar; hydrogen; sustainability; net zero

1. Global Community for Sustainability

Fossil fuels have enormously contributed to our demands for heating, power, and chemical products. However, these resources are nonrenewable, have limited amounts, and have led to severe environmental pollution problems worldwide after the Industrial Revolution. These problems include air pollution, thermal pollution, acid rain, etc. In particular, on account of vast emissions of carbon dioxide, the primary byproduct of burning fossil fuels, into the atmosphere, people are encountering more severe environmental challenges, such as the deteriorated atmospheric greenhouse effect, global warming, and climate change [1]. The rising CO_2 concentration and accumulation in the atmosphere even lead to ocean acidification [2], another noticeable issue impacting marine ecosystems.

The global community has made many efforts to solve these environmental and resource challenges. Significant milestones and collaborative initiatives have pushed these efforts toward sustainability, as shown in Figure 1. Beginning with the Earth Summit in 1992, this pivotal event laid the groundwork for international environmental governance. It emphasized the need for sustainable development and set the stage for subsequent collaborative efforts. The United Nations Framework Convention on Climate Change (UNFCCC) was established in 1995 to combat global climate change. In the same year, the first Conference of the Parties (COP1) in Berlin paved the way for international cooperation on climate action. Kyoto Protocol, held in 1997, set binding emission reduction targets for developed countries. It aimed to mitigate greenhouse gas emissions and promote sustainable practices. Re100, launched in 2014, was a global initiative that united influential businesses, such as 3M, Apply, Adobe, Airbnb, IKEA, TSMC, and Intel, committed to using 100% renewable electricity. Then, the 2015 Paris Agreement sought to curb global warming by ensuring that the rise in average temperature remains below 2 °C compared to pre-industrial levels. It encouraged countries to submit nationally determined contributions (NDCs) outlining their emission reduction actions and adaptation measures. This landmark agreement entered into force in 2016. Subsequently, all United Nations Member States adopted the Sustainable Development Goals (SDGs) in 2015. The 17 SDGs, along with 169 targets, were outlined in the outcome document titled "Transforming our world: the 2030 Agenda for Sustainable Development." The 17 global objectives addressed poverty, inequality, climate change, and other critical challenges to create a more sustainable and equitable world. Of the 17 SDGs, SDG 7 (affordable and clean energy) is directly related to green energy and fuel development. The newest conference of the parties (COP) event, COP28, was held in Dubai, UAE, in 2023. Representatives from different countries gathered to address critical climate challenges, implement the Paris Agreement, and accelerate efforts to control global temperature rise to 1.5 °C by the end of this century.

In addition to the events mentioned above, "net zero emissions (or simply net zero)" is also worth paying attention to for sustainability. Net zero is defined as the state where the amount of greenhouse gases emitted by human activities is entirely offset by carbon removal from the atmosphere. The net zero concepts for climate change and greenhouse gas emissions started gaining significant attention around the early to mid-2000s. However, it wasn't until the late 2010s that it became a prominent goal within climate policy discussions and corporate sustainability strategies. The Paris Agreement of 2015 played a crucial role in elevating the prominence of net zero. It underscored the significance of restricting global warming to significantly less than 2 °C and trying to confine it to 1.5 °C above the levels recorded before the industrial era [3]. Since then, the net zero target has become increasingly adopted by governments, businesses, and organizations worldwide as a vital approach for addressing climate change and attaining enduring sustainability.

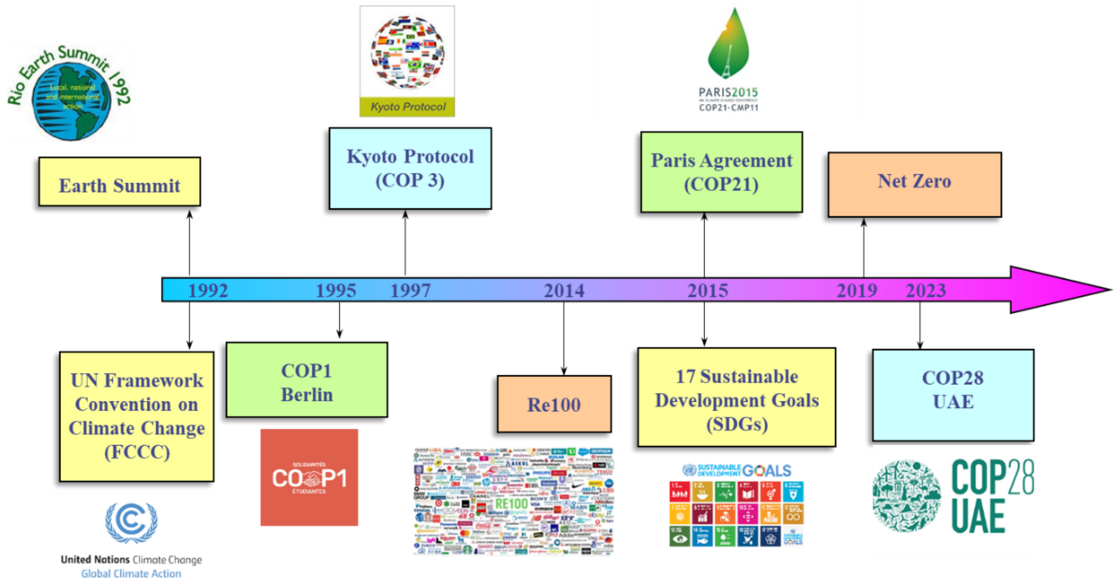

Figure 1. Global community efforts for sustainability.

2. Green Energy

As described earlier, burning fossil fuels to gain energy is the primary reason causing environmental problems. For this reason, many countries have spurred a shift toward renewable energy sources like solar, wind, marine, biomass, geothermal, and hydropower to mitigate global warming. While people grapple with the challenges posed by fossil fuels, the transition to green energy becomes essential for a sustainable future. Green energies comprise solar, wind, biomass, hydropower, marine, and geothermal. No CO_2 is emitted into the atmosphere when utilizing these green energies, so carbon neutralization and decarbonization can be achieved.

2.1. Solar Energy

Solar energy is recognized as a sustainable alternative energy source that is inexpensive, inexhaustible, and widely accessible. Solar energy consists of solar photovoltaic (PV) and concentrating solar power (CSP). Solar energy used for global electricity production is still low, at around 3.6% [4]. Nevertheless, there was a significant surge of around 22% in the installed solar energy capacity from 2021 to 2022. In recent years, considerable progress has been made in materials and systems within solar energy technology to improve efficiency and lower costs [5]. Besides power generation, solar energy can also be applied to materials processing, metallurgy and materials, the cement industry and ceramics, and the recycling of materials' wastes [6].

2.2. Wind Energy

Like solar energy, wind energy is a mature technology and has been highly commercialized. It directly converts wind mechanical energy into electricity, so it is a promising renewable energy source, offering clean and relatively affordable usage [7]. There is ample potential for expansion in installed wind power capacity, evidenced by the substantial global increase in onshore wind capacity. For instance, in 2010, the capacity stood at a mere 178 GW, whereas by 2021, it had surged to 769 GW [8]. Wind turbines can be classified as horizontal and vertical axis wind turbines in accordance with design. To effectively harvest wind energy for electricity generation, much effort has been made in wind turbine design [9] and wind farm array optimization [10].

2.3. Bioenergy

In contemporary times, bioenergy ranks as the fourth most significant primary energy source, following oil, coal, and natural gas [11]; it is also the largest renewable energy resource. Unlike solar and wind energy, which primarily contribute to electricity generation, bioenergy is focused mainly on producing biofuels. These biofuels can be applied to heating, power generation, and transportation. Through biorefinery, biomass can be converted to a variety of biofuels and chemicals. Moreover, waste valorization and a circular bioeconomy [12] can be achieved when biomass wastes are employed as feedstocks. Much attention has recently focused on the relationship between bioenergy and carbon neutrality [13].

2.4. Hydropower

Hydropower, or hydroelectric power, is a sustainable energy source that harnesses power by manipulating natural water flow using dams or diversion structures in rivers or other water bodies. Hydropower globally supplies around 62% of all renewable electricity [14] and around 16% of global electricity demand [15]. At the heart of a hydropower plant lies the hydro turbine, pivotal in converting water’s potential energy into mechanical energy, propelling the generator to produce electricity. Turbines are categorized into two main types: impulse and reaction turbines [16]. Recently, small-scale and micro hydropower development has been an important research topic, particularly for its applications in rural and remote areas [17].

2.5. Marine Energy

Marine energy, also called ocean energy, consists of ocean currents, tides, wave energy, ocean thermal energy conversion (OTEC), and salinity gradient energy. Because the ocean covers approximately 71% of the Earth’s surface, marine energy resources are abundant and geographically distributed. Theoretical estimates suggest that marine energy sources could offer a potential of approximately 151,300 terawatt-hours per year [18]. However, most marine energy technologies are still in the pre-commercial phase, and substantial advancements are needed in research and development and in demonstrating and validating these technologies [19]. These efforts aim to enhance their performance and reliability, ultimately reducing the associated levelized cost of energy (LCoE). To make marine energy more efficient and ready for commercialization, more efforts are needed on energy converter design and optimization [20], the deployment of tidal turbines and generators [21], and the development of materials and structures to withstand harsh marine environments [22].

2.6. Geothermal Energy

It is estimated that the Earth’s core temperature is around 5700 °C, so a tremendous amount of heat is contained in the Earth’s interior. Geothermal energy is also a renewable and sustainable energy resource and is reliable and stable when harvesting geothermal energy. It was reported that 88 countries have directly utilized geothermal energy [23]. Geothermal energy, manifested as hot water and steam, can be used for power generation, greenhouse and space heating, aquaculture pond and raceway heating, industrial applications, etc. Due to heat in the deep underground, resource assessment is the most crucial work for developing geothermal energy. Developing efficient and cost-effective geothermal power plants [24] and heat pump systems [25] is also paramount. Moreover, geothermal energy production’s environmental, economic, and social impacts also attract much attention to geothermal sustainability [26].

3. Green Fuels

Green fuels intrinsically are sustainable fuels. They are alternatives to traditional fossil fuels and are characterized by no net carbon emissions. So, green fuels can reduce greenhouse gas emissions and mitigate global warming and climate change. They can even promote the energy security of a country. Some common examples of green fuels include biofuels, hydrogen, and synthesis fuels.

3.1. Biofuels

Biofuels are produced from biomass. Biomass is an abundant resource, mainly lignocellulosic and algal biomass [27,28]. Organic wastes such as crop residues are also crucial for developing bioenergy. Raw biomass, like wood, can be consumed or burned directly for bioenergy. However, its utilization efficiency is low. Solid, liquid, and gas biofuels can be produced through various conversion technologies, such as physical (grinding, palletization, compression or densification, etc.), thermochemical (combustion, gasification, pyrolysis, torrefaction, liquefaction, etc.), chemical (transesterification), or biological (fermentation, digestion, etc.) conversion [11]. The classification of biofuels in terms of their phases is shown in Figure 2.

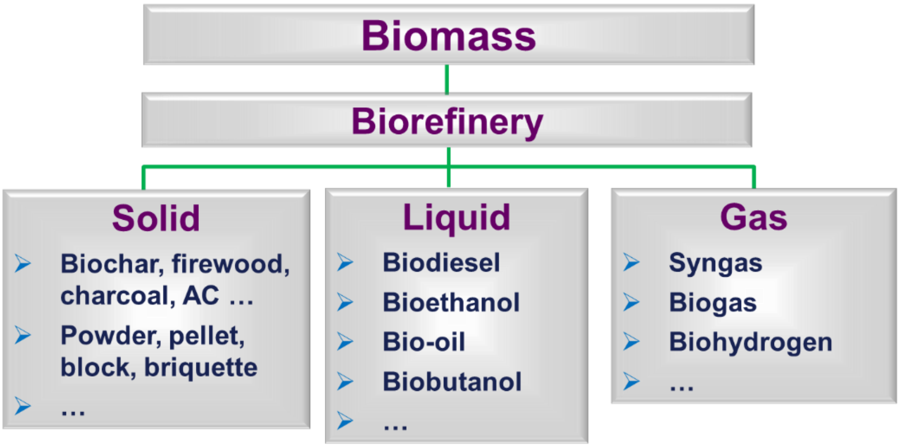

Figure 2. Classification of biofuels.

3.1.1. Solid Biofuel

Wood as a solid biofuel has been consumed for a long time. Wood pellets from the densification of sawdust, wood shavings, or other wood residues are widely used for heating, cooking, power generation, and combined heat and power (CHP) plants [29]. Furthermore, charcoal from carbonization has been widely employed because of its higher energy density. Recently, biochar production through torrefaction and pyrolysis has been extensively investigated [30,31]. In addition to fuel usage, biochar can be used for wastewater treatment to remove dyes, heavy metals, antibiotics, etc. [32], achieving environmental remediation. Moreover, biochar can also be applied to soil amendment and even to the target of carbon negativity.

3.1.2. Liquid Biofuel

Biodiesel and bioethanol production techniques are mature, and the two biofuels have been widely used for vehicles. Biodiesel, a non-toxic and biodegradable fuel, is made from vegetable oils, animal fats, or recycled cooking oils through transesterification. Though biodiesel has been commercialized, research on feedstock selection, catalyst development, fuel stability, and storage for biodiesel quality deserves further investigation [33,34]. Alternatively, bioethanol is made from fermenting sugars or starches in corn, sugarcane, wheat, barley, etc. However, to avoid food storage problems from bioethanol production, using food waste and lignocellulosic biomass as feedstocks is a growing field of research. When using lignocellulosic biomass as a feedstock for bioethanol production, choosing effective pretreatment methods for breaking down complex recalcitrance carbohydrates into fermentable sugars is also a critical topic [35]. Bio-oil is produced from biomass pyrolysis and contains various organic compounds, including phenols, acids, aldehydes, ketones, furans, etc. [28]. Bio-oil can be used as a feedstock to produce high-valued chemicals, solvents, and resins. However, bio-oil has a high water content and is unstable; therefore, upgrading bio-oil is crucial for its application [36]. Another liquid biofuel is biobutanol, which can be produced through the microbial fermentation of biomass-derived sugars, starches, or cellulose [37].

3.1.3. Gas Biofuel

Syngas (synthesis gas), composed of hydrogen and carbon monoxide, produced from biomass gasification is called bio-syngas. Bio-syngas can be burned for heat and power generation in gas turbines, steam boilers, or as a fuel in fuel cells. It can be further processed to produce methanol, dimethyl ether (DME), and liquid transportation fuels such as synthetic gasoline) [38,39]. Bio-syngas cleanup to remove impurities such as sulfur compounds, ammonia, tars, and particulates is an essential issue for biomass gasification development and scale-up. Biogas is generated when microorganisms anaerobically digest organic materials in an oxygen-free environment. It primarily comprises CH_4 and CO_2, along with small amounts of H_2S, N_2, and trace impurities. Process optimization is a potential topic for enhancing biogas production [40]. Biogas purification and upgrading are also essential for producing biomethane [41]. Bio-hydrogen is a biologically produced hydrogen generated from biological processes using renewable biomass as a feedstock. Bio-hydrogen can be produced through dark fermentation, photo-fermentation, and water photolysis [42]. Suitable and advanced microbial strain selection and engineering, reactor design, process optimization, substrate selection and pretreatment, and hydrogen purification play essential roles in bio-hydrogen development [43,44].

3.2. Hydrogen

The evolution of fuel usage is highly related to the atomic caron-to-hydrogen ratio in fuel. Humans' fossil fuel consumption proceeded with coal, petroleum, and natural gas. Coal has an atomic carbon-to-hydrogen ratio of around 10, gasoline has a ratio of around 0.5 (close to wood), and CH_4 has a ratio of 0.25. Hydrogen is gaining significant attention worldwide as a clean fuel and an energy carrier. Since hydrogen has no carbon in gas hydrogen (its atomic carbon-to-hydrogen ratio is 0), using it is conducive to achieving net zero and decarbonization targets [45].

Hydrogen is classified into (1) grey hydrogen, produced from fossil fuel without incorporating carbon capture and storage (CCS) technology; (2) blue hydrogen, produced from natural gas with CCS [46]; (3) green hydrogen, produced via water electrolysis using green power like wind or solar energy; (4) turquoise hydrogen, produced from methane pyrolysis or thermal decomposition to produce pure hydrogen and carbon [47]; (5) pink hydrogen, produced by water electrolysis powered by nuclear energy [46]; and (6) white hydrogen, also known as "natural," "gold," or "geologic" hydrogen, is a naturally occurring form of hydrogen found in the Earth's crust [48].

The future of the hydrogen economy is promising and is expected to play a significant role in the global energy transition. The critical tasks to overcome to approach the hydrogen economy include lowering green hydrogen production costs, hydrogen delivery development, innovative hydrogen storage technology, and hydrogen utilization (fuel cell vehicles, aviation, power production, railway, etc.) [49,50].

3.3. Ammonia

Ammonia has been widely applied in the industry for fertilizer, chemicals, cleaners and sanitizers, refrigerators, pharmaceuticals and healthcare, food additives, water and metal surface treatment, etc. Due to the net-zero target, ammonia, a carbon-free fuel, has also gained significant global interest as a candidate for the transition toward renewable energy [51]. Ammonia is a hydrogen carrier. Compared to hydrogen, ammonia is easy to store and deliver. The first step in the ammonia supply chain is green ammonia production [52], which involves water electrolysis to produce green hydrogen using renewable electricity (green power) and the Haber-Bosch process to synthesize ammonia. Currently, high production costs and scale-up are the main obstacles to green ammonia production [51]. Like hydrogen, ammonia has no carbon, so no carbon dioxide is produced and emitted when burning ammonia. Ammonia can be applied to internal combustion engines, gas turbines, power generation, etc. It can also be blended with other fuels (CO, syngas, dimethyl ether, diethyl ether, coal) to be combusted for industrial applications. Although NH_3 combustion does not emit CO_2, it has pronounced barriers such as high NO_x emissions, low burning velocity, and lower stability [53].

3.4. Synthetic Fuel and Renewable Natural Gas (RNG)

Synthetic fuels are also known as e-fuels or power-to-liquid fuels. Synthetic fuels are produced from the combination of hydrogen, stemming from water electrolysis using renewable electrolysis, and carbon dioxide, whether extracted from the atmosphere or generated by industrial activities. Synthetic fuels include synthetic e-methane, e-methanol, e-ammonia, e-gasoline, e-diesel, and e-jet fuel [54]. E-gasoline, e-diesel, and e-jet fuel can be produced from e-Fischer-Tropsch synthesis (e-FT), implying that Fischer-Tropsch (FT) synthesis uses green electricity to convert syngas and CO_2 to liquid fuels. Though e-fuels appear to be a promising solution for the future of green mobility, they still face several challenges, such as high production costs, energy conversion efficiency and loss, and significant infrastructure development fuel [55].

Renewable natural gas (RNG) or biomethane is the biogas produced from organic waste's anaerobic digestion or thermochemical processes followed by purification. Therefore, unlike biogas containing methane, carbon dioxide, and other small amounts of gases, RNG is a nearly pure form of methane, generated either by upgrading biogas or by gasifying solid biomass and then methanating it. The resulting RNG has a methane content of at least

90%. So, RNG can be used as a direct replacement for natural gas in heating, electricity generation, and transportation, reducing methane emissions from waste. The concerns of RNG development include production costs, feedstock, upgrading technology, environmental impact, and efficiency [56,57].

4. Perspectives and Challenges in Green Energy and Fuel Research

4.1. Perspectives

Green energy and fuel research encompasses various perspectives, focusing on developing sustainable and renewable energy sources to replace fossil fuels. Key areas of research and perspectives aim to address global energy needs while reducing environmental impacts and improving energy security. Some perspectives are described as follows.

(1) Advanced biofuels: Research in this area focuses on developing biofuels from renewable biological sources such as third-generation feedstocks (i.e., macroalgae and microalgae). These biofuels offer a sustainable alternative to conventional fossil fuels, with ongoing studies addressing these technologies' challenges and future potential [58]. Developing advanced biofuel combining waste valorization, biorefinery, and circular bioeconomy is promising [12].

(2) Market and economic perspectives**:** To fulfill the transition to a sustainable society, it is necessary to analyze the market dynamics and economic viability of green energy technologies, exploring multiple perspectives to understand the business case for renewable energy investments [59].

(3) Emerging materials in energy applications: Integrating nanomaterials, such as graphene, into energy technologies is a rapidly advancing field. These materials can enhance the efficiency and performance of solar cells, fuel cells, and batteries [60]. Perovskites are another emerging material with a specific structure that has received a great deal of attention recently. Perovskites can be used in solar cells, batteries, supercapacitors, thermoelectric materials, energy storage, photocatalysis, lighting emitting diodes (LEDs), solid oxide fuel cells (SOFCs), hydrogen evolution reaction, and oxygen evolution reaction [61,62].

(4) Renewable energy integration: It involves adopting and optimizing renewable energy resources, such as solar, wind, hydrogen, geothermal, etc, to create sustainable energy systems [63].

(5) Artificial intelligence (AI) applications: AI is playing a pivotal role in green energy and fuel research, significantly enhancing the development and utilization of renewable energy sources. Through data analysis, evolutionary computation, machine learning, and optimization algorithms, AI technologies can effectively improve the efficiency of green energy and fuel forecasting and management [64,65].

4.2. Challenges

Green energy and fuel research faces several significant challenges. These challenges range from technical and economic issues to policy and social acceptance hurdles. They are described below.

(1) Technical challenges: One of the primary technical challenges is improving the efficiency and performance of renewable energy technologies. For instance, solar panels and wind turbines need advancements in material science to enhance energy conversion efficiency. Storing energy efficiently remains a significant hurdle. Technologies like batteries and supercapacitors need further development to provide reliable storage solutions that balance the intermittent nature of renewable energy sources [66].

(2) Economic challenges: The initial investment for renewable energy infrastructure is often high. While the long-term benefits and operational costs might be lower, the upfront costs can be prohibitive for widespread adoption [66]. Meanwhile, renewable energy markets are influenced by various factors, including subsidies for fossil fuels, market demand, and the economic viability of renewable energy projects [59].

(3) Social and acceptance challenges: Public acceptance is crucial for successful renewable energy projects. Community opposition to renewable energy installations like wind farms or solar parks can delay or even halt projects. Increasing public awareness and understanding of the benefits and necessity of renewable energy is essential for gaining broader acceptance [67].

(4) Environmental and resource challenges: While renewable energy is generally environmentally friendly, the production and disposal of renewable energy technologies can have environmental impacts that need to be managed [68]. Meanwhile, the availability of resources needed for renewable energy technologies, such as rare earth elements for batteries and solar panels, can pose significant challenges [69].

5. Conclusions

The transition to green energy and sustainable fuel sources is essential to mitigate the adverse environmental impacts caused by the reliance on fossil fuels. This research has highlighted the significant strides made in various green energy sectors and outlines the challenges that must be addressed to advance these technologies further. Considerable advancements have been made in solar, wind, bioenergy, hydropower, marine, and geothermal technologies. Each of these sectors offers promising avenues for sustainable energy generation with varying degrees of maturity and commercial readiness. Solar and wind energies have substantially increased capacity and efficiency improvements, while marine and geothermal energy still require extensive research and development to become commercially viable. The development of biofuels, hydrogen, ammonia, and synthetic fuels represents a crucial component of the green energy landscape. Biofuels from lignocellulosic and algal biomass, hydrogen production through electrolysis using renewable energy, and the synthesis of fuels from carbon capture and renewable electricity are highlighted as key focus areas. Each fuel type presents unique advantages, such as carbon neutrality and potential integration into existing infrastructure. Improving the efficiency and performance of renewable energy technologies, along with addressing energy storage issues, are identified as primary technical challenges. Economically, the high initial investment costs and market dynamics, including subsidies for fossil fuels, pose significant barriers to widespread adoption. Effective regulatory frameworks and supportive policies are critical for advancing green energy technologies. In addition, public acceptance and awareness are essential to overcoming resistance and ensuring the successful implementation of renewable energy projects. While renewable energy technologies generally have lower environmental impacts, producing and disposing of these technologies can still pose environmental and ecological challenges. The availability of critical resources, such as rare earth elements, is also a concern that needs to be addressed. The transition to green energy and sustainable fuels is a multifaceted endeavor that requires continued innovation, supportive policies, and public engagement. In summary, research with a collaborative approach to overcoming the existing challenges and realizing the full potential of renewable energy technologies for a sustainable future still needs much effort.

Funding: This research received financial support from the National Science and Technology Council, Taiwan, R.O.C, under the contracts NSTC 113-2218-E-006-012-, NSTC 113-2218-E-002-029-, NSTC NSTC 113-2221-E-006-195-MY3, NSTC 112-2622-E-006-029-, and NSTC 112-2221-E-006-111-MY3.

Institutional Review Board Statement: Not applicable.

Informed Consent Statement: Not applicable.

Data Availability Statement: Not applicable.

Conflicts of Interest: The author declares no conflict of interest.

References

1. Paraschiv, S.; Paraschiv, L.S. Trends of carbon dioxide (CO_2) emissions from fossil fuels combustion (coal, gas and oil) in the EU member states from 1960 to 2018. *Energy Rep.* **2020**, *6*, 237–242.
2. Iida, Y.; Takatani, Y.; Kojima, A.; et al. Global trends of ocean CO_2 sink and ocean acidification: An observation-based reconstruction of surface ocean inorganic carbon variables. *J. Oceanogr.* **2021**, *77*, 323–358.
3. Van Soest, H.L.; den Elzen, M.G.; van Vuuren, D.P. Net-zero emission targets for major emitting countries consistent with the Paris Agreement. *Nat. Commun.* **2021**, *12*, 2140.
4. Pourasl, H.H.; Barenji, R.V.; Khojastehnezhad, V.M. Solar energy status in the world: A comprehensive review. *Energy Rep.* **2023**, *10*, 3474–3493.
5. Dada, M.; Popoola, P. Recent advances in solar photovoltaic materials and systems for energy storage applications: A review. *Beni-Suef Univ. J. Basic Appl. Sci.* **2023**, *12*, 66.
6. Fernández-González, D. A state-of-the-art review on materials production and processing using solar energy. *Miner. Process. Extr. Metall. Rev.* **2023**, 1–43.
7. Zhang, Z.; Liu, X.; Zhao, D.; et al. Overview of the development and application of wind energy in New Zealand. *Energy Built Environ.* **2023**, *4*, 725–742.
8. Jung, C.; Schindler, D. Efficiency and effectiveness of global onshore wind energy utilization. *Energy Convers. Manag.* **2023**, *280*, 116788.
9. Hand, B.; Kelly, G.; Cashman, A. Aerodynamic design and performance parameters of a lift-type vertical axis wind turbine: A comprehensive review. *Renew. Sustain. Energy Rev.* **2021**, *139*, 110699.

10. Azlan, F.; Kurnia, J.; Tan, B.; et al. Review on optimisation methods of wind farm array under three classical wind condition problems. *Renew. Sustain. Energy Rev.* **2021**, *135*, 110047.
11. Chen, W.-H.; Lin, B.-J.; Lin, Y.-Y.; et al. Progress in biomass torrefaction: Principles, applications and challenges. *Prog. Energy Combust. Sci.* **2021**, *82*, 100887. https://doi.org/10.1016/j.pecs.2020.100887.
12. Ubando, A.T.; Felix, C.B.; Chen, W.-H. Biorefineries in circular bioeconomy: A comprehensive review. *Bioresour. Technol.* **2020**, *299*, 122585.
13. Saravanakumar, A.; Vijayakumar, P.; Hoang, A.T.; et al. Thermochemical conversion of large-size woody biomass for carbon neutrality: Principles, applications, and issues. *Bioresour. Technol.* **2023**, *370*, 128562.
14. Shaktawat, A.; Vadhera, S. Risk management of hydropower projects for sustainable development: A review. *Environ. Dev. Sustain.* **2021**, *23*, 45–76.
15. Wasti, A.; Ray, P.; Wi, S.; et al. Climate change and the hydropower sector: A global review. *Wiley Interdiscip. Rev. Clim. Chang.* **2022**, *13*, e757.
16. Kumar, K.; Saini, R. A review on operation and maintenance of hydropower plants. *Sustain. Energy Technol. Assess.* **2022**, *49*, 101704.
17. Elbatran, A.; Yaakob, O.; Ahmed, Y.M.; et al. Operation, performance and economic analysis of low head micro-hydropower turbines for rural and remote areas: A review. *Renew. Sustain. Energy Rev.* **2015**, *43*, 40–50.
18. Taveira-Pinto, F.; Rosa-Santos, P.; Fazeres-Ferradosa, T. Marine renewable energy. *Renew. Energy* **2020**, *150*, 1160–1164.
19. Bhuiyan, M.A.; Hu, P.; Khare, V.; et al. Economic feasibility of marine renewable energy. *Front. Mar. Sci.* **2022**, *9*, 988513.
20. Garcia-Teruel, A.; Forehand, D. A review of geometry optimisation of wave energy converters. *Renew. Sustain. Energy Rev.* **2021**, *139*, 110593.
21. Walker, S.; Thies, P. A review of component and system reliability in tidal turbine deployments. *Renew. Sustain. Energy Rev.* **2021**, *151*, 111495.
22. Qu, F.; Li, W.; Dong, W.; et al. Durability deterioration of concrete under marine environment from material to structure: A critical review. *J. Build. Eng.* **2021**, *35*, 102074.
23. Lund, J.W.; Toth, A.N. Direct utilization of geothermal energy 2020 worldwide review. *Geothermics* **2021**, *90*, 101915.
24. Hackstein, F.V.; Madlener, R. Sustainable operation of geothermal power plants: Why economics matters. *Geotherm. Energy* **2021**, *9*, 10.
25. Farzanehkhameneh, P.; Soltani, M.; Kashkooli, F.M.; et al. Optimization and energy-economic assessment of a geothermal heat pump system. *Renew. Sustain. Energy Rev.* **2020**, *133*, 110282.
26. Soltani, M.; Kashkooli, F.M.; Souri, M.; et al. Environmental, economic, and social impacts of geothermal energy systems. *Renew. Sustain. Energy Rev.* **2021**, *140*, 110750.
27. Chen, W.-H.; Lin, B.-J.; Huang, M.-Y.; et al. Thermochemical conversion of microalgal biomass into biofuels: A review. *Bioresour. Technol.* **2015**, *184*, 314–327. https://doi.org/10.1016/j.biortech.2014.11.050.
28. Chen, W.-H.; Ho, K.-Y.; Aniza, R.; et al. A review of noncatalytic and catalytic pyrolysis and co-pyrolysis products from lignocellulosic and algal biomass using Py-GC/MS. *J. Ind. Eng. Chem.* **2024**, *134*, 51–64.
29. Sarker, T.R.; Nanda, S.; Meda, V.; et al. Densification of waste biomass for manufacturing solid biofuel pellets: A review. *Environ. Chem. Lett.* **2023**, *21*, 231–264.
30. Chen, W.-H.; Peng, J.; Bi, X.T. A state-of-the-art review of biomass torrefaction, densification and applications. *Renew. Sustain. Energy Rev.* **2015**, *44*, 847–866. https://doi.org/10.1016/j.rser.2014.12.039.
31. Li, Y.; Gupta, R.; Zhang, Q.; et al. Review of biochar production via crop residue pyrolysis: Development and perspectives. *Bioresour. Technol.* **2023**, *369*, 128423.
32. Chen, W.-H.; Hoang, A.T.; Nižetić, S.; et al. Biomass-derived biochar: From production to application in removing heavy metal-contaminated water. *Process Saf. Environ. Prot.* **2022**, *160*, 704–733.
33. Mohiddin, M.N.B.; Tan, Y.H.; Seow, Y.X.; et al. Evaluation on feedstock, technologies, catalyst and reactor for

sustainable biodiesel production: A review. *J. Ind. Eng. Chem.* **2021**, *98*, 60–81.

34. Hazrat, M.; Rasul, M.; Khan, M.; et al. Techniques to improve the stability of biodiesel: A review. *Environ. Chem. Lett.* **2021**, *19*, 2209–2236.
35. Ocreto, J.B.; Chen, W.-H.; Ubando, A.T.; et al. A critical review on second-and third-generation bioethanol production using microwaved-assisted heating (MAH) pretreatment. *Renew. Sustain. Energy Rev.* **2021**, *152*, 111679.
36. Zhang, M.; Hu, Y.; Wang, H.; et al. A review of bio-oil upgrading by catalytic hydrotreatment: Advances, challenges, and prospects. *Mol. Catal.* **2021**, *504*, 111438.
37. Ndaba, B.; Chiyanzu, I.; Marx, S. n-Butanol derived from biochemical and chemical routes: A review. *Biotechnol. Rep.* **2015**, *8*, 1–9.
38. Huang, M.-H.; Lee, H.-M.; Liang, K.-C.; et al. An experimental study on single-step dimethyl ether (DME) synthesis from hydrogen and carbon monoxide under various catalysts. *Int. J. Hydrog. Energy* **2015**, *40*, 13583–13593.
39. Galadima, A.; Muraza, O. From synthesis gas production to methanol synthesis and potential upgrade to gasoline range hydrocarbons: A review. *J. Nat. Gas Sci. Eng.* **2015**, *25*, 303–316.
40. Djimtoingar, S.S.; Derkyi, N.S.A.; Kuranchie, F.A.; et al. A review of response surface methodology for biogas process optimization. *Cogent Eng.* **2022**, *9*, 2115283.
41. Mulu, E.; M'Arimi, M.M.; Ramkat, R.C. A review of recent developments in application of low cost natural materials in purification and upgrade of biogas. *Renew. Sustain. Energy Rev.* **2021**, *145*, 111081.
42. Xu, X.; Zhou, Q.; Yu, D. The future of hydrogen energy: Bio-hydrogen production technology. *Int. J. Hydrog. Energy* **2022**, *47*, 33677–33698.
43. Akhlaghi, N.; Najafpour-Darzi, G. A comprehensive review on biological hydrogen production. *Int. J. Hydrog. Energy* **2020**, *45*, 22492–22512.
44. Yahaya, E.; Lim, S.W.; Yeo, W.S.; et al. A review on process modeling and design of biohydrogen. *Int. J. Hydrog. Energy* **2022**, *47*, 30404–30427.
45. Nnabuife, S.G.; Oko, E.; Kuang, B.; et al. The prospects of hydrogen in achieving net zero emissions by 2050: A critical review. *Sustain. Chem. Clim. Action* **2023**, *2*, 100024.
46. Shirizadeh, B.; Quirion, P. Long-term optimization of the hydrogen-electricity nexus in France: Green, blue, or pink hydrogen? *Energy Policy* **2023**, *181*, 113702.
47. Teso, A.; Cloete, S.; del Pozo, C.A.; et al. Integration assessment of turquoise hydrogen in the European energy sector. *Energy Convers. Manag.* **2024**, *307*, 118334.
48. Hand, E. *Hidden Hydrogen*; Science: New York, NY, USA, 2023; Volume 379, pp. 630–636.
49. Man, J.; Ma, T.; Yu, Y.; et al. Levelized costs and potential production of green hydrogen with wind and solar power in different provinces of mainland China. *J. Renew. Sustain. Energy* **2024**, *16*, 025902.
50. Qureshi, F.; Yusuf, M.; Khan, M.A.; et al. A State-of-The-Art Review on the Latest trends in Hydrogen production, storage, and transportation techniques. *Fuel* **2023**, *340*, 127574.
51. El-Shafie, M.; Kambara, S. Recent advances in ammonia synthesis technologies: Toward future zero carbon emissions. *Int. J. Hydrog. Energy* **2023**, *48*, 11237–11273.
52. Olabi, A.; Abdelkareem, M.A.; Al-Murisi, M.; et al. Recent progress in Green Ammonia: Production, applications, assessment; barriers, and its role in achieving the sustainable development goals. *Energy Convers. Manag.* **2023**, *277*, 116594.
53. Kang, L.; Pan, W.; Zhang, J.; et al. A review on ammonia blends combustion for industrial applications. *Fuel* **2023**, *332*, 126150.
54. Nemmour, A.; Inayat, A.; Janajreh, I.; et al. Green hydrogen-based E-fuels (E-methane, E-methanol, E-ammonia) to support clean energy transition: A literature review. *Int. J. Hydrog. Energy* **2023**, *48*, 29011–29033.
55. Shi, K.; Guan, B.; Zhuang, Z.; et al. Perspectives and Outlook of E-fuels: Production, Cost Effectiveness, and Applications. *Energy Fuels* **2024**, *38*, 7665–7692.

56. Du, G.; Shami, H.O.; Mostafa, L.; et al. Life cycle cost and life cycle environmental analysis of the different waste-to-renewable natural gas pathways: An effort to identify an optimal pathway under different Multi-criteria decision-based scenarios. *Process Saf. Environ. Prot.* **2024**, *183*, 1082–1101.
57. Hoffman, A.; Kurumbail, U.; Rhodes, N.; et al. Renewable natural gas: A case study of Minnesota. *Biomass Bioenergy* **2024**, *183*, 107163.
58. Mathushika, J.; Gomes, C. Development of microalgae-based biofuels as a viable green energy source: Challenges and future perspectives. *Biointerface Res. Appl. Chem.* **2022**, *12*, 3849–3882.
59. Qadir, S.A.; Al-Motairi, H.; Tahir, F.; et al. Incentives and strategies for financing the renewable energy transition: A review. *Energy Rep.* **2021**, *7*, 3590–3606.
60. Salahdin, O.D.; Sayadi, H.; Solanki, R.; et al. Graphene and carbon structures and nanomaterials for energy storage. *Appl. Phys. A: Mater. Sci. Process.* **2022**, *128*, 703.
61. Monama, G.R.; Ramohlola, K.E.; Iwuoha, E.I.; et al. Progress on perovskite materials for energy application. *Results Chem.* **2022**, *4*, 100321.
62. Fakharuddin, A.; Gangishetty, M.K.; Abdi-Jalebi, M.; et al. Perovskite light-emitting diodes. *Nat. Electron.* **2022**, *5*, 203–216.
63. Alzahrani, A.; Ramu, S.K.; Devarajan, G.; et al. review on hydrogen-based hybrid microgrid system: Topologies for hydrogen energy storage, integration, and energy management with solar and wind energy. *Energies* **2022**, *15*, 7979.
64. Chen, W.-H.; Eng, C.F.; Lin, Y.-Y.; et al. Two-step thermodegradation kinetics of cellulose, hemicelluloses, and lignin under isothermal torrefaction analyzed by particle swarm optimization. *Energy Convers. Manag.* **2021**, *238*, 114116.
65. Chen, W.-H.; Lu, C.-Y.; Chou, W.-S.; et al. Design and optimization of a crossflow tube reactor system for hydrogen production by combining ethanol steam reforming and water gas shift reaction. *Fuel* **2023**, *334*, 126628.
66. Elavarasan, R.M.; Shafiullah, G.; Padmanaban, S.; et al. A comprehensive review on renewable energy development, challenges, and policies of leading Indian states with an international perspective. *IEEE Access* **2020**, *8*, 74432–74457.
67. Gareiou, Z.; Drimili, E.; Zervas, E. Public acceptance of renewable energy sources. In *Low Carbon Energy Technologies in Sustainable Energy Systems*; Elsevier: Amsterdam, The Netherlands, 2021; pp. 309–327.
68. Sharma, H.B.; Vanapalli, K.R.; Barnwal, V.K.; et al. Evaluation of heavy metal leaching under simulated disposal conditions and formulation of strategies for handling solar panel waste. *Sci. Total Environ.* **2021**, *780*, 146645.
69. Jyothi, R.K.; Thenepalli, T.; Ahn, J.W.; et al. Review of rare earth elements recovery from secondary resources for clean energy technologies: Grand opportunities to create wealth from waste. *J. Clean. Prod.* **2020**, *267*, 122048.

Green Energy and Fuel Research

Review

Life Cycle Assessment of Microalgal Carbon Fixation and Torrefaction for Carbon Neutralization: A State-of-the-Art Review

Congyu Zhang *, Jin Fang, Yong Zhan, Xin Wang, Tao Chen, Kuifeng Hao, Jiaqi Ma and Yuting Wang

School of Resources and Environment, Northeast Agricultural University, Harbin 150030, China
* Correspondence: ztdw7727@163.com
Received: 23 May 2024; Revised: 12 August 2024; Accepted: 5 September 2024; Published: 10 September 2024

Abstract: In the past decades, a series of phenomena such as global warming, glacier melting, sea level rise, and haze weather caused by the greenhouse effect have been reported, which seriously threaten the future of humans. To address this challenge, several countries have initiated interventions to prevent climate change, such as carbon neutralization. Given the current economic, social development and environmental protection requirements, microalgal carbon fixation appears to be a suitable approach to achieve carbon net zero emission while also promoting microalgal biofuel production. This promotes the realization of energy structure transformation and optimization of carbon neutralization. This article provides a comprehensive and state-of-the-art review of research progress on microalgal carbon capture and solid biofuel production via the torrefaction process, with focus on the efficiency and capacity of microalgal carbon fixation, as well as the principle and application of microalgal torrefaction. The detailed review includes the practical value and development prospect of microalgal torrefied biochar, fuel performance conversion, and mechanism in the torrefaction process. Furthermore, the environmental impact of microalgal carbon fixation and torrefaction process are discussed to evaluate the overall environmental benefits of microalgal utilization via life cycle assessment (LCA) method. The technical difficulties of microalgal carbon fixation and torrefaction process are also discussed. This review paper is beneficial to guide the scheme demonstration and specific implementation of microalgal carbon neutralization and thus lead to the efficient establishment of microalgal carbon reduction, biomass accumulation, and biofuel production techniques.

Keywords: life cycle assessment; microalgal carbon fixation; microalgal torrefaction; integrative analysis; carbon neutralization

1. Introduction

Microalgae, also known as microscopic algae, are tiny photosynthetic organisms found in various aquatic environments, such as freshwater and marine habitats [1]. They are single-celled or multicellular organisms belonging to various microorganisms called algae. Microalgae carry out photosynthesis, using sunlight as the energy source to convert carbon dioxide (CO_2) and water into organic compounds, primarily sugars and oxygen (O_2) [2]. They are involved in global carbon fixation, producing a significant volume of O_2 and removing CO_2 from the atmosphere. Microalgae can be widely used in various fields, such as food, feed, biofuels, cosmetics, medicine, etc [3]. In recent years, the application of microalgae in the energy field has received increasing attention. Due to the absorption of a large amount of CO_2 during the growth process of microalgae, they can be converted into solid biofuels through the pyrolysis process. Thus, the microalgae can be used to achieve carbon neutralization and renewable energy [4,5].

Microalgal carbon fixation refers to the process in which microalgae absorb a large amount of CO_2 through photosynthesis, convert it into organic matter, and fix it in biomass [6]. Microalgae can efficiently convert CO_2 from the atmosphere into organic carbon and store it within cells, making it a vital carbon storage medium [7]. This process not only helps to reduce the concentration of CO_2 in the atmosphere, but also sustainably sequesters carbon during the utilization of microalgal biomass. Microalgae possess the following advantages in carbon fixation: (1) Compared to other plants, microalgae possess higher photosynthetic efficiency and can more effectively absorb CO_2 from the atmosphere [8]. (2) Microalgae possess the characteristic of rapid growth, which can quickly accumulate a large amount of biomass and fix a large amount of carbon inside the cells. (3) Microalgae are classified into numerous species, each with unique adaptability under different environmental conditions, exhibiting significant potential for carbon sequestration [9]. (4) The growth of microalgae is a renewable process, and its biomass can be utilized to produce a range of valuable products, including food, feed, and biofuels. This makes its carbon fixation process more sustainable. Due to its efficient absorption of CO_2 and rapid growth, microalgae carbon fixation is considered a potential carbon neutralization technology [10]. Utilizing microalgae to fix and store carbon helps reduce CO_2 concentration in the atmosphere, alleviate the global greenhouse effect, and provide a sustainable solution for addressing climate change.

Microalgal torrefaction is a process in which microalgae are thermally treated in the absence of O_2 at 200–300 °C. This process aims to improve microalgal biomass's properties and energy density for efficient conversion into biofuels or other valuable products [11]. During microalgal torrefaction, the biomass undergoes various physical and chemical changes. The process typically involves the removal of moisture and volatile matter, resulting in increased carbon content and energy density [12]. The main objectives of microalgal torrefaction are increasing the energy density, improving stability and handling, and enhancing conversion efficiency. It is important to note that microalgal torrefaction is still an emerging technology, and further research and development are needed to optimize the process parameters, understand the effects on different microalgal species, and evaluate the overall techno-economic feasibility [13]. Nonetheless, microalgal torrefaction holds potential as a sustainable and renewable pathway for energy production and utilization of microalgal biomass.

Combining microalgal carbon fixation and microalgal torrefaction can potentially achieve carbon neutralization or even carbon negative effects [14]. Microalgae are photosynthetic organisms that can capture CO_2 from the atmosphere and convert it into organic biomass through photosynthesis. The process involves utilizing sunlight, water, and CO_2 to produce carbohydrates, lipids, and proteins [15]. Cultivating microalgae in large-scale systems can fix and store significant amounts of CO_2 within the microalgal biomass [16]. After microalgae have been cultivated and harvested, they can undergo torrefaction process. In such systems, the CO_2 emitted during energy production from torrefied microalgae is captured and recycled back into the microalgal cultivation process. This creates a continuous cycle where CO_2 is repeatedly fixed and utilized, resulting in a net zero or even negative carbon footprint [17]. Combining microalgal carbon fixation with microalgal torrefaction may yield a carbon neutral or negative effect. The captured CO_2 is effectively stored within the microalgal biomass, and the subsequent energy production does not contribute to additional CO_2 emissions when a closed-loop system is implemented.

Life cycle assessment (LCA) is a common method for evaluating the environmental effects of a product or process throughout its entire life cycle. When conducting an LCA analysis of the overall process of microalgal carbon fixation and microalgal torrefaction, several key aspects can be considered, including microalgal cultivation, harvesting and drying, torrefaction process, energy production, end-of-life options, and additional inputs and processes [18]. The LCA analysis may help to assess the overall environmental performance of the microalgal carbon fixation and torrefaction process, revealing its potential environmental benefits and identifying areas for further improvement [19]. It helps decision-makers evaluate the sustainability of the technology and make informed choices to minimize potential negative impacts on the environment.

2. Microalgal Carbon Neutralization of Fixation and Conversion

2.1. A Brief Introduction to Carbon Neutralization

Carbon neutralization is the process of balancing or offsetting carbon emissions by compensating for them through activities that remove or reduce an equivalent amount of CO_2 from the atmosphere. The primary goal of carbon neutralization is to achieve a net-zero carbon footprint, where the emissions produced are balanced by actions that actively remove or prevent the release of CO_2 [20]. Human activities, such as burning fossil fuels, deforestation, and industrial processes, contribute to the accumulation of greenhouse gases in the atmosphere, leading to global warming and climate change. Carbon neutralization aims to mitigate these effects by reducing and counterbalancing the CO_2 emitted into the atmosphere. Several approaches are used to achieve carbon neutralization [21]. One common method involves reducing emissions at their source through energy efficiency measures, transitioning to renewable energy sources, or adopting cleaner technologies. By minimizing the amount of carbon emissions generated, the need for offsetting is reduced [22].

Offsetting plays a crucial role in carbon neutralization by investing in projects or initiatives that remove or reduce CO_2 from the atmosphere. This can include activities such as afforestation (planting trees), reforestation, carbon capture and storage (CCS) technologies, or supporting renewable energy projects [23]. These actions can offset the remaining carbon emissions that cannot be eliminated directly. Various standards and certifications have been established to ensure the credibility and transparency of carbon neutralization efforts. These frameworks verify and certify the authenticity and impact of offset projects, ensuring that they genuinely contribute to carbon reduction or removal [24]. Carbon neutralization is vital to address climate change and achieve sustainability goals. It allows individuals, businesses, and organizations to take responsibility for their carbon emissions and actively contribute to a greener and more sustainable future [25]. Implementation of carbon neutralization measures at individual and collective levels may achieve a balanced carbon cycle and mitigate the harmful effects of climate change.

2.2. Carbon Neutralization Value of Microalgal Carbon Fixation

The carbon neutralization value of microalgal carbon fixation refers to the ability of microalgae to absorb and convert CO_2 into organic biomass through photosynthesis. This process helps to offset carbon emissions and reduce the overall concentration of CO_2 in the atmosphere, thus contributing to carbon neutralization. Microalgae are highly efficient in capturing and utilizing CO_2 due to their rapid growth rates and high photosynthetic activity [3]. They can fix significant amounts of CO_2, often surpassing other terrestrial plants in their carbon sequestration potential. It is estimated that microalgae can capture several times more CO_2 per unit area compared to traditional land-based crops like trees. Moreover, microalgal biomass obtained through carbon fixation can be utilized in various ways [26]. It can be converted into biofuels, such as biodiesel or bioethanol, serving as alternative and renewable energy sources. Additionally, microalgae can be used as a feedstock for producing food supplements, animal feed, fertilizers, and other valuable products. Therefore, microalgal carbon fixation has significant carbon neutralization value as it not only helps to reduce greenhouse gas emissions but also provides potential solutions for sustainable energy production and resource utilization.

The carbon neutralization value of microalgal carbon fixation depends on several factors, including microalgae species, growth conditions, and cultivation methods. Different species have varying carbon uptake rates, with some being more efficient than others [27]. The carbon fixation conditions of different microalgae are listed in Table 1. Optimizing growth conditions, such as light intensity, temperature, and nutrient availability, can further enhance carbon fixation capacity. Furthermore, the utilization of microalgal biomass can also contribute to carbon neutralization. Microalgae can be used as a feedstock for biofuels, such as biodiesel and bioethanol, replacing fossil fuel-derived alternatives. By using microalgal biomass as a renewable energy source, carbon emissions can be reduced [28]. Overall, microalgal carbon fixation has the potential to play a significant role in carbon neutralization efforts due to its ability to capture and convert CO_2 into biomass, and its versatile applications in various sectors.

Table 1. The carbon fixation conditions of different microalgae.

Microalgae Species	CO_2 Fixation Rate (g_{CO2} $L^{-1}\cdot d^{-1}$)	CO_2 Fixation Efficiency (%)	Biomass Productivity ($g_{biomass}$ $L^{-1}\cdot d^{-1}$)	Reference
Chlorella fusca LEB 111	0.23	35.70%	0.12	[29]
Chlorella sp. AT1	0.57	64.00%	0.24	[30]
Scenedesmus sp.	0.16	33.00%	0.08	[31]
Spirulina sp.	0.18	21.80%	0.10	[32]
Scenedesmus obliquus SA1	1.04	10.30%	0.55	[33]
Chlorella fusca	0.26	63.40%	0.14	[34]
Chlorella vulgaris	1.28	12.00%	0.36	[35]
Spirulina sp. LEB 18	0.10	15.80%	0.06	[36]
Coelastrum sp.	7.25	59.80%	0.27	[37]
Spirulina platensis	1.44	85.00%	0.43	[38]
Scenedesmus dimorphus	0.80	63.40%	0.44	[39]

2.3. Mechanism and Application of Carbon Fixation and Reduction by Microalgae

Microalgal carbon fixation is the process by which microalgae convert CO_2 from the atmosphere into organic compounds through photosynthesis. This process plays a crucial role in mitigating climate change by reducing the concentration of CO_2. The mechanism of carbon fixation by microalgae primarily involves the process of photosynthesis [40]. Microalgae, like other plants and algae, use sunlight, CO_2, and water to produce organic compounds through photosynthesis. The process steps are summarized as follows: (1) Absorption of sunlight. Microalgae utilize pigments, such as chlorophyll, to absorb sunlight energy [41]. (2) Carbon dioxide uptake. Microalgae extract CO_2 from the atmosphere or dissolved carbon sources in water. (3) Photosynthetic reaction. In the presence of sunlight and the enzyme RuBis CO (Ribulose-1,5-bisphosphate carboxylase/oxygenase), CO_2 is converted into organic compounds, primarily carbohydrates. (4) Oxygen release. As a byproduct of photosynthesis, microalgae release oxygen into their environment [42]. The profiles of microalgal carbon fixation and conversion are shown in Figure 1.

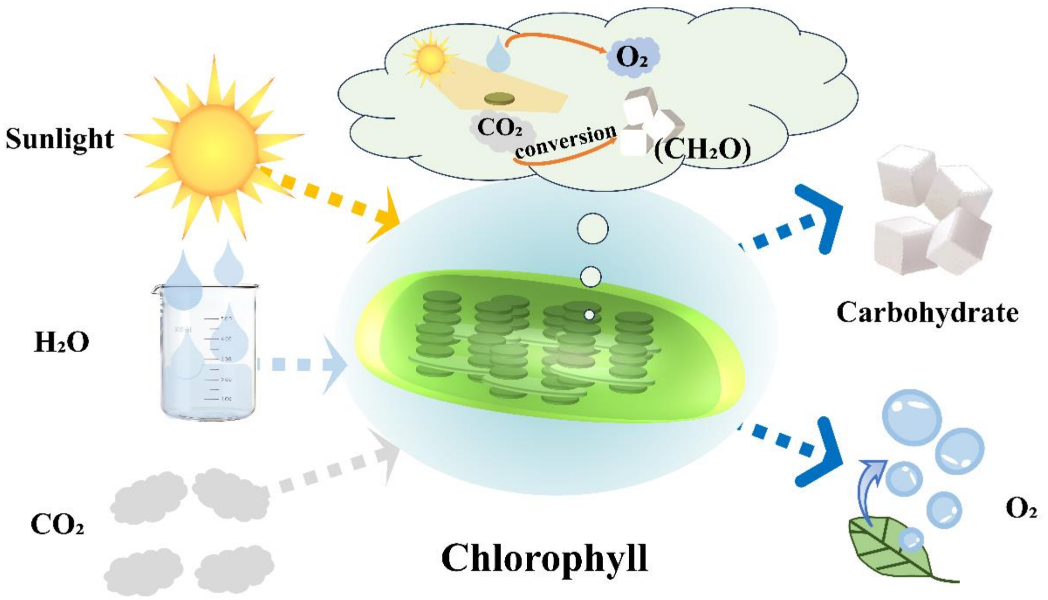

Figure 1. The profiles of microalgal carbon fixation and conversion.

Microalgal carbon fixation and reduction has multiple applications, including (1) Carbon sequestration. Microalgae can capture and store substantial amounts of CO_2, contributing to mitigating greenhouse gas emissions. By cultivating microalgae in large-scale open ponds or closed photobioreactors, significant quantities of CO_2 can be absorbed and converted into biomass [43]. (2) Biofuel production. Microalgae can be used as a feedstock to produce biofuels like biodiesel and bioethanol. The lipids accumulated in microalgae can be extracted and processed into biodiesel, which can directly substitute for fossil fuels. Additionally, the carbohydrates present in microalgae may undergo fermentation to produce bioethanol [44]. (3) Food and feed production. Some species of microalgae have high nutritional value and can be used as a food source for humans or animals. Microalgae contain proteins, essential fatty acids, vitamins, and minerals, making them suitable for inclusion in various food and feed products [45]. (4) Wastewater treatment. Microalgae can remove nutrients, such as nitrogen and phosphorus, from wastewater through their growth and metabolic activities, purifying the water in the process [46]. (5) Carbon capture and utilization (CCU). Microalgal biomass can be used as a carbon source for bioplastics, biochemicals, and other valuable products, thereby reducing reliance on fossil fuel-derived raw materials [47]. These applications highlight the versatility of microalgae and their potential to contribute to carbon fixation, reduction, and sustainable resource utilization.

3. High-Value Carbon-Neutral Biofuel Production via the Torrefaction Process

3.1. An Overview of Torrefaction Technology

Torrefaction is a thermal treatment process that involves heating biomass, typically wood or agricultural residues, in the absence of oxygen [48]. The torrefaction process triggers the production of a dry and relatively stable solid fuel known as torrefied biomass or biochar. The main objective of torrefaction is to improve the properties of biomass, making it more suitable for energy conversion processes such as combustion, gasification, and co-firing with coal [49,50]. Some key aspects and characteristics of torrefaction technology are shown as follows:

(1) Temperature and residence time. In the torrefaction process, biomass is heated at temperatures ranging from 200 to 300 °C. The heating period is usually around 15–60 min, depending on the scale and design of the torrefaction reactor [51].

(2) Drying and volatile release. During torrefaction, moisture content and volatile compounds like methane, CO_2, and water vapor are removed from the biomass. This helps in increasing the energy density of the resulting torrefied biomass.
(3) Enhanced fuel properties. Torrefied biomass exhibits improved fuel characteristics compared to raw biomass. It has reduced moisture content, higher energy density, improved grindability, increased hydrophobicity (water resistance), and enhanced stability [52]. These improved properties make torrefied biomass easier to handle, transport, and store.
(4) Reduced emissions and environmental impact. The torrefaction process reduces the emission of greenhouse gases, such as CO_2 and methane, compared to the combustion of raw biomass [53]. Additionally, torrefied biomass possesses lower emissions of volatile organic compounds and other pollutants during combustion.
(5) Utilization in various energy conversion systems. Torrefied biomass can be used in existing coal-fired power plants, co-fired with coal, or utilized in dedicated biomass power plants and heating systems. It can also be processed further through gasification to produce synthesis gas (syngas) required to generate biofuels or other chemicals.
(6) Storage and transportation advantages. Torrefied biomass has improved storage properties due to its hydrophobic nature, making it resistant to moisture absorption. It can be stored for more extended periods without degradation [54]. The higher energy density of torrefied biomass allows for more efficient transportation over longer distances with reduced shipping costs.
(7) Carbon neutralization and sustainability. Using torrefied biomass as a renewable energy source contributes to carbon neutralization since the carbon released during combustion is balanced by the carbon absorbed by the feedstock during growth [55]. Additionally, torrefaction technology can utilize agricultural residues and forestry waste, promoting sustainable resource utilization and reducing environmental impacts.

Song et al. [56] selected maple sawdust as the feedstock and explored the coalification effect of the torrefaction process. They figured out that the main reaction mechanisms are the decomposition of unstable oxygenated functional groups, the degradation of celluloses, and the condensation of aromatic carbons. Jiang et al. [57] investigated the pelleting performance of torrefied microalga *Nannochloropsis Oceanica* residues, and indicated that the activation energies of pellets range from 5.83 to 77.71 kJ/mol. Mei et al. [58] explored the effect of temperature oscillation on the biomass torrefaction process, and pointed out that such an operation inhibited the intensity of the subsequent pyrolysis reaction. Overall, torrefaction technology is a promising approach for converting biomass into a more efficient and convenient form of solid fuel, and can be applied in various energy conversion systems while reducing emissions and enhancing sustainability.

3.2. The Carbon Neutralization Potential of Microalgal Torrefaction

Microalgal torrefaction is a thermal processing technique that involves the heating of microalgal biomass in the absence of oxygen to produce a solid, carbon-rich biochar [59]. This biochar can be used as a renewable energy source or as a soil amendment. In terms of carbon neutralization potential, microalgal torrefaction can sequester and store CO_2 from the atmosphere [60]. During microalgae growth, they absorb CO_2 through photosynthesis, converting it into organic compounds. Torrefaction of microalgae results in the formation of biochar containing the captured carbon, which effectively prevents its release back into the atmosphere. Furthermore, using microalgal biochar as a soil amendment can improve soil fertility, enhance nutrient retention, and promote carbon sequestration in soils [17]. This can contribute to reducing greenhouse gas emissions by storing carbon in the soil for extended periods. Microalgal torrefaction has the potential to be a carbon-neutral process as it allows for the sequestration and storage of CO_2, preventing its release into the atmosphere, and promoting carbon capture in soils [61]. However, the exact carbon neutralization potential would depend on various factors, such as the specific microalgae species used, the torrefaction process parameters, and the end-use applications of the resulting biochar. The results of elemental analysis and HHVs of various microalgae are listed in Table 2, and the systematic diagram of microalgal torrefaction process is shown in Figure 2.

Table 2. The results of elemental analysis and higher heating values (HHVs) of microalgae.

Microalgae Species	Elemental Analysis (wt %)				HHV (MJ/kg)	Reference
	C	H	N	O		
S. obliquus CNW-N	37.37	5.80	6.82	50.02	16.10	[62]
C. sp. JSC4	41.49	6.83	3.34	48.34	19.27	[63]
C. sp. JSC4 residue	48.06	7.62	3.81	40.51	16.91	[64]
C. *sorrokiniana* CY1	45.07	7.64	3.88	35.52	20.40	[65]
Chlorella vulgaris ESP-31 residue	47.78	7.85	4.14	40.23	17.90	[66]
Chlorella vulgaris ESP-31	53.01	8.67	3.26	35.05	22.02	[67,68]
Nannochloropsis Oceanica	53.98	8.18	8.42	29.42	21.02	[17]
Chlorella sp.	51.06	7.64	9.90	31.40	22.01	[17]
Chlorella vulgaris	45.66	5.90	9.05	31.95	18.77	[69]
Arthrospira platensis	36.49	6.12	7.89	49.51	12.66	[70]
spirulina platensis	45.70	7.71	11.26	25.69	20.46	[71]

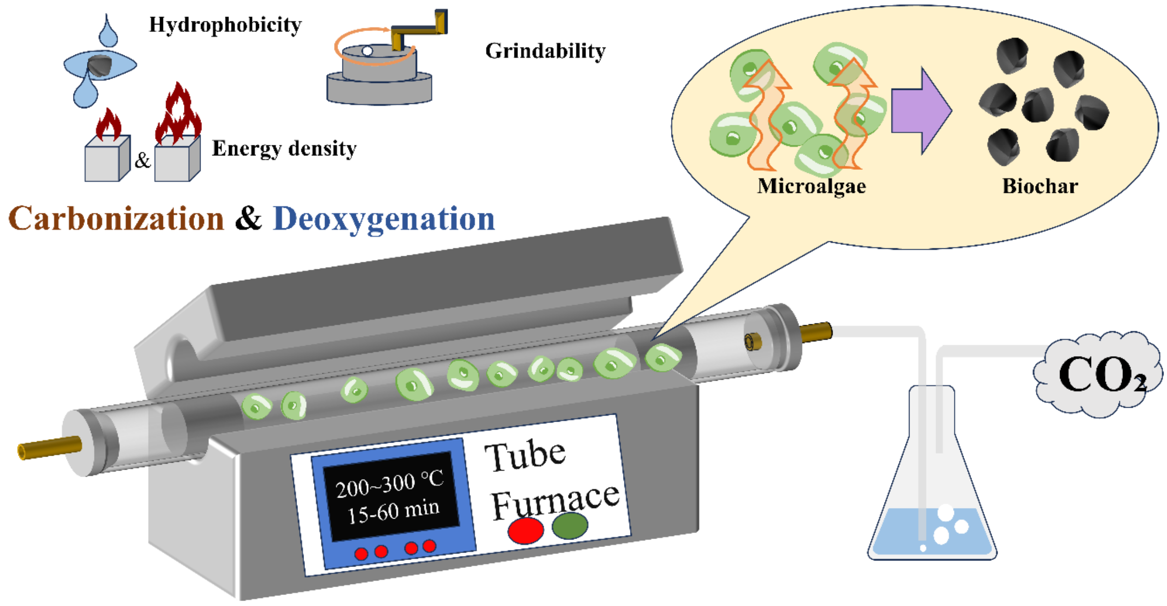

Figure 2. Systematic diagram of microalgal torrefaction process.

The carbon neutralization potential of microalgal torrefaction lies in its ability to sequester carbon and reduce greenhouse gas emissions [72]. The moisture and volatile components are removed from the microalgal torrefaction process, leaving behind a carbon-rich material. The torrefied microalgae can be used as a carbon sink by locking away carbon for an extended period. Furthermore, microalgal torrefaction produces a solid residue with a higher energy density than raw microalgae [73]. This torrefied microalgal biomass can be used as a renewable energy source, replacing fossil fuels and reducing CO_2 emissions from conventional energy production. In summary, microalgal torrefaction can contribute to carbon neutralization by sequestering carbon as torrefied microalgae and providing a renewable energy source that reduces greenhouse gas emissions [74]. However, further research are needed to optimize the process and assess its environmental and economic viability on a larger scale.

3.3. Practical Value and Development Prospect of Microalgal Carbon Neutral Biochar

Microalgal carbon neutral biochar, also known as microalgal biochar or microalgal-derived biochar, refers to the biochar produced from the torrefaction or pyrolysis of microalgae. It offers several practical values and has promising development prospects:

(1) Carbon sequestration. Microalgal carbon-neutral biochar acts as a long-term carbon sink by locking away carbon in a stable form. This helps to mitigate climate change by reducing greenhouse gas emissions [8].

(2) Soil improvement. Microalgal biochar improves soil fertility, water retention, and nutrient availability when applied to soils. It enhances soil structure, microbial activity, and nutrient cycling, improving crop growth and yield [75].
(3) Waste utilization. Microalgal carbon-neutral biochar can be produced from various types of microalgae, including those grown for wastewater treatment or CO_2 capture. This allows for converting waste biomass into a valuable product, contributing to waste management and resource recovery.
(4) Renewable energy production. The torrefaction or pyrolysis process to produce microalgal biochar generates biochar, bio-oil, and syngas [76]. These byproducts can be utilized as renewable energy sources, providing an alternative to fossil fuels and reducing greenhouse gas emissions.
(5) Sustainable agriculture. Applying microalgal biochar in agriculture can enhance soil health and reduce the need for chemical fertilizers. It promotes sustainable farming practices by minimizing nutrient leaching and improving soil resilience.
(6) Water quality improvement. Using microalgal carbon neutral biochar in water treatment systems can help remove pollutants, such as heavy metals and organic contaminants from wastewater [77]. This aids in water purification and contributes to environmental protection.

In terms of development prospects, microalgal carbon-neutral biochar holds significant potential. As research and technology advancements continue, there are opportunities to optimize production processes, develop innovative cultivation methods for microalgae, and explore the commercial viability of utilizing microalgal biochar in various industries [78,79]. However, additional research and pilot-scale studies are needed to fully understand its long-term effects, optimize production efficiency, and assess the economic viability of large-scale implementation. The profiles of application potential of microalgal carbon neutral biochar are shown in Figure 3.

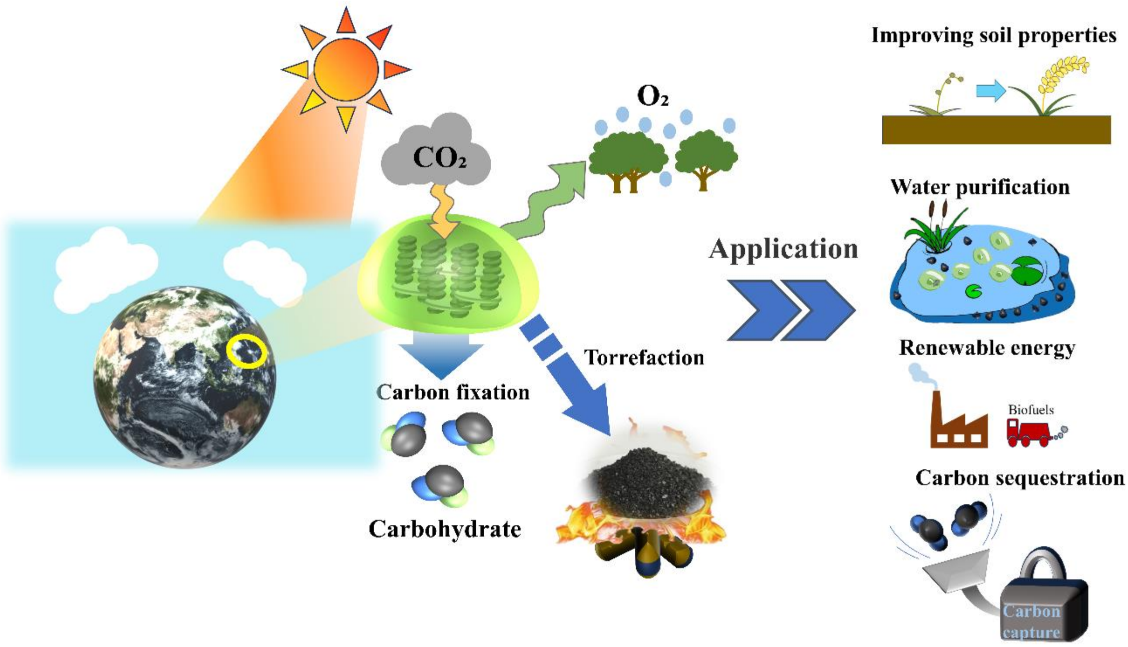

Figure 3. The profiles of application potential of microalgal carbon neutral biochar.

4. LCA for Environmental Impact Analysis of the Carbon Neutralization Process

4.1. A Brief Introduction of LCA in Microalgal Utilization

LCA is a methodology used to evaluate a product's or process's environmental impact throughout its entire life cycle, from raw material extraction to disposal. LCA provides a systematic and quantitative analysis of the environmental inputs and outputs associated with a particular system [3,80]. The application of LCA in microalgal utilization facilitates the assessment of the environmental performance of various microalgal-based products and processes. It considers factors such as resource consumption, energy use, emissions, and waste generation at each stage of the microalgal production and utilization chain [81].

LCA in microalgal utilization involves several key steps:

(1) Goal definition. Clearly defining the scope, objectives, and boundaries of the study. This includes specifying the purpose of the assessment, the functional unit being analyzed (e.g., per kilogram of microalgal biomass), and the system boundaries (e.g., from cultivation to end use) [82].
(2) Inventory analysis: Collecting data on the inputs (e.g., water, nutrients, energy) and outputs (e.g., biomass, CO_2 emissions) associated with each stage of the microalgal production and utilization process. This includes accounting for all relevant inputs and outputs, both direct and indirect [83].
(3) Impact assessment. Evaluating the environmental impacts of the system based on the inventory data. This involves categorizing the inventory data into impact categories such as greenhouse gas emissions, water consumption, land use, and toxicity. Different impact assessment methods can be used to quantify the impacts [84].
(4) Interpretation. Analyzing and interpreting the results to identify hotspots, areas of concern, and potential improvement opportunities. This step helps inform decision-making by considering the trade-offs and identifying strategies for reducing environmental impacts [85].

When evaluating the use of microalgae, LCA enables the comparison of various scenarios, technologies, and products to identify those with a lower environmental impact. It supports the development of sustainable microalgal-based applications, such as biofuels, feed additives, and wastewater treatment systems, by providing insights into the environmental implications throughout the life cycle [86,87]. The findings of LCA studies can guide researchers, policymakers, and industry stakeholders in making informed decisions to minimize the environmental footprint of microalgal utilization. The systematic diagram of microalgal carbon neutralization based on LCA is shown in Figure 4.

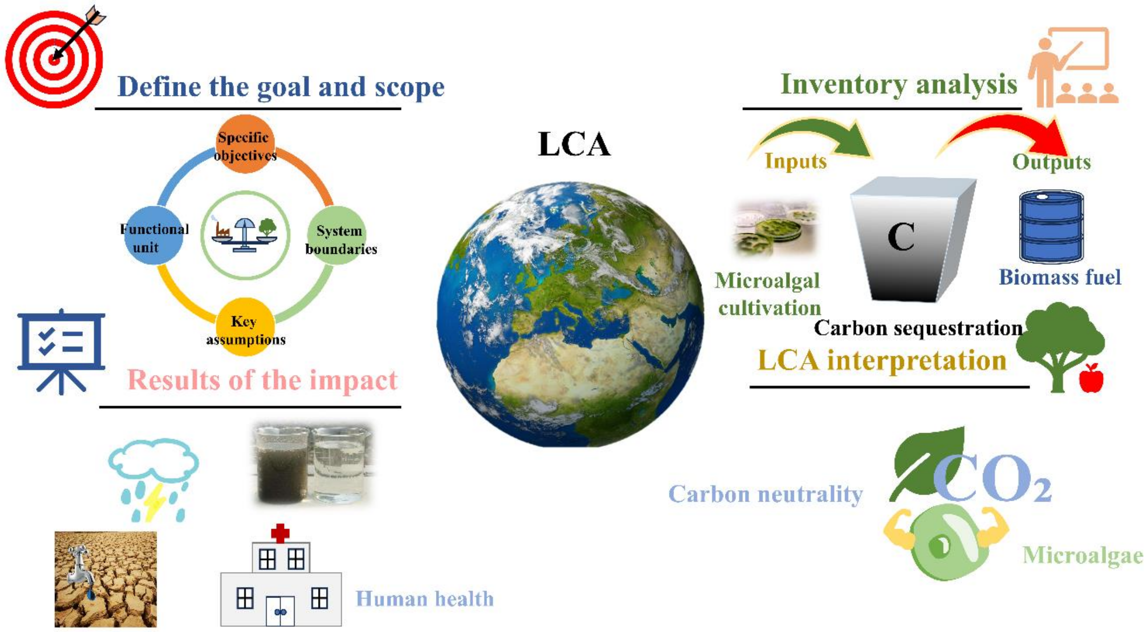

Figure 4. Systematic diagram of microalgal carbon neutralization based on LCA.

4.2. Environmental Impact Analysis of Microalgal Carbon Neutralization Process

The environmental impact analysis of the microalgal carbon neutralization process involves assessing the various environmental impacts associated with the production and use of microalgal carbon neutral products, such as biochar, biofuels, and other valuable byproducts [88]. The carbon footprint of the microalgal carbon neutralization process measures the total greenhouse gas emissions associated with the entire life cycle of the product. This includes emissions from cultivating microalgae, processing, transportation, and end-use applications [89]. The goal is to minimize or offset these emissions to achieve carbon neutralization. The energy consumption of the process is assessed to evaluate the efficiency and sustainability of microalgal carbon-neutral products [90]. It includes energy inputs required for cultivation, harvesting, processing, and conversion into desired products. The cultivation of microalgae requires land and water resources. Environmental analysis considers the potential impact on ecosystems, water availability, and land use change. Sustainable practices, such as using non-arable land or utilizing wastewater for cultivation, can mitigate these impacts [91,92].

Assessing the impact of microalgal cultivation on local biodiversity is crucial. Changes in land use, introduction of non-native species, and use of fertilizers or chemicals can potentially harm local ecosystems. Mitigation measures include the selection of native microalgal strains and minimizing chemicals use [93,94]. Proper management of waste generated during the process is essential to prevent pollution. This includes the responsible disposal or reuse of residual biomass, process byproducts, and wastewater. Recycling these materials can minimize environmental impacts. The process should be analyzed for potential water and air pollution. Nutrient-rich wastewater from microalgal cultivation can lead to eutrophication if not adequately managed [95]. Emissions from energy-intensive processes should also be controlled to avoid air pollution. Environmental impact assessment considers the economic and social aspects of the microalgal carbon neutralization process [96]. This includes assessing the feasibility of large-scale implementation, potential job creation, and overall benefits to local communities.

Life cycle assessment is commonly used to conduct a comprehensive environmental impact analysis. LCA evaluates the environmental impacts associated with each stage of the product's life cycle, from raw material extraction to end-of-life disposal [97]. This helps identify hotspots and prioritize improvements to minimize the overall environmental footprint of microalgal carbon-neutral products. Therefore, comprehensive environmental impact assessments and LCA for the microalgal carbon neutralization process should be conducted to ensure its sustainability and minimize any potential negative environmental effects [98]. These assessments provide valuable information for decision-making, process optimization, and the development of sustainable microalgal-based technologies.

4.3. Analysis of Microalgal Carbon Neutralization Based on LCA

The LCA assessment of microalgal carbon neutralization involves evaluation of the environmental impacts associated with the entire life cycle of microalgal-based carbon sequestration processes. Notably, LCA provides a systematic approach to quantifying and assessing the potential environmental burdens and benefits of a product or process, from raw material extraction to end-of-life disposal [99]. The first step in the LCA is to define the goal and scope of the study. This involves identifying the specific objectives, functional units, system boundaries, and critical assumptions for the assessment of microalgal carbon neutralization. For inventory analysis, data on inputs (e.g., water, nutrients, energy) and outputs (e.g., biomass, waste, emissions) throughout the life cycle of microalgal-based carbon sequestration are collected and quantified [100]. This includes data on microalgal cultivation, harvesting, processing, transportation, and utilization. The collected inventory data are evaluated for its potential environmental effects using impact assessment methods. These methods consider various impact categories such as climate change, acidification, eutrophication, resource depletion, and human health effects. They help to understand the overall environmental performance of the microalgal carbon neutralization process [101].

The results of the impact assessment are interpreted to identify significant environmental hotspots and evaluate the sustainability of the microalgal carbon neutralization process. Sensitivity analysis and uncertainty analysis may also be conducted to assess the robustness of the results and address data limitations and uncertainties [102]. The findings of the LCA analysis provide valuable insights into the environmental performance of the microalgal carbon neutralization process. This information can identify improvement opportunities and guide the development of more sustainable practices, technologies, and strategies. Applying LCA to the microalgal carbon neutralization process makes it possible to identify areas where environmental impacts are the most significant and explore ways to optimize resource efficiency, reduce emissions, and minimize environmental footprints [103]. Moreover, LCA can assist in making informed decisions and developing sustainable microalgal-based carbon sequestration systems. LCA provides a holistic and quantitative approach to assess the environmental performance of microalgal carbon neutralization processes [104]. By identifying areas for improvement, LCA can assist decision-formulators to make informed choices toward more sustainable and environmentally friendly microalgal-based technologies.

5. Challenges and Prospects

5.1. Technical Difficulties of Microalgal Carbon Fixation and Torrefaction Process

The technical difficulties of microalgal carbon fixation and torrefaction processes are mainly reflected in the following aspects:

(1) Microalgal cultivation. Cultivating microalgae at a large scale can be challenging. Factors such as optimal nutrient supply, light intensity, temperature control, and minimizing contamination need to be

carefully managed. Maintaining high growth rates and biomass productivity while ensuring microalgal biomass's desired composition and quality is essential.

(2) Harvesting and dewatering. Efficiently separating microalgae from the culture medium and concentrating the biomass poses technical challenges. Traditional methods, such as centrifugation or filtration, can be energy-intensive and costly. Developing cost-effective and scalable harvesting and dewatering technologies is crucial to minimize energy consumption and maximize biomass recovery.

(3) Biomass drying. After harvesting, the moisture content in the microalgal biomass needs to be reduced for further processing. Drying microalgae can be energy-intensive due to the high moisture content. Developing energy-efficient drying methods, such as low-temperature or solar drying techniques, can help reduce energy requirements and associated costs.

(4) Torrefaction process optimization. Torrefaction is a thermal conversion process that involves heating biomass in the absence of oxygen to convert it into a more energy-dense, stable, and hydrophobic solid. Optimizing the torrefaction conditions, such as temperature, residence time, and heating rate, to maximize energy efficiency, carbon retention, and biochar quality is a technical challenge. Achieving consistent and uniform torrefaction across the biomass is also essential.

(5) Process integration and scale-up. Integrating microalgal cultivation, carbon fixation, and torrefaction processes into a complete and efficient system is complex. Scaling up processes from the laboratory to commercially viable levels presents technical challenges in reactor design, heat transfer, logistics, and economic viability. Addressing these challenges requires continuous research, development, and pilot-scale testing.

(6) Biomass quality and composition. The composition of microalgal biomass can vary depending on factors such as species, cultivation conditions, and harvesting methods. Variations in lipid content, protein composition, and nutrient levels can impact the torrefaction process and biochar properties. Therefore, understanding and controlling biomass quality and composition is critical for consistent and high-quality biochar production.

These technical challenges can be addressed through interdisciplinary research, involving collaborations between researchers and industry experts. Through continuous innovation, such efforts will optimize microalgal carbon fixation and torrefaction processes for maximum efficiency, environmental performance, and economic viability.

5.2. Prospects

The LCA of microalgal torrefaction for carbon neutralization has several prospects contributing to its potential as a sustainable solution. Here are some of the key prospects:

(1) Carbon neutralization. Microalgal torrefaction involves the conversion of microalgal biomass into a biochar-like product through thermal treatment. This process may lead to carbon-neutral or even carbon-negative outcomes. LCA can reveal greenhouse gas emissions and carbon sequestration potential throughout the entire life cycle, demonstrating the effectiveness of microalgal torrefaction in carbon neutralization.

(2) Renewable energy generation. The torrefied microalgal biomass obtained from the process can be used as solid biofuel for energy production. LCA can assess the environmental impacts associated with the combustion or gasification of torrefied biomass, including greenhouse gas emissions, air pollutants, and resource depletion. It facilitates the identification of the potential benefits and drawbacks of utilizing torrefied microalgal biomass as a renewable energy source.

(3) Waste valorization. Microalgae cultivation for torrefaction requires a substantial amount of biomass feedstock. LCA enables the evaluation of the environmental implications associated with producing and managing microalgal biomass, such as land use, water consumption, and nutrient inputs. By identifying the potential environmental burdens, LCA can aid in developing strategies to optimize resource utilization and minimize waste generation.

(4) Comparative analysis. LCA allows for a comparative analysis of microalgal torrefaction with other carbon neutralization and renewable energy technologies. By assessing the environmental performance of different options, decision-makers can make informed choices based on sustainability criteria. LCA provides insights into the strengths and weaknesses of microalgal torrefaction, helping to position it within the broader context of carbon neutralization strategies.

(5) Optimization and improvement. LCA serves to identify environmental hotspots and improvement opportunities within the microalgal torrefaction process. It facilitates the identification of specific areas

for optimization, including energy consumption, resource utilization efficiency, and emissions reduction. By incorporating the findings from LCA, researchers and engineers can make informed decisions to enhance the overall sustainability of microalgal torrefaction.

In summary, the benefits of applying LCA for microalgal torrefaction lie in its ability to assess the carbon neutralization potential, evaluate environmental impacts, facilitate waste valorization, enable comparative analysis, and support the optimization and improvement of the process. This comprehensive assessment can guide decision-making, promote sustainable practices, and contribute to developing a carbon-neutral future.

6. Conclusions

The life cycle assessment of microalgal torrefaction for carbon neutralization highlights the immense potential of this technology in achieving sustainable and environmentally friendly carbon neutralization. The review encompasses a comprehensive analysis of the environmental impacts associated with microalgal torrefaction throughout its entire life cycle. The LCA approach allows for a holistic evaluation of microalgal torrefaction, considering factors such as greenhouse gas emissions, resource consumption, waste generation, and renewable energy production. By quantifying these environmental indicators, LCA provides valuable insights into the process's strengths, weaknesses, and opportunities for improvement. The prospects identified through this review demonstrate the significant role that microalgal torrefaction can play in carbon neutralization efforts. Not only does it have the potential to achieve carbon-neutral or even carbon-negative outcomes, but it also offers opportunities for renewable energy generation and waste valorization. These aspects contribute to both mitigating climate change and fostering a circular economy.

Furthermore, the comparative analysis enabled by LCA allows decision-makers to evaluate microalgal torrefaction alongside other carbon neutralization technologies, facilitating informed choices based on sustainability criteria. This data-driven approach supports the formulation and execution of effective strategies for achieving carbon neutrality. Overall, this review highlights the critical role of integrating LCA into the development and application of microalgal torrefaction to promote carbon neutrality. Harnessing the full potential of this technology and utilizing LCA as an analytical tool will provide a strategy for achieving a sustainable future characterized by reduced greenhouse gas emissions, efficient resource utilization, and a thriving circular economy.

Author Contributions: writing—reviewing and editing, C.Z.; visualization, investigation, Y.Z., X.W. and T.C.; data curation, writing—original draft preparation, J.F., K.H., J.M. and Y.W.

Funding: This work was supported by China Postdoctoral Science Foundation (2023MD744171) and high-level talent introduction project of Northeast Agricultural University.

Institutional Review Board Statement: Not applicable.

Informed Consent Statement: Not applicable.

Data Availability Statement: Not applicable.

Conflicts of Interest: The authors declare no conflict of interest.

References

1. Sathya, A.B.; Thirunavukkarasu, A.; Nithya, R.; et al. Microalgal biofuel production: Potential challenges and prospective research. *Fuel* **2023**, *332*, 126199.
2. Kong, F.; Torres, I.; Warakanont, J.; et al. Lipid catabolism in microalgae. *New Phytol.* **2018**, *218*, 1340–1348.
3. Wang, Y.; Yang, S.; Liu, J.; et al. Realization process of microalgal biorefinery: The optional approach toward carbon net-zero emission. *Sci. Total Environ.* **2023**, *901*, 165546.
4. Peter, A.P.; Khoo, K.S.; Chew, K.W.; et al. Microalgae for biofuels, wastewater treatment and environmental monitoring. *Environ. Chem. Lett.* **2021**, *19*, 2891–2904.
5. Yusoff, I.I.; Rohani, R.; Zaman, N.K.; et al. Comprehensive evaluation of the integrated membrane contactor-microalgae photobioreactor system for simultaneous H_2 purification and CO_2 treatment from biomass fermented gases. *J. Clean. Prod.* **2021**, *318*, 128608.
6. Fu, J.; Huang, Y.; Xia, A.; et al. How the sulfur dioxide in the flue gas influence microalgal carbon dioxide fixation: From gas dissolution to cells growth. *Renew. Energy* **2022**, *198*, 114–122.
7. Tamburic, B.; Evenhuis, C.R.; Crosswell, J.R.; et al. An empirical process model to predict microalgal carbon fixation

rates in photobioreactors. *Algal Res.* **2018**, *31*, 334–346.
8. Zhao, B.; Su, Y. Process effect of microalgal-carbon dioxide fixation and biomass production: A review. *Renew. Sustain. Energy Rev.* **2014**, *31*, 121–132.
9. de Pablo, J.G.; Lindley, M.; Hiramatsu, K.; et al. Label-free live microalgal starch screening via Raman flow cytometry. *Algal Res.* **2023**, *70*, 102993.
10. Feng, L.; Wang, Z.; Jia, D.; et al. Functional metabolism pathways of significantly regulated genes in Nannochloropsis oceanica with various nitrogen/phosphorus nutrients for CO2 fixation. *Sci. Total Environ.* **2023**, *883*, 163318.
11. Yong, Y.G.; Ong, H.C.; Show, P.L.; et al. Torrefaction of microalgal biochar as potential coal fuel and application as bio-adsorbent. *Energy Convers. Manag.* **2018**, *165*, 152–162.
12. Zhang, C.; Ho, S.-H.; Chen, W.-H.; et al. Oxidative torrefaction performance of microalga Nannochloropsis Oceanica towards an upgraded microalgal solid biofuel. *J. Biotechnol.* **2021**, *338*, 81–90.
13. Zhang, C.; Li, F.; Ho, S.-H.; et al. Oxidative torrefaction of microalga Nannochloropsis Oceanica activated by potassium carbonate for solid biofuel production. *Environ. Res.* **2022**, *212*, 113389.
14. Ubando, A.T.; Rivera, D.R.T.; Chen, W.-H.; et al. A comprehensive review of life cycle assessment (LCA) of microalgal and lignocellulosic bioenergy products from thermochemical processes. *Bioresour. Technol.* **2019**, *291*, 121837.
15. Lin, J.-Y.; Xue, C.; Tan, S.-I.; et al. Pyridoxal kinase PdxY mediated carbon dioxide assimilation to enhance the biomass in Chlamydomonas reinhardtii CC-400. *Bioresour. Technol.* **2021**, *322*, 124530.
16. Lababpour, A. A dynamic model for the prediction of flue gas carbon dioxide removal by the microalga Chlorella vulgaris in column photobioreactor. *Alex. Eng. J.* **2018**, *57*, 3311–3320.
17. Zhang, C.; Wang, C.; Cao, G.; et al. Comparison and characterization of property variation of microalgal biomass with non-oxidative and oxidative torrefaction. *Fuel* **2019**, *246*, 375–385.
18. Lu, Y.; Mu, D.; Xue, Z.; et al. Life cycle assessment of industrial production of microalgal oil from heterotrophic fermentation. *Algal Res.* **2021**, *58*, 102404.
19. Sun, J.; Yang, L.; Xiao, S.; et al. A promising microalgal wastewater cyclic cultivation technology: Dynamic simulations, economic viability, and environmental suitability. *Water Res.* **2022**, *217*, 118411.
20. Ma, J.; Yang, L.; Wang, D.; et al. Digitalization in response to carbon neutrality: Mechanisms, effects and prospects. *Renew. Sustain. Energy Rev.* **2024**, *191*, 114138.
21. Yang, Y.; Tong, L.; Yin, S.; et al. Status and challenges of applications and industry chain technologies of hydrogen in the context of carbon neutrality. *J. Clean. Prod.* **2022**, *376*, 134347.
22. Gao, H.; Liu, Q.; Yan, C.; et al. Mitigation of greenhouse gas emissions and improved yield by plastic mulching in rice production. *Sci. Total Environ.* **2023**, *880*, 162984.
23. Dubey, A.; Arora, A. Advancements in carbon capture technologies: A review. *J. Clean. Prod.* **2022**, *373*, 133932.
24. Zeng, J.; Yang, M. Digital technology and carbon emissions: Evidence from China. *J. Clean. Prod.* **2023**, *430*, 139765.
25. Liu, Y.; Weng, Z.; Han, B.; et al. Recent studies on the comprehensive application of biochar in multiple environmental fields. *J. Clean. Prod.* **2023**, *421*, 138495.
26. Goveas, L.C.; Nayak, S.; Vinayagam, R.; et al. Microalgal remediation and valorisation of polluted wastewaters for zero-carbon circular bioeconomy. *Bioresour. Technol.* **2022**, *365*, 128169.
27. Ruiz-Ruiz, P.; Gómez-Borraz, T.L.; Saldivar, A.; et al. Diluted methane mitigation by a co-culture of alkaliphilic methanotrophs and the microalgae Scenedesmus obtusiusculus towards carbon neutrality. *Biochem. Eng. J.* **2024**, *203*, 109211.
28. Zhang, J.-T.; Wang, J.-X.; Liu, Y.; et al. Microalgal-bacterial biofilms for wastewater treatment: Operations, performances, mechanisms, and uncertainties. *Sci. Total Environ.* **2024**, *907*, 167974.
29. da Rosa, G.M.; de Morais, M.G.; Costa, J.A.V. Green alga cultivation with monoethanolamine: Evaluation of CO_2 fixation and macromolecule production. *Bioresour. Technol.* **2018**, *261*, 206–212.
30. Kuo, C.-M.; Jian, J.-F.; Sun, Y.-L.; et al. An efficient Photobioreactors/Raceway circulating system combined with

alkaline-CO_2 capturing medium for microalgal cultivation. *Bioresour. Technol.* **2018**, *266*, 398–406.

31. Ketheesan, B.; Nirmalakhandan, N. Feasibility of microalgal cultivation in a pilot-scale airlift-driven raceway reactor. *Bioresour. Technol.* **2012**, *108*, 196–202.
32. Cheng, J.; Guo, W.; Ameer Ali, K.; et al. Promoting helix pitch and trichome length to improve biomass harvesting efficiency and carbon dioxide fixation rate by Spirulina sp. in 660 m^2 raceway ponds under purified carbon dioxide from a coal chemical flue gas. *Bioresour. Technol.* **2018**, *261*, 76–85.
33. Basu, S.; Sarma Roy, A.; Ghoshal, A.K.; et al. Operational strategies for maximizing CO_2 utilization efficiency by the novel microalga Scenedesmus obliquus SA1 cultivated in lab scale photobioreactor. *Algal Res.* **2015**, *12*, 249–257.
34. Duarte, J.H.; Fanka, L.S.; Costa, J.A.V. Utilization of simulated flue gas containing CO_2, SO_2, NO and ash for Chlorella fusca cultivation. *Bioresour. Technol.* **2016**, *214*, 159–165.
35. Lam, M.K.; Lee, K.T. Effect of carbon source towards the growth of Chlorella vulgaris for CO_2 bio-mitigation and biodiesel production. *Int. J. Greenh. Gas Control* **2013**, *14*, 169–176.
36. da Rosa, G.M.; Moraes, L.; Cardias, B.B.; et al. Chemical absorption and CO2 biofixation via the cultivation of Spirulina in semicontinuous mode with nutrient recycle. *Bioresour. Technol.* **2015**, *192*, 321–327.
37. Kargupta, W.; Ganesh, A.; Mukherji, S. Estimation of carbon dioxide sequestration potential of microalgae grown in a batch photobioreactor. *Bioresour. Technol.* **2015**, *180*, 370–375.
38. Kumar, A.; Yuan, X.; Sahu, A. K.; et al. A hollow fiber membrane photo-bioreactor for CO_2 sequestration from combustion gas coupled with wastewater treatment: A process engineering approach. *J. Chem. Technol. Biotechnol.* **2010**, *85*, 387–394.
39. Arroyo, C.A.; Contreras, J.L.; Zeifert, B.; et al. CO_2 Capture of the Gas Emission, Using a Catalytic Converter and Airlift Bioreactors with the Microalga Scenedesmus dimorphus. *Appl. Sci.* **2019**, *9*, 3212.
40. Zhao, X.; Zhang, T.; Dang, B.; et al. Microalgae-based constructed wetland system enhances nitrogen removal and reduce carbon emissions: Performance and mechanisms. *Sci. Total Environ.* **2023**, *877*, 162883.
41. Li, P.; Wang, D.; Hu, Z.; et al. Insight into the potential mechanism of bicarbonate assimilation promoted by mixotrophic in CO_2 absorption and microalgae conversion system. *Chemosphere* **2024**, *349*, 140903.
42. Burlacot, A.; Peltier, G. Energy crosstalk between photosynthesis and the algal CO_2-concentrating mechanisms. *Trends Plant Sci.* **2023**, *28*, 795–807.
43. Yan, Z.; Shen, T.; Li, W.; et al. Contribution of microalgae to carbon sequestration in a natural karst wetland aquatic ecosystem: An in-situ mesocosm study. *Sci. Total Environ.* **2021**, *768*, 144387.
44. Li, P.; Luo, Y.; Yuan, X. Life cycle and techno-economic assessment of source-separated wastewater-integrated microalgae biofuel production plant: A nutrient organization approach. *Bioresour. Technol.* **2022**, *344*, 126230.
45. Lucas, B.F.; Brunner, T.A. Attitudes and perceptions towards microalgae as an alternative food: A consumer segmentation in Switzerland. *Algal Res.* **2024**, *78*, 103386.
46. Chen, S.; Li, X.; Ma, X.; et al. Lighting the way to sustainable development: Physiological response and light control strategy in microalgae-based wastewater treatment under illumination. *Sci. Total Environ.* **2023**, *903*, 166298.
47. Oliva, G.; Galang, M.G.; Buonerba, A.; et al. Carbon capture and utilization in waste to energy approach by leading-edge algal photo-bioreactors: The influence of the illumination wavelength. *Case Stud. Chem. Environ. Eng.* **2023**, *7*, 100348.
48. Zhang, C.; Ho, S.-H.; Chen, W.-H.; et al. Torrefaction performance and energy usage of biomass wastes and their correlations with torrefaction severity index. *Appl. Energy* **2018**, *220*, 598–604.
49. Chen, W.H.; Lin, B.J.; Lin, Y.Y.; et al. Progress in biomass torrefaction: Principles, applications and challenges. *Prog. Energy Combust. Sci.* **2021**, *82*, 100887.
50. Zhang, C.; Zhan, Y.; Chen, W.-H.; et al. Correlations between different fuel property indicators and carbonization degree of oxidatively torrefied microalgal biomass. *Energy* **2024**, *286*, 129693.
51. Chen, W.-H.; Aniza, R.; Arpia, A.A.; et al. A comparative analysis of biomass torrefaction severity index prediction from

machine learning. *Appl. Energy* **2022**, *324*, 119689.

52. Zhang, C.; Chen, W.-H.; Ho, S.-H.; et al. Comparative advantages analysis of oxidative torrefaction for solid biofuel production and property upgrading. *Bioresour. Technol.* **2023**, *386*, 129531.
53. Zhang, C.; Yang, W.; Chen, W.-H.; et al. Effect of torrefaction on the structure and reactivity of rice straw as well as life cycle assessment of torrefaction process. *Energy* **2021**, *240*, 122470.
54. Chen, W.H.; Lin, B.J.; Colin, B.; et al. Hygroscopic transformation of woody biomass torrefaction for carbon storage. *Appl. Energy* **2018**, *231*, 768–776.
55. Zhang, C.; Chen, W.-H.; Zhang, Y.; et al. Influence of microorganisms on the variation of raw and oxidatively torrefied microalgal biomass properties. *Energy* **2023**, *276*, 127612.
56. Song, Y.; Chen, Z.; Li, Y.; et al. Regulation of energy properties and thermal behavior of bio-coal from lignocellulosic biomass using torrefaction. *Energy* **2024**, *289*, 129949.
57. Jiang, Y.; Zhou, G.; Zhang, H.; et al. Coupling effects of heating pelleting and torrefaction on black pellets production from microalga Nannochloropsis Oceanica residues. *Fuel* **2023**, *353*, 129007.
58. Mei, Y.; Chen, Y.; Zhang, S.; et al. Effect of temperature oscillation on torrefaction and pyrolysis of elm branches. *Energy* **2023**, *271*, 127055.
59. Ho, S.-H.; Zhang, C.; Tao, F.; et al. Microalgal Torrefaction for Solid Biofuel Production. *Trends Biotechnol.* **2020**, *38*, 1023–1033.
60. Zhang, C.; Wang, M.; Chen, W.-H.; et al. A comparison of conventional and oxidative torrefaction of microalga Nannochloropsis Oceanica through energy efficiency analysis and life cycle assessment. *J. Clean. Prod.* **2022**, *369*, 133236.
61. Bates, R.B.; Ghoniem, A.F. Biomass torrefaction: Modeling of volatile and solid product evolution kinetics. *Bioresour. Technol.* **2012**, *124*, 460–469.
62. Chen, W.H.; Wu, Z.Y.; Chang, J.S. Isothermal and non-isothermal torrefaction characteristics and kinetics of microalga Scenedesmus obliquus CNW-N. *Bioresour. Technol.* **2014**, *155*, 245–251.
63. Chen, Y.C.; Chen, W.H.; Lin, B.J.; et al. Impact of torrefaction on the composition, structure and reactivity of a microalga residue. *Appl. Energy* **2016**, *181*, 110–119.
64. Chen, W.H.; Huang, M.Y.; Chang, J.S.; et al. An energy analysis of torrefaction for upgrading microalga residue as a solid fuel. *Bioresour. Technolgy* **2015**, *185*, 285–293.
65. Chen, W.H.; Huang, M.Y.; Chang, J.S.; et al. Thermal decomposition dynamics and severity of microalgae residues in torrefaction. *Bioresour. Technol.* **2014**, *169*, 258–264.
66. Chen, W.H.; Huang, M.Y.; Chang, J.S.; et al. Torrefaction operation and optimization of microalga residue for energy densification and utilization. *Appl. Energy* **2015**, *154*, 622–630.
67. Bach, Q.V.; Chen, W.H.; Lin, S.C.; et al. Wet torrefaction of microalga Chlorella vulgaris ESP-31 with microwave-assisted heating. *Energy Convers. Manag.* **2016**, *141*, 163–170.
68. Bach, Q.V.; Chen, W.H.; Sheen, H.K.; et al. Gasification kinetics of raw and wet-torrefied microalgae Chlorella vulgaris ESP-31 in carbon dioxide. *Bioresour. Technol.* **2017**, *244*, 1393–1399.
69. Phusunti, N.; Phetwarotai, W.; Tekasakul, S. Effects of torrefaction on physical properties, chemical composition and reactivity of microalgae. *Korean J. Chem. Eng.* **2017**, *35*, 503–510.
70. Ho, S.-H.; Zhang, C.; Chen, W.-H.; et al. Characterization of biomass waste torrefaction under conventional and microwave heating. *Bioresour. Technol.* **2018**, *264*, 7–16.
71. Wu, K.T.; Tsai, C.J.; Chen, C.S.; et al. The characteristics of torrefied microalgae. *Appl. Energy* **2012**, *100*, 52–57.
72. Moreira, D.; Pires, J.C.M. Atmospheric CO2 capture by algae: Negative carbon dioxide emission path. *Bioresour. Technol.* **2016**, *215*, 371–379.
73. Raheem, A.; Prinsen, P.; Vuppaladadiyam, A.K.; et al. A review on sustainable microalgae based biofuel and bioenergy production: Recent developments. *J. Clean. Prod.* **2018**, *181*, 42–59.

74. Song, W.; He, Y.; Huang, R.; et al. Life cycle assessment of deep-eutectic-solvent-assisted hydrothermal disintegration of microalgae for biodiesel and biogas co-production. *Appl. Energy* **2023**, *335*, 120758.
75. Wu, G.; Tham, P.E.; Chew, K.W.; et al. Net zero emission in circular bioeconomy from microalgae biochar production: A renewed possibility. *Bioresour. Technol.* **2023**, *388*, 129748.
76. Yu, K.L.; Chen, W.-H.; Sheen, H.-K.; et al. Production of microalgal biochar and reducing sugar using wet torrefaction with microwave-assisted heating and acid hydrolysis pretreatment. *Renew. Energy* **2020**, *156*, 349–360.
77. Yu, K.L.; Show, P.L.; Ong, H.C.; et al. Microalgae from wastewater treatment to biochar—Feedstock preparation and conversion technologies. *Energy Convers. Manag.* **2017**, *150*, 1–13.
78. Sadvakasova, A.K.; Kossalbayev, B.D.; Bauenova, M.O.; et al. Microalgae as a key tool in achieving carbon neutrality for bioproduct production. *Algal Res.* **2023**, *72*, 103096.
79. Min Woon, J.; Shiong Khoo, K.; Akermi, M.; et al. Reviewing biohydrogen production from microalgal cells through fundamental mechanisms, enzymes and factors that engendering new challenges and prospects. *Fuel* **2023**, *346*, 128312.
80. Zhang, C.; Chen, W.-H.; Ho, S.-H. Economic feasibility analysis and environmental impact assessment for the comparison of conventional and microwave torrefaction of spent coffee grounds. *Biomass Bioenergy* **2023**, *168*, 106652.
81. Bhar, R.; Tiwari, B.R.; Sarmah, A.K.; et al. A comparative life cycle assessment of different pyrolysis-pretreatment pathways of wood biomass for levoglucosan production. *Bioresour. Technol.* **2022**, *356*, 127305.
82. Zhu, X.; Labianca, C.; He, M.; et al. Life-cycle assessment of pyrolysis processes for sustainable production of biochar from agro-residues. *Bioresour. Technol.* **2022**, *360*, 127601.
83. Zhou, H.; Zhang, W.; Li, L.; et al. Environmental impact and optimization of lake dredged-sludge treatment and disposal technologies based on life cycle assessment (LCA) analysis. *Sci. Total Environ.* **2021**, *787*, 147703.
84. Lee, J.G.; Chae, H.G.; Cho, S.R.; et al. Impact of plastic film mulching on global warming in entire chemical and organic cropping systems: Life cycle assessment. *J. Clean. Prod.* **2021**, *308*, 127256.
85. Puig-Samper Naranjo, G.; Bolonio, D.; Ortega, M.F.; et al. Comparative life cycle assessment of conventional, electric and hybrid passenger vehicles in Spain. *J. Clean. Prod.* **2021**, *291*, 125883.
86. Cvetković, S.M.; Radoičić, T.K.; Kijevčanin, M.; et al. Life Cycle Energy Assessment of biohydrogen production via biogas steam reforming: Case study of biogas plant on a farm in Serbia. *Int. J. Hydrog. Energy* **2021**, *46*, 14130–14137.
87. Hosseinzadeh-Bandbafha, H.; Rafiee, S.; Mohammadi, P.; et al. Exergetic, economic, and environmental life cycle assessment analyses of a heavy-duty tractor diesel engine fueled with diesel–biodiesel-bioethanol blends. *Energy Convers. Manag.* **2021**, *241*, 114300.
88. Li, R.; Zhang, C.; Chen, W.-H.; et al. Multistage utilization of soybean straw-derived P-doped biochar for aquatic pollutant removal and biofuel usage. *Bioresour. Technol.* **2023**, *387*, 129657.
89. Liu, G.; Zhang, X.; Liu, H.; et al. Biochar/layered double hydroxides composites as catalysts for treatment of organic wastewater by advanced oxidation processes: A review. *Environ. Res.* **2023**, *234*, 116534.
90. Quiroz, D.; Greene, J.M.; Quinn, J.C. Regionalized Life-Cycle Water Impacts of Microalgal-Based Biofuels in the United States. *Environ. Sci. Technol.* **2022**, *56*, 16400–16409.
91. Cao, B.; Zhang, T.; Zhang, W.; et al. Enhanced technology based for sewage sludge deep dewatering: A critical review. *Water Res.* **2021**, *189*, 116650.
92. Zhang, J.; Zhang, X.; Yang, M.; et al. Transforming lignocellulosic biomass into biofuels enabled by ionic liquid pretreatment. *Bioresour. Technol.* **2021**, *322*, 124522.
93. Thengane, S.K.; Burek, J.; Kung, K.S.; et al. Life cycle assessment of rice husk torrefaction and prospects for decentralized facilities at rice mills. *J. Clean. Prod.* **2020**, *275*, 123177.
94. Huang, X.; Bai, S.; Liu, Z.; et al. Fermentation of pigment-extracted microalgal residue using yeast cell-surface display: Direct high-density ethanol production with competitive life cycle impacts. *Green Chem.* **2020**, *22*, 153–162.
95. Wang, X.; Liu, F.; Li, Y.; et al. Development of a facile and bi-functional superhydrophobic suspension and its applications in superhydrophobic coatings and aerogels in high-efficiency oil–water separation. *Green Chem.* **2020**, *22*,

7424–7434.

96. Zhang, L.-J.; Qian, L.; Ding, L.-Y.; et al. Ecological and toxicological assessments of anthropogenic contaminants based on environmental metabolomics. *Environ. Sci. Ecotechnology* **2021**, *5*, 100081.
97. Aresti, L.; Christodoulides, P.; Florides, G.A. An investigation on the environmental impact of various Ground Heat Exchangers configurations. *Renew. Energy* **2021**, *171*, 592–605.
98. Choi, H.I.; Lee, J.S.; Choi, J.W.; et al. Performance and potential appraisal of various microalgae as direct combustion fuel. *Bioresour. Technol.* **2019**, *273*, 341–349.
99. Sun, P.; Liu, C.; Li, A.; et al. Using carbon dioxide-added microalgal-bacterial granular sludge for carbon-neutral municipal wastewater treatment under outdoor conditions: Performance, granule characteristics and environmental sustainability. *Sci. Total Environ.* **2022**, *848*, 157657.
100. Valente, A.; Iribarren, D.; Dufour, J. How do methodological choices affect the carbon footprint of microalgal biodiesel? A harmonised life cycle assessment. *J. Clean. Prod.* **2019**, *207*, 560–568.
101. Zaimes, G.G.; Khanna, V. Integrating the Role of Thermodynamics in LCA: A Case Study of Microalgal Biofuels. In *Encyclopedia of Sustainable Technologies*, Abraham, M.A., Ed.; Elsevier: Oxford, 2017; pp. 397–406.
102. Liang, D.; Wu, J.; Lu, L.; et al. Coupling with in-situ electrochemical reactive chlorine species generation and two-phase partitioning method for enhanced microalgal biodiesel production. *Bioresour. Technol.* **2022**, *364*, 128100.
103. Czyrnek-Delêtre, M.M.; Rocca, S.; Agostini, A.; et al. Life cycle assessment of seaweed biomethane, generated from seaweed sourced from integrated multi-trophic aquaculture in temperate oceanic climates. *Appl. Energy* **2017**, *196*, 34–50.
104. Wang, S.; Lu, W.; Esakkimuthu, S.; et al. Life cycle assessment of carbon-based adsorbent preparation from algal biomass. *J. Clean. Prod.* **2023**, *427*, 139269.

Green Energy and Fuel Research

Article

Heating Performance and Energy Efficiency Analysis of Air-Source Heat Pumps in Public Buildings Across Different Climate Zonings

Junbao Fan [1], Yilin Liu [1,]*, Jing Ma [2], Ying Cao [1,2], Zhibin Zhang [1], Xin Cui [1] and Liwen Jin [1,]*

[1] School of Human Settlements and Civil Engineering, Xi'an Jiaotong University, No. 28 Xianning West Road, Xi'an 710049, China

[2] China Architecture Design and Research Group, Beijing 100044, China

* Correspondence: ylliu@xjtu.edu.cn (Y.L.); lwjin@xjtu.edu.cn (L.J.)

Received: 11 July 2024; Revised: 3 September 2024; Accepted: 5 September 2024; Published: 20 September 2024

Abstract: Public buildings exhibit the highest operational energy consumption and contribute the most to carbon emissions compared to other types of building. The electrification of energy terminals in public buildings is crucial for the energy conservation and emission reduction, especially the energy-saving retrofitting of heating systems. Given the significant impact of climate on the performance of air-source heat pumps, this study explored the performance and energy efficiency of air-source heat pump systems in public buildings across different climate zonings. Using Design Builder software, the physical models of three types of public buildings (commercial, hotel, and office) were constructed, and the annual variations in the building load was analyzed. Considering the effects of defrosting and low-temperature conditions, an air-source heat pump heating system models were developed using TRNSYS software. The simulation results showed that the average COP of the heat pump system on the coldest day in Harbin, Beijing, and Shanghai were 1.7, 2.46 and 2.49, respectively. Moreover, the analysis factor correlation analysis reveals that the COP of the heat pump system is positively correlated with the dry-bulb temperature, negatively correlated with the building load. Surprisingly, the COP is not affected by the types of public buildings. The findings of this study are expected to provide valuable guidance for the application and regulation of air-source heat pumps in the public buildings.

Keywords: air-source heat pump; public building; heating; coefficient of performance; correlation analysis

1. Introduction

As of 2021, public buildings had the highest operational energy consumption intensity among all building types. Although the total area of public buildings is only 14.7 billion square meters, much smaller than that of urban and rural residential buildings, public buildings account for the largest proportion of total operational energy consumption in China, approximately 34.7%, amounting to 386 million tons of standard coal equivalent. Correspondingly, the carbon emissions from the operation of public buildings also constitute the highest proportion of total building operational carbon emissions, approximately 32.7%, reaching 720 million tons of CO_2 [1]. Accelerating the adjustment of the energy structure, increasing the proportion of clean energy, promoting electrification, and reducing the dependence on fossil fuels are effective ways to achieve the "dual carbon" goals [2]. The electrification of building energy terminals is a key measure to reach these goals, especially in enhancing the electrification level of the heating in public buildings.

In recent years, air-source heat pumps, as an efficient and energy-saving clean heating technology, have effectively utilized low-grade energy from the ambient air, thereby conserving the higher-grade energy sources [3–6]. They are currently widely used in regions with hot-summers and cold-winters in China, such as the Yangtze River Basin and its southern areas [7]. In the northeastern and northwestern regions, the growth and potential for air-source heat pumps are substantial due to coal policy restrictions and increasing coal prices [8]. Researchers have conducted extensive studies on the factors affecting the performance of air-source heat pumps and their application strategies [9,10].

The air-source heat pump is prone to frosting at low ambient temperatures, which can significantly impair its operating performance. Integrating the air-source heat pump with other energy systems or optimizing the circulating system can effectively enhance system performance. Xu et al. [11] investigated the impact of climate conditions on the frost formation in air-source heat pumps and proposed a characterization parameter, namely the hours of the frost formation. By analyzing the hours of the frost formation under various characteristic temperature differences and combining the frost characteristics of different types of air-source heat pumps, the climate division for China was conducted to provide a reference for the climate-adaptive design and defrost control strategies for air-source heat pumps. Wu et al. [12] experimentally tested the long-term performance of an air-source heat pump system under cold climate conditions. The experimental data showed that the system coefficient of performance (COP) is highly correlated with the outdoor temperature. When the supply water temperature increased by approximately 6 °C and the outdoor temperature was around −5 °C, the corresponding COP decreased by 14.2%. Additionally, the relative humidity had a minimal impact on the system COP. Wu et al. [13] constructed a heating system combining an air-source heat pump with a water storage tank and conducted a long-term performance monitoring in an actual building in Beijing. The coupled system allowed the air-source heat pump to operate continuously at higher ambient temperatures. The results revealed that, compared to the continuous operation, the daily average COP of the air-source heat pump increased by 14.0% and the SCOP increased by 26.1% on the coldest days. Long et al. [14] proposed a hybrid combined heating system integrating the solar hot water with an air-source heat pump, and analyzed its energy efficiency during the cold season. The results indicated that the solar radiation intensity and the ambient temperature were the crucial factors affecting the energy efficiency of various connection methods within the combined system. Changes in the return water temperature had the greatest impact on the series configuration and the least impact on the parallel configuration. By switching the connection method between solar heat water (SHW) and air-source heat pump (ASHP) based on outdoor weather conditions, the HSAHP combined with the heating system can achieve significant energy-saving benefits.

In general, the research on the air-source heat pump mainly focuses on its design optimization, environmental applications, and integration with other heating methods, primarily in residential buildings [15–20]. There is a lack of research concerning its use in the heating system of public buildings. The application of ASHP in public buildings significantly differs from the residential settings in terms of building load magnitude, hourly load variation, and system operation times. Additionally, the ASHP is commonly used as single units in residential buildings, whereas large public buildings typically require simultaneous use of multiple units. Moreover, importantly, in low-temperature environments, the performance of ASHP may decline significantly due to frost formation. Furthermore, the performance of air-source heat pump systems exhibits significant variations under different building types and climate zonings. Therefore, it is imperative to explore the suitability and actual performance trends of ASHPs in different public building types across different climate zonings in China.

In this study, to explore the effects of building types and climate zonings on the performance of air-source heat pumps, the representative cities (Harbin, Beijing, and Shanghai) were selected for severe cold, cold, and hot-summer and cold-winter regions, respectively. The physical models of three typical types of public buildings (commercial, hotel, and office) were constructed using Design Builder software to analyze the annual variations in the building load. Considering the effects of defrosting and low-temperature conditions, the air-source heat pump heating system models were developed using TRNSYS software. By utilizing annual hourly load data from three types of public buildings in the three representative cities, the operational characteristics and performance influencing factors of air-source heat pump systems on the typical days (hottest day, moderate-temperature day, and coldest day) were simulated and analyzed. The findings of this study are expected to provide effective guidance for the application and control strategies of air-source heat pump systems in public buildings.

2. Model Development of Air Source Heat Pump System

2.1. Selection of Typical Cities

There is a vast territory with significant climate differences across various regions in China, which can be classified into five climate zones: severe cold, cold, hot-summer and cold-winter, hot summer and warm winter, and mild regions. The air-source heat pump is primarily used for the heating in low-temperature areas, with the heating performance greatly influenced by outdoor climate parameters. Therefore, this study focuses on the severe cold, cold, and hot-summer and cold-winter zones. The climatic features of severely cold regions are predominantly characterized by extremely cold and prolonged winters, significant annual and daily temperature variations, with the temperature in winter frequently dropping below −10 ° C.In cold regions, the climate is characterized by cold and dry winters, accompanied by large annual and daily temperature differences. The temperature in winter typically ranges from −10 ° Cto 0 ° C,with a considerable number of days where the daily average temperature is lower than 5 ° C.On the other hand, the climatic features of hot-summer and cold-winter regions are more intricate, featuring sultry and humid summers and chilly and dry winters. The temperature in summer often exceeds 30 °C, while the temperature in winter may dip to around 0 °C. The comprehensive investigation identifies the representative cities for these three climate zones as Harbin, Beijing, and Shanghai, respectively. The heating durations for these three cities are shown in Table 1.

Given the diverse types of public buildings, this study selects three typical categories as the research subjects: commercial, hotel, and office buildings. Referring to the actual building information provided by China Architecture Design and Research Group, the physical model of typical public buildings: commercial, hotels, and office buildings were built based on the Design Builder software, as shown in Figure 1. The office building has a floor-to-ceiling height of 7 stories, a total building height of 30.6 m, and a total floor area of 9280 square meters. The primary room functions include office spaces and meeting rooms. The hotel building comprises a 3-story low-rise section and a 15-story high-rise section, with a total building height of 52.5 m and a total floor area of 34,000 square meters. The main room functions encompass dining, lodging, and various other facilities. The commercial building has a floor-to-ceiling height of 4 stories, a total building height of 23 m, and a total floor area of 135,000 square meters. The key functions include retail, dining, supermarkets, and cinemas. The annual hourly heat load variations for three Harbin, Beijing, and Shanghai public buildings were simulated and analyzed. The resulting load data served as the input parameters for the operation simulation of air-source heat pump system.

Table 1. The heating durations for three typical cities.

Climate Zonings	City	Heating Condition	Heating Duration
Severe cold	Harbin	$T_{ave} \leq 5$ °C	10.17~04.10
Cold	Beijing	$T_{ave} \leq 5$ °C	11.12~03.14
Hot-summer and cold-winter	Shanghai	$T_{ave} \leq 8$ °C	12.05~03.07

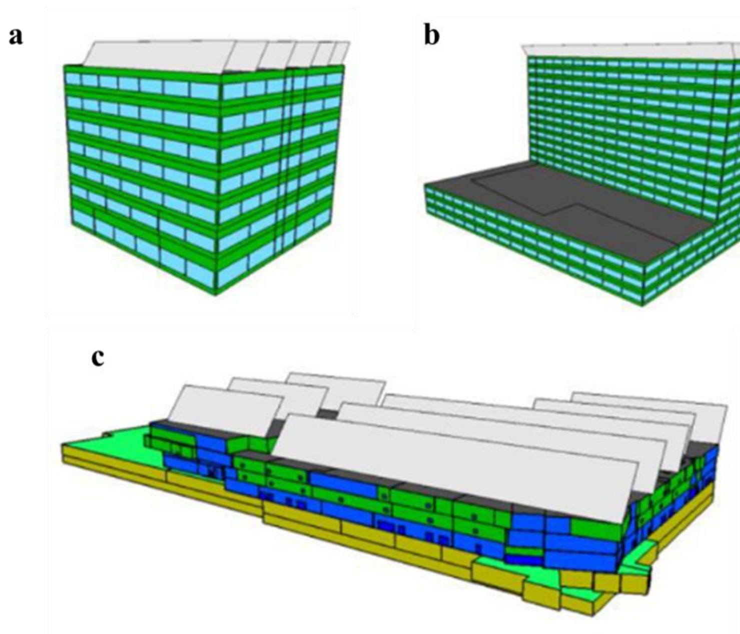

Figure 1. The model diagrams constructed using design builder: (**a**) Office building; (**b**) Hotel building; (**c**) Commercial building.

2.2. Air-Source Heat Pump System Model

The TRNSYS software can perform the transient energy consumption simulations for systems, featuring high visualization capabilities and good openness, which is widely used in multi-zone building models and HVAC systems [21]. As shown in Figure 2, the air-source heat pump heating system model is constructed based on the TRNSYS software. The system comprises an air-source heat pump circuit (red loop) and a terminal heating circuit (purple loop). The red loop section comprises an air-source heat pump module, a buffer tank, a heat pump-side circulating pump, and a heat pump quantity control module. Specifically, the buffer tank collects the heat output from the air-source heat pump module for the terminal heating. Through a comprehensive feedback mechanism, the control module adjusts the number of operating heat pumps based on the hourly heat load, the stored heat in the buffer tank, and the output heat of air-source heat pump. By contrast, the purple loop section includes a buffer tank, supply and return piping, a terminal heating module, and a load-side circulating pump. The buffer tank is controlled by adjusting the water pump speed to provide the heat to the terminal heating module, thereby satisfying the real-time building load. Additionally, switching the two blue lines completes the switching of the cooling and heating cycles.

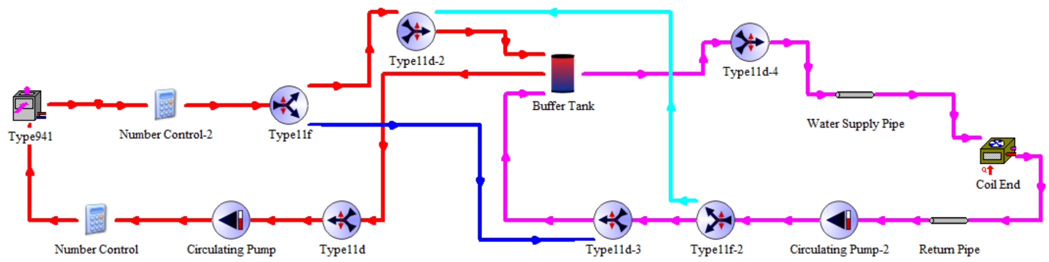

Figure 2. The air-source heat pump heating system.

The air-source heat pump heating system model is established using TRNSYS software, which utilizes various standard components to form a complete loop and generate data output. In the simulation and analysis of heating system, the specific modules are invoked to record data. The simulations are conducted under given input conditions, and the numerical results are collected through the output module. The main standard components involved in the air-source heat pump heating system model used in this study are listed in Table 2.

Table 2. Standard components selected in the TRNSYS model for this study.

Type	Component Name	Type	Component Description
Type941	Air-source Heat Pump	Type165	Controller
Type158	Thermal Storage Tan	Type515	Seasonal Schedule
Type673	Energy Rate Control Load	Type14h	Time Forcing Function
Type11f	Diverter/Mixer Valve	Type9e	General Data File Reader
Type110	Circulation Pump	Type15-3	Energy Climate File
Type31	Circulation Pump	Type65c	Online Plotter
Type24	Integrator	Type46a	Output

2.3. Correction Method for Low Temperature and Defrosting of Air-Source Heat Pumps

To analyze the variable condition performance of air-source heat pumps, this study utilizes performance fitting equations that account for the effects of low temperatures and defrosting to reflect the decay in the heating capacity and input power of air-source heat pump. To analyze the performance of air source heat pump under variable operating conditions, the performance fitting equation considering the effect of low temperature and defrosting on heat pump heating capacity attenuation is adopted in this paper.

(a) Heating capacity correction of the air-source heat pump for low-temperature

The heating capacity of the air-source heat pump on variable operating conditions is positively correlated with the outdoor temperature and negatively correlated with the outlet water temperature of the condenser. The correction coefficient equation for the heating capacity on variable operating conditions is as follows [22].

$$K_1 = a_1 + a_2 t_a + a_3 t_{out,a} + a_4 t_a{}^2 + a_5 t_a t_{out,a} + a_6 t_{out,a}{}^2 \tag{1}$$

where K_1 denotes the correction coefficient of heat produced by heat pump under low-temperature condition; $a_{1\sim}a_6$ represents the fitting coefficients; t_a denotes the outdoor temperature, °C; $t_{out,a}$ denotes the condenser outlet water temperature, °C.

(b) Heating capacity correction of the air-source heat pump for defrosting

Defrosting in the air-source heat pumps generally involves a reverse heating cycle, which reduces the heating capacity of the heat pump. When the temperature is below 7 °C and above 7 °C, the correction factors for the heating capacity during the defrosting are as follows [7].

$$t_a < 7\ °C,\ K_2 = 1 + 0.0027(t_a - 7) - 0.1801\exp(-t_a{}^2/5) \tag{2}$$

$$t_a > 7\ °C,\ K_2 = 1 - 0.1801\exp(-t_a{}^2/5) \tag{3}$$

where K_2 is the correction coefficient of heat produced by heat pump under defrosting condition.

(c) Input power correction of the air-source heat pump for low-temperature

The input power of the air-source heat pump on the variable operating conditions is influenced by both the outdoor temperature and the outlet water temperature of the condenser. Therefore, the fitted equation for the input power of the air-source heat pump on variable operating conditions is as follows.

$$K_3 = b_1 + b_2 t_a + b_3 t_{out,a} + b_4 t_a^2 + b_5 t_a t_{out,a} + b_6 t_{out,a}^2 \tag{4}$$

where K_3 represents the correction coefficient for the variable operating condition input power of the air-source heat pump; b_1~b_6 represent the fitting coefficient.

2.4. Performance Characterization Parameters of Air-Source Heat Pump

To evaluate the performance of air-source heat pumps under different setting parameters, three performance indicators are introduced: daily average load, daily average COP, and maximum load. The daily average load (Q_{H-ave}) is calculated with Equation (5), expressed as the arithmetic mean of heat loads during all working hours of the day. The daily average *COP* (COP_{ave}) is determined by Equation (6), which represents the arithmetic mean of the *COP* during all working hours of the day when the heat pump is operating normally. The maximum load occurs at the time point with the maximum absolute value of load during the calculation day.

$$Q_{H-ave} = \sum_{h=1}^{24} Q_H \tag{5}$$

$$COP_{ave} = \sum_{h=1}^{24} COP_h \tag{6}$$

where Q_{H-ave} is the daily average load, and Q_H is the hourly heat load. COP_{ave} is the average coefficient of performance, and *COP* is the hourly coefficient of performance.

2.5. Selection of Air-Source Heat Pumps

Considering the building load magnitudes in severe cold, cold, and hot-summer and cold-winter zones, the variable frequency air-source heat pump with the heating capacity of 165 kW from Midea is selected. Its performance and design parameters are listed in Tables 3 and 4. Based on the data provided by the manufacturer regarding the outlet water temperature, heat output, and input power of the heat pump under different outdoor ambient temperatures, the aforementioned performance fitting equations are employed to fit the actual performance data. The fitting results yield the heat output correction coefficient K_1 and input power coefficient K_3 of the heat pump under different outdoor ambient temperatures and outlet water temperatures. The correction coefficients for low temperature and defrosting are calculated using Equations (1–4), which are listed in Table 5.

Table 3. The performance parameters of air-source heat pump.

Operation Modes	Parameters	Unit	Value
Nominal heating mode	Nominal heating capacity	kW	110
	Nominal Heating power	kW	41.98
	Water flow rate	m^3/h	18.90
	COP		2.62
Nominal cooling mode	Nominal cooling capacity	kW	142
	Nominal cooling power	kW	41.89
	Water flow rate	m^3/h	24.42
	COP		3.39
Low-temperature heating mode	Low-temperature heating capacity	kW	90
	Low-temperature heating power	kW	50.1
	Water flow rate	m^3/h	18.6
	COP		1.8
Rated heating mode	Rated heating capacity	kW	165
	Rated heating power	kW	44.35
	Water flow rate	m^3/h	28.5
	COP		3.72

Table 4. Design parameters for supply/return water temperature of air-source heat pump heating system in different climate zones.

Climate Zones	Sever Cold	Cold	Hot-Summer and Cold-Winter
Supply/return water temperature	38/33 °C	41/36 °C	45/40 °C

Table 5. Correction and Fitting Coefficients for Variable Operating Condition Heating Capacity and Input Power.

Coefficients	$K_1(\times10^{-4})$	Coefficients	$K_3\ (\times10^{-4})$
a_1	7001.3	b_1	7938.6
a_2	133.2	b_2	−13.3
a_3	89.8	b_3	−142.5
a_4	−1.45	b_4	−0.22
a_5	0.36	b_5	0.73
a_6	−1.25	b_6	4.96

3. Dynamic Operating Characteristics of Air-Source Heat Pump Systems

3.1. Distribution Characteristics of Annual Hourly Dynamic Heat Load

To compare and analyze the hourly heat load distribution patterns throughout the year for three regions, Figure 3 presents the annual load and outdoor dry-bulb temperature variation curves for commercial buildings in Harbin, Beijing, and Shanghai. Clearly, the building load is closely correlated with outdoor dry-bulb temperatures, exhibiting different trends across the three regions. In Harbin and Beijing, with lower outdoor temperatures, the building heat load reaches the peak during the middle of heating duration. In contrast, the building load in Shanghai shows a more moderate variation throughout the year. Regarding the heat load data, the building load in Harbin are significantly higher than those in Beijing and Shanghai. The maximum heat load for commercial buildings is 9335.78 kW, with an annual average heat load of 1465.06 kW.

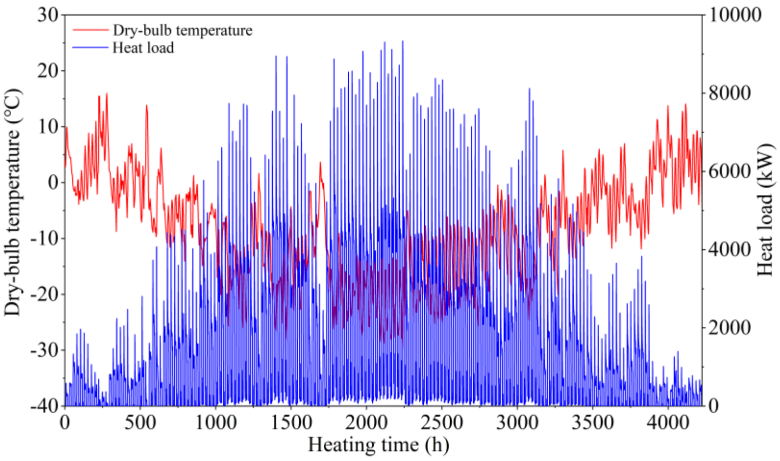

(a)

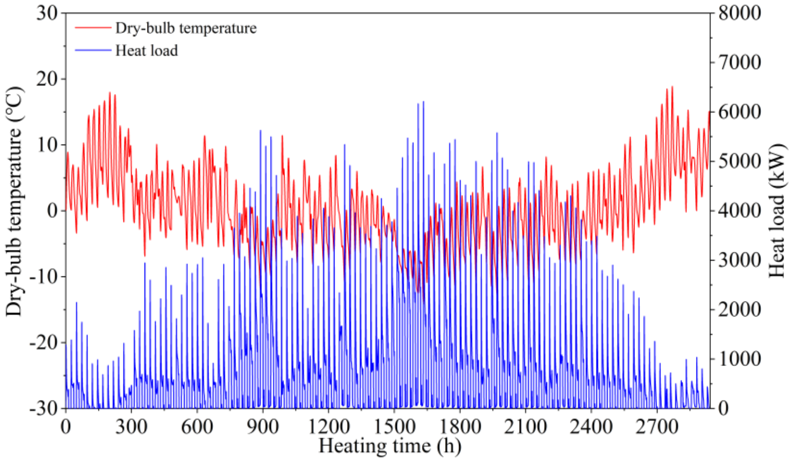

(**b**)

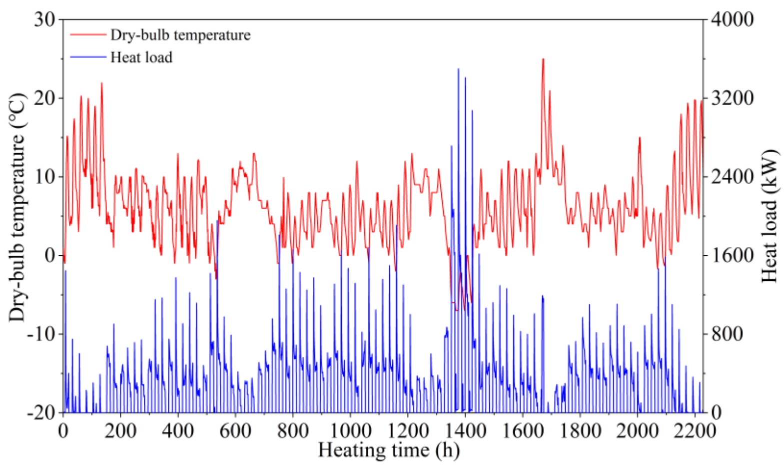

(**c**)

Figure 3. Annual hourly load variations of commercial buildings across different regions: (**a**) Harbin, (**b**) Beijing, (**c**) Shanghai.

3.2. Impact of Outdoor Dry-Bulb Temperature on the Heat Pump Operating Characteristics

The performance of the air-source heat pump systems is significantly influenced by the outdoor meteorological parameters. Focusing on the commercial buildings in Beijing, the impact of outdoor dry-bulb temperatures on the operating characteristics of air-source heat pump systems is investigated in this section. Based on the outdoor temperature data during the heating duration in Beijing, the coldest day (−11.7 °C), the hottest day (0.6 °C), and the moderate-temperature day (a day with average temperature during the heating period, −6.3 °C) were selected for the performance analysis. As shown in Figure 4, the variation trends in the operating units and the system COP of air-source heat pump system on three typical days were simulated.

The results show that the operating unit of heat pump closely follows the variation trend of the building load. As shown in Figure 4a, on the coldest day, to ensure that the indoor temperature in the office buildings does not drop below 5 °C, there is still a low heat load during the non-working hours. However, as shown in Figure 3b, the heat pump system does not need to operate because the thermal storage tank is sufficient to meet the building's heating demand. Additionally, from Figure 4d, f, on the moderate temperature day and the hottest day, there are 1–2 h of temporary shutdown for the heat pump system. This is because the thermal storage tank can meet the heating demand during the durations. Subsequently, as the building load increases, the stored heat in the tank becomes insufficient to meet the demand, causing the heat pump system to restart. During peak load periods on three representative days, the heat pump system needs to operate 39, 17, and 3 units, respectively, to meet the heating demand on the coldest, moderate-temperature, and warmest days. Additionally, the daily average COP of the heat pump system decreases with the decline in the average temperature of the typical days, being 3.1, 2.8 and 2.5, respectively.

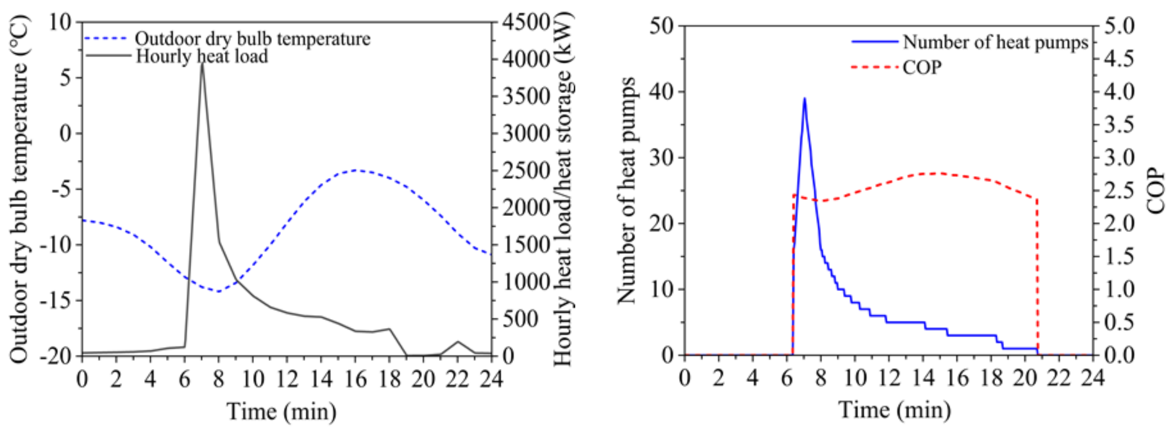

(**a**) (**b**)

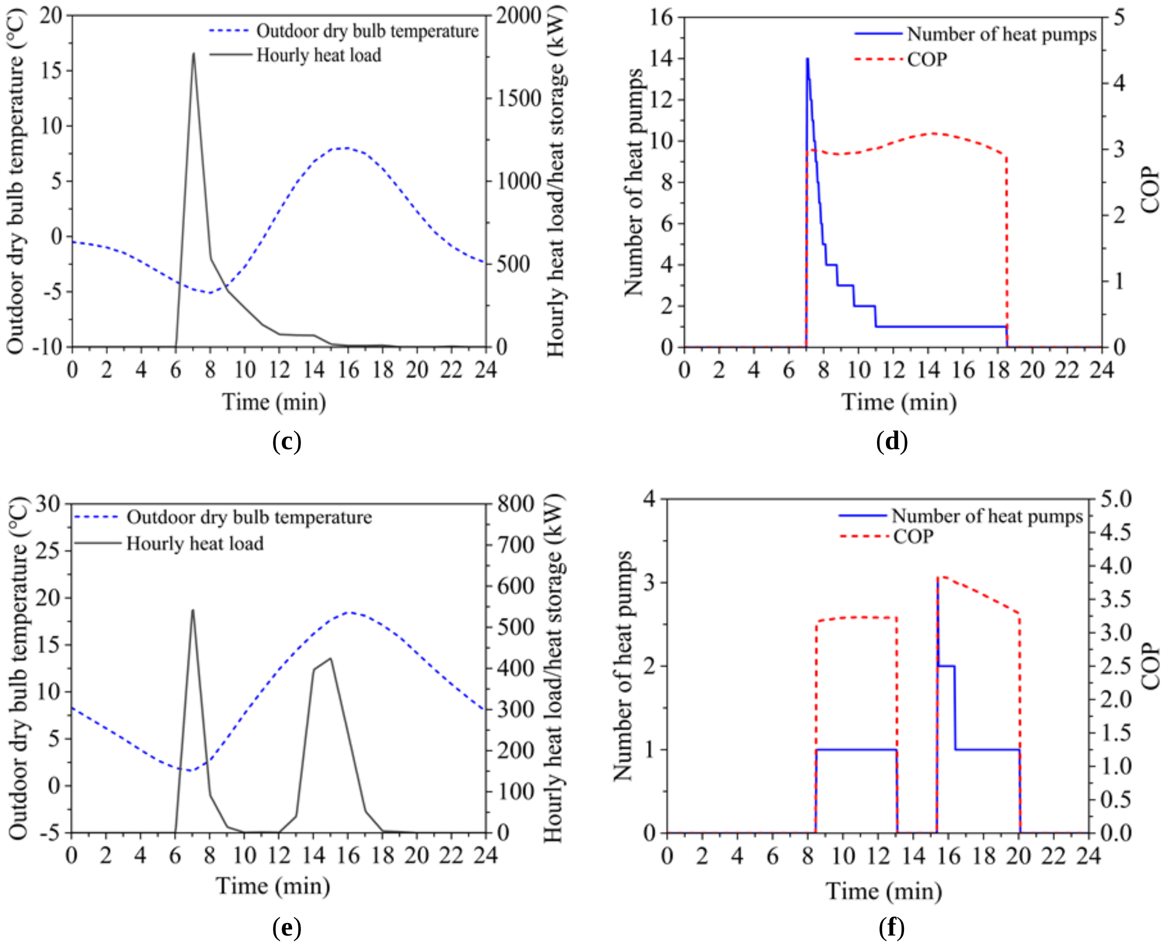

Figure 4. Variation of building load: (**a**) Coldest day; (**c**) Moderate-temperature day; (**e**) Hottest day, and heat pump system operating characteristics: (**b**) Coldest day; (**d**) Moderate-temperature day; (**f**) Hottest day.

3.3. Impact of Climate Zonings on the Heat Pump Operating Characteristics

In the different climate zonings, the setup requirements for air-source heat pump systems vary, including aspects such as supply/return water temperatures, defrosting, and low-temperature corrections, all of which can impact the overall performance of the heat pump system. Therefore, this section will analyze the working characteristics of an air-source heat pump system in the office building under three different climate zonings, with a focus on its performance on the coldest day. As shown in Figure 5, the heat load of office buildings exhibits two peak values, occurring at the beginning and end of the working hours, mainly influenced by the trend of outdoor temperature changes. Additionally, in Harbin, the lower outdoor temperatures at night result in a minimal heat load required to maintain indoor temperatures above 5 °C during non-working hours.

The operating characteristics of the heat pump system vary significantly across the three cities. In Harbin, the heat pump system operates during both working and non-working hours, with up to 15 units running at peak times. During the certain non-working periods, 1–3 units are still required to maintain the heating demand. The hourly fluctuations in the system COP are more pronounced in Harbin compared to Beijing and Shanghai, with a daily average COP of 1.7. In Beijing, due to the smaller heat load, the installation of thermal storage tank allows the heat pump system to operate only during the certain working hours (7 AM to 1 PM), with a maximum of 3 units running. The daily average COP of the heat pump system in Beijing is 2.46, slightly lower than that in Shanghai, which is 2.49.

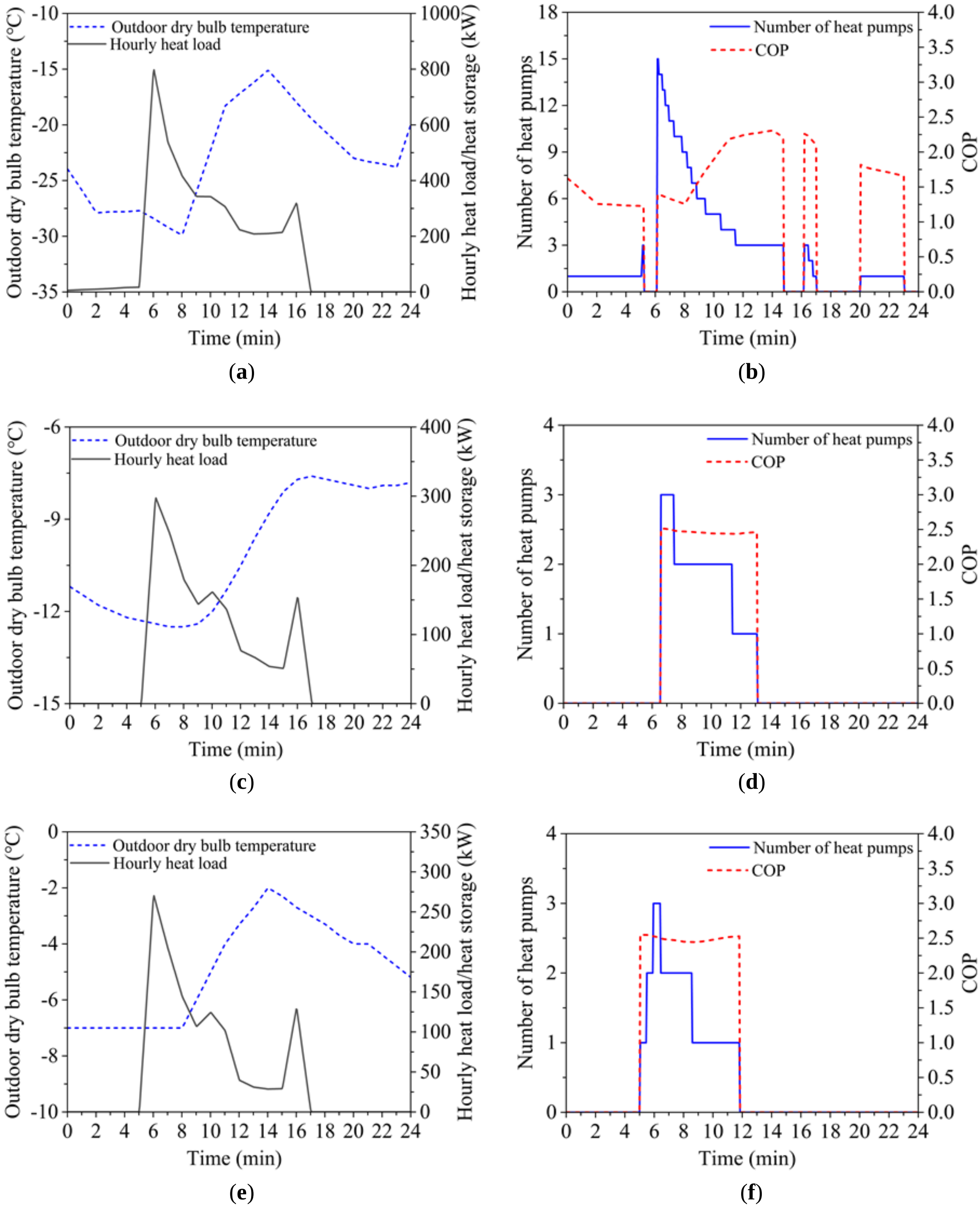

Figure 5. Variation of building load: (**a**) Harbin; (**c**) Beijing; (**e**) Shanghai, and heat pump system operating characteristics: (**b**) Harbin; (**d**) Beijing; (**f**) Shanghai.

3.4. Impact of Public Building Type on the Heat Pump Operating Characteristics

The office, hotel, and commercial buildings differ significantly regarding building area, operating hours, and building load. Focusing on the moderate-temperature day in Shanghai, the impact of public building types on the operating characteristics of air-source heat pump systems is discussed in this section. As descripted in Figure 6, the heat load variation trends of the three types of public buildings show differences in both the load magnitude and heating duration. On moderate-temperature days, the peak load for the office, hotel, and commercial buildings are 70 kW, 1050 kW, and 900 kW, respectively. Additionally, the hotel buildings have the heat load almost 24 hours on moderate-temperature day.

The variation in the operating unit number of heat pump in the hotel building closely aligns with the changes in the building load, with brief periods of shutdown observed. In contrast, with the assistance of the thermal storage tank, only a few heat pumps need to operate in office and commercial buildings during the certain periods to meet the heating demand. The daily average temperatures on the moderate-temperature days are 1.38 °C for the office building, 2.83 °C for the hotel, and 4.07 °C for the commercial building. The daily average COP of the heat pump systems for the office, hotel, and commercial buildings are 2.76, 2.88, and 3.09, respectively. Thus, it can be inferred that the COP of the heat pump systems in different public buildings will exhibit slight differences when the outdoor temperatures are similar.

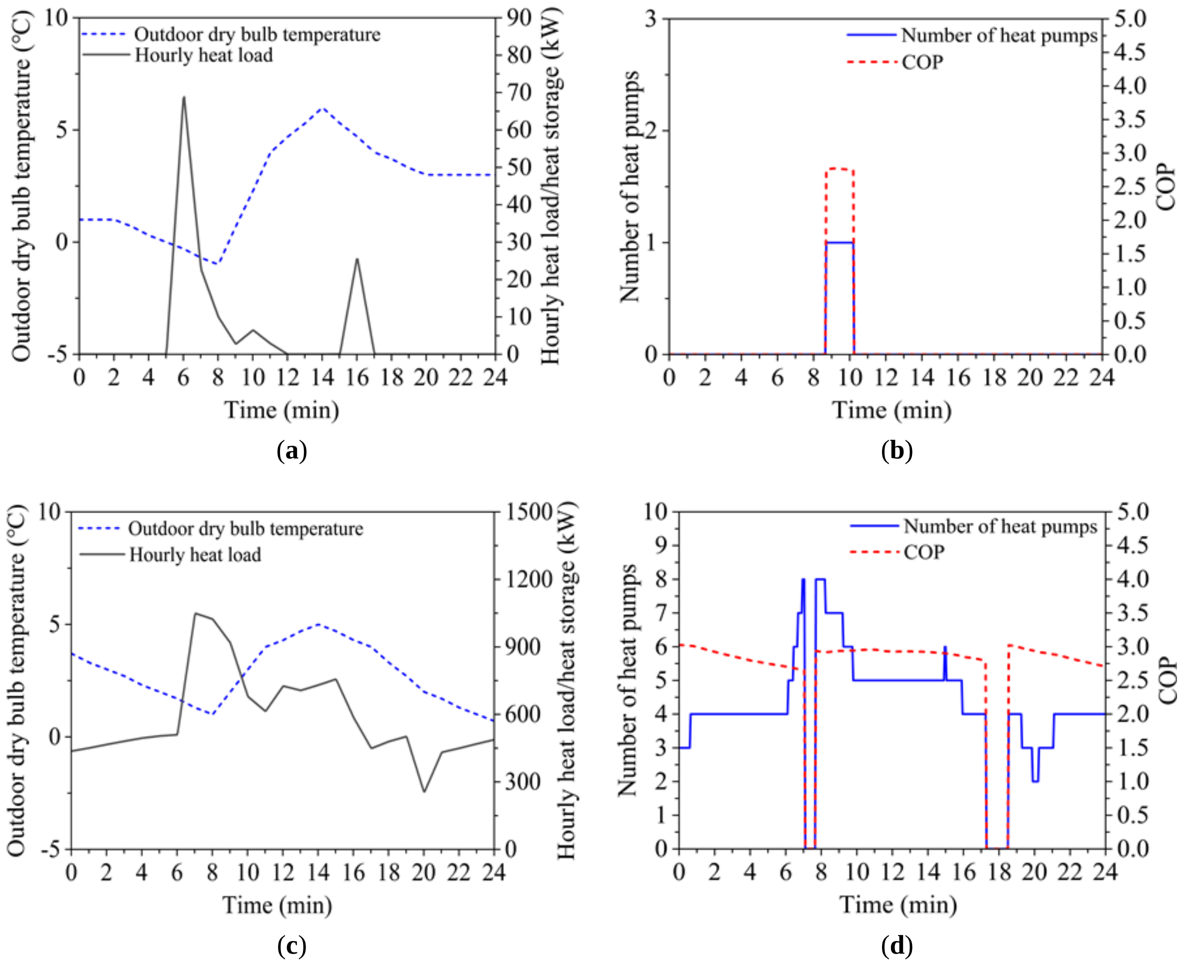

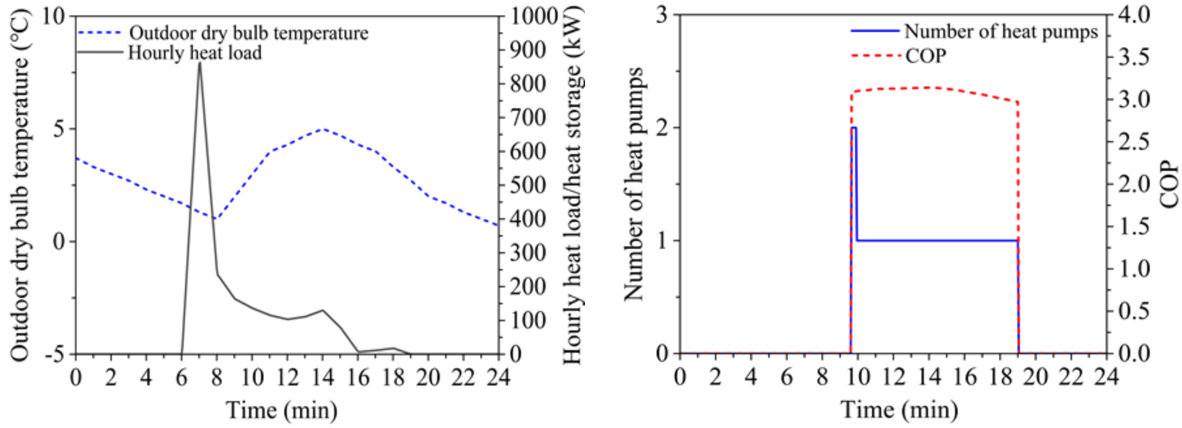

(e) **(f)**

Figure 6. Variation of building load: (a) Office; (c) Hotel; (e) Commercial, and heat pump system operating characteristics:(a) Office; (c) Hotel; (e) Commercial.

4. Correlation Analysis of Factors Affecting Heat Pump System Performance

The previous analysis of air-source heat pump heating systems reveals that the dry-bulb temperature significantly affects the system's COP. The building load also affects the system COP, while the building type has a negligible influence on the system COP. To validate the impact of these factors on the system COP, a correlation analysis is required. In this analysis, the dry-bulb temperature, building load, and COP are continuous variables, whereas the public building type is a categorical variable.

For the correlation analysis between the continuous data, Pearson correlation coefficient is used when the data sets of two variables satisfy the normal distribution and show a linear relationship. Spearman correlation coefficient is used when the data sets do not satisfy the normal distribution and linear relationship but show a monotonic relationship. The Pearson and Spearman correlation coefficients are calculated based on Equations (7) and (8), respectively. A one-way analysis of variance (ANOVA) is used to analyze the correlation between continuous data and unordered categorical data.

$$R = \frac{\sum (X - \bar{X})(Y - \bar{Y})}{\sqrt{\sum (X - \bar{X})^2 (Y - \bar{Y})^2}} \tag{7}$$

where R represents the correlation coefficient, and $\bar{X}$ and $\bar{Y}$ are the means of the variables X and Y, respectively.

$$R_S = 1 - \frac{6\sum d^2}{n(n^2 - 1)} \tag{8}$$

where R_S represents the correlation coefficient, d is the difference in ranks between two variables, and n is the sample number.

The Pearson and Spearman correlation coefficients range between −1 and 1, with the values closer to −1 or 1 indicating a stronger correlation. When the coefficient is above 0.5, the variables are positively correlated. When the coefficient is below −0.5, they are negatively correlated. The significance of both correlation coefficients is determined by a *p*-value below 0.05, indicating a significant correlation between the variables. In one-way ANOVA, the F-value represents the ratio of between-group variance to within-group variance, indicating the extent of the factor influence on the dependent variable. A larger F-value suggests greater significance of differences between groups and smaller significance within groups. A significance level of *p*-value below 0.05 indicates the significant differences between the different categories of the dependent variable, thereby demonstrating a correlation between the two variables.

The data on the dry bulb temperature, building load, and the COP of air-source heat pump systems for three types of buildings in different regions on the typical days are shown in Table 6. According to the correlation analysis, the Pearson correlation coefficient between the dry-bulb temperature and COP is 0.924, with a *p*-value of 8.67×10^{-16} below 0.05. The Spearman correlation coefficient is 0.941, with a *p*-value of 1.59×10^{-17} below 0.05. It indicates that the correlation between the dry-bulb temperature and COP is significant and positively correlated. The Pearson correlation coefficient between building load and COP is −0.643, with a *p*-value of 0.000024 below 0.05, while the Spearman correlation coefficient is −0.580, with a *p*-value of 0.000207 below 0.05. This indicates that the correlation between building load and COP is significant and negatively correlated. The results of the one-way ANOVA for building types and COP are presented in Table 7. The homogeneity of variance tests all yielded values above 0.05, validating the use of the one-way ANOVA. These results indicate that there is no correlation between building types and COP.

Table 6. The dry-bulb temperature, building load, and system COP on the typical days.

Cities	Typical Day	Building Type	Dry−Bulb Temperature/°C	Heat Load/kW	COP
Harbin	Hottest day	Commercial	7.36	116.48	3.32
		Hotel	10.71	183.31	3.56
		Office	7.91	19.57	3.51
	Coldest day	Commercial	−23.56	1099.65	1.64
		Hotel	−22.99	1832.50	1.78
		Office	−23.54	177.86	1.70
	Moderate−temperature day	Commercial	−8.10	294.42	2.77
		Hotel	−4.13	751.41	3.06
		Office	−3.43	189.12	3.04
Beijing	Hottest day	Commercial	13.22	46.03	3.41
		Hotel	4.81	351.02	3.14
		Office	0.56	163.05	3.12
	Coldest day	Commercial	−7.70	764.18	2.57
		Hotel	−8.52	1084.09	2.61
		Office	−11.65	149.02	2.46
	Moderate−temperature day	Commercial	2.48	208.94	3.07
		Hotel	0.54	669.10	3.06
		Office	−6.30	112.66	2.75
Shanghai	Hottest day	Commercial	10.85	30.37	3.58
		Hotel	10.50	248.02	3.15
		Office	10.37	52.92	3.07
	Coldest day	Commercial	−4.57	235.91	2.81
		Hotel	−4.92	1035.13	2.52
		Office	−5.95	141.84	2.49
	Moderate−temperature day	Commercial	4.07	74.35	3.09
		Hotel	2.83	585.37	2.88
		Office	1.38	4.66	2.76

Table 7. One-way ANOVA of building types and cop.

Cities	Homogeneity of Variance	F-Value	*p*-Value	Correlation
Harbin	0.978 > 0.05	0.043	0.958 > 0.05	NA
Beijing	0.699 > 0.05	0.390	0.679 > 0.05	NA
Shanghai	0.893 > 0.05	0.343	0.712 > 0.05	NA

5. Conclusions

Considered the influence of low temperatures and defrosting conditions, this study established an air-source heat pump heating system model using TRNSYS. The effects of outdoor meteorological parameters, climate zonings, and building types on the operational characteristics and energy efficiency of air-source heat pump systems were simulated and analyzed. By thoroughly comprehending the intricacies of these characteristics and patterns, and integrating them with the actual demands of buildings for intelligent adjustments, the heat pump systems can achieve substantial improvements in energy efficiency, ensuring a comfortable indoor environment simultaneously. The key conclusions of this study are as follows.

1. In terms of the annual load variation, the building heat load in Harbin and Beijing reach the peak in the middle of the heating season, whereas that in Shanghai shows a more moderate variation in annual building load. The variations in the operation unit number of heat pump system closely mirror the variation in the building load.

2. The performance of air-source heat pumps is closely tied to climate zonings. On the coldest day of the heating duration, the daily average COP of air-source heat pump heating systems in Harbin, Beijing, and Shanghai was as follows: Shanghai (2.49) > Beijing (2.46) > Harbin (1.7).

3. Through the combination of correlation coefficients and one-way ANOVA, it was found that the COP of air-source heat pump heating systems is positively correlated with dry bulb temperature and negatively correlated with the building load, independent of the building type in the public buildings.

Author Contributions: J.F.: software, data curation, writing-original draft preparation; Y.L.: conceptualization, methodology, writing-reviewing and editing; J.M.: visualization, investigation; Y.C.: data curation, supervision; Z.Z.: software, validation; X.C.: validation, supervision; L.J.: supervision, writing-reviewing and editing. All authors have read and agreed to the published version of the manuscript.

Funding: This research was funded by National Natural Science Foundation of China, 52406109, Fundamental Research Funds for the Central Universities, xzy012024075, Shaanxi Postdoctoral Science Foundation, 2023BSHEDZZ51 and Postdoctoral Fellowship Program of CPSF, GZC20232076.

Institutional Review Board Statement: Not applicable.

Informed Consent Statement: Written informed consent has been obtained from the patients to publish this paper.

Data Availability Statement: Not applicable.

Conflicts of Interest: The authors declare no conflict of interest.

Reference

1. Shan, Y.; Guan, D.; Zheng, H.; et al. China CO_2 emission accounts 1997–2015. *Sci. Data* **2018**, *5*, 170201.
2. Du, W.; Li, X.; Chen, Y.; Shen, G. Household air pollution and personal exposure to air pollutants in rural China—A review. *Environ. Pollut.* **2018**, *237*, 625–638.
3. Cai, J.Y.; Zhou, H.H.; Xu, L.J.; et al. Experimental and numerical investigation on the heating performance of a novel multi-functional heat pump system with solar-air composite heat source. *Sustain. Cities Soc.* **2021**, *73*, 103118.
4. Ni, L.; Dong, J.; Yao, Y.; et al. A review of heat pump systems for heating and cooling of buildings in China in the last decade. *Renew. Energy* **2015**, *84*, 30–45.
5. Vieira, A.S.; Stewart, R.A.; Beal, C.D. Air source heat pump water heaters in residential buildings in Australia: Identification of key performance parameters. *Energy Build.* **2015**, *91*, 148–162.
6. Wei, W.Z.; Wu, C.S.; Ni, L.; et al. Performance optimization of space heating using variable water flow air source heat pumps as heating source: Adopting new control methods for water pumps. *Energy Build.* **2022**, *255*, *111654*.
7. Zhang, Q.; Zhang, L.; Nie, J. Techno-economic analysis of air source heat pump applied for space heating in northern China. *Appl. Energy* **2017**, *207*, 533–542.
8. Zhang, L.; Jiang, Y.; Dong, J. Advances in vapor compression air source heat pump system in cold regions: A review. *Renew. Sustain. Energy Rev.* **2018**, *81*, 353–365.
9. Safa, A.A.; Fung, A.S.; Kumar, R. Comparative thermal performances of a ground source heat pump and a variable capacity air source heat pump systems for sustainable houses. *Appl. Therm. Energy* **2015**, *81*, 279–287.
10. Zhang, H.; Jiang, L.; Zheng, W.; et al. Experimental study on a novel thermal storage refrigerant-heated radiator coupled with air source heat pump heating system. *Build. Environ.* **2019**, *164*, 106341.
11. Xu, X.; Fang, Z.; Wang, Z. Climatic division based on frosting characteristics of air-source heat pumps. *Energy Build.* **2020**, *224*, 110219.
12. Wu, C.; Liu, F.; Li, X.; et al. Low-temperature air source heat pump system for heating in severely cold area: Long-term applicability evaluation. *Build. Environ.* **2022**, *208*, 108594.
13. Wu, P.; Wang, Z.; Li, X.; et al. Energy-saving analysis of air source heat pump integrated with a water storage tank for heating applications. *Build. Environ.* **2020**, *180*, 107029.
14. Long, J.; Xia, K.; Zhong, H.; et al. Study on energy-saving operation of a combined heating system of solar hot water and air source heat pump. *Energy Convers. Manag.* **2021**, *229*, 113624.
15. Song, M.; Deng, S.; Dang, C. Review on improvement for air source heat pump units during frosting and defrosting. *Appl. Energy* **2018**, *211*, 1150–1170.
16. Wang, X.; Yu, J.; Xing, M. Performance analysis of a new ejector enhanced vapor injection heat pump cycle. *Energy Convers. Manag.* **2015**, *100*, 242–248.
17. Wei, W.; Ni, L.; Zhou, C. Performance analysis of a quasi-two stage compression air source heat pump in severe cold region with a new control strategy. *Appl. Therm. Eng.* **2020**, *174*, 115317.
18. Li, Y.; Yu, J. Theoretical analysis on optimal configurations of heat exchanger and compressor in a two-stage compression air source heat pump system. *Appl. Therm. Eng.* **2016**, *96*, 682–689.
19. Soltani, R.; Dincer, I.; Rosen, M.A. Comparative performance evaluation of cascaded air-source hydronic

heat pumps. *Energy Convers. Manag.* **2015**, *89*, 577–587.
20. Shen, J.; Guo, T.; Tian, Y. Design and experimental study of an air source heat pump for drying with dual modes of single stage and cascade cycle. *Appl. Therm. Eng.* **2018**, *129*, 280–289.
21. Karami, M.; Abdshahi, H. Energy and exergy analysis of the transient performance of a qanat-source heat pump using TRNSYS-MATLAB co-simulator. *Energy Environ.* **2023**, *34*, 560–585.
22. Loïc, C.; Rowley, P. Towards low carbon homes—A simulation analysis of building-integrated air-source heat pump systems. *Energy Build.* **2012**, *34*, 127–136.

Review

A Review of Geothermal Energy Coupled Hybrid System for Building Heat Supply

Jianke Hao [1], Guosheng Jia [1,]*, Zhendi Ma [1], Zhibin Zhang [1], Congfu Ma [1], Chonghua Cheng [2] and Liwen Jin [1,]*

[1] School of Human Settlements and Civil Engineering, Xi'an Jiaotong University, Xi'an 710049, China
[2] Shaanxi Yateer Scientific and Technological Innovation Construction Co., Ltd., Xi'an 710076, China
* Correspondence: jiaguosheng@xjtu.edu.cn (G.J.); lwjin@xjtu.edu.cn (L.J.)
Received: 3 September 2024; Revised: 8 October 2024; Accepted: 10 October 2024; Published: 11 October 2024

Abstract: Recently, there has been significant emphasis on studying the combination of geothermal energy with other forms of renewable energy. This has become an important area of research in sustainable energy development. The notable characteristic of this integration is its ability to improve the overall efficiency and reliability of the heat supply system. This study reviews the research conducted on the building heating system, which combines geothermal energy with solar energy, wind energy, and air-source energy. A thorough analysis of how previous studies have utilized renewable energy sources to address the drawbacks of geothermal heating systems has been performed, with a specific focus on energy consumption efficiency, soil temperature variations, system power supply, and cost analysis. Geothermal energy coupled with solar energy can mitigate the instability of the solar energy supply and reduce the ground temperature attenuation. The integration of geothermal and wind energy can produce electricity, thereby satisfying the power requirements. The combination of geothermal energy with an air-source heat pump system can enhance the overall performance and reduce the borehole heat exchanger depth. Through the detailed analysis of these hybrid systems, we aim to promote the development and popularization of the coupled system and provide a reference for renewable energy utilization.

Keywords: geothermal energy, renewable energy, hybrid building heating system, coupled system efficiency

1. Introduction

As economic globalization continues to advance, the increasing energy consumption has exerted tremendous pressure on the environment and resources. Therefore, the main direction of energy development is shifting to increase the utilization of renewable energy instead of fossil fuels to decrease greenhouse gas emissions [1,2]. The comprehensive use of renewable energy is particularly important as it contributes to societal sustainability [3], ecological balance [4], and the reduction of atmospheric pollution [5,6]. Geothermal energy is a kind of renewable resource that is widespread and clean [7–10]. It can be efficiently utilized through technologies such as geothermal heat pumps to obtain high-temperature heat sources [11,12]. It is applicable for various purposes, including building heating, electricity generation, greenhouse cultivation, and swimming pool heating [13,14].

Geothermal energy has numerous advantages, such as vast reserves and widespread distribution [15,16]. Its development is currently progressing rapidly. The ground source heat pump (GSHP) technology has been proven to be an effective way for building heating all over the world. The buried heat exchanger (BHE) is the main equipment in the GSHP system and there have been many investigations about the BHE heat transfer mechanism, numerical simulation and performance optimization. However, some problems and limitations arise during the utilization process [17,18]. One of the major unresolved issues is that the long-term operation of BHE will lead to ground temperature attenuation. The BHE is usually buried underground to absorb heat from the high-temperature strata. If the system operates for a long time, the ground temperature might decrease year by year, and the BHE heat extraction efficiency might not satisfy the energy demands [19,20]. Therefore, combining geothermal energy with other renewable energy sources has become a feasible method to solve this problem [21,22]. Through the integration of geothermal energy with other renewable energy resources [23,24], the system efficiency can be improved essentially [25,26]. Typically, combining solar energy with geothermal energy can mitigate the intermittent nature of solar energy and improve the reliability of the energy supply [27,28]. Integrating geothermal energy with air-source heat pump systems can significantly decrease operational expenses and enhance energy consumption efficiency [29,30]. By combining geothermal energy with wind energy, it is possible to have a continuous and reliable source of electricity supply throughout the year, enhancing the dependability of the power grid [31].

This literature focuses on the utilization of geothermal energy combined with other renewable energy sources to improve the reliability and efficiency of the building heating system. The primary goal is to assess the advancements in geothermal energy-coupled hybrid systems. In pursuit of this objective, we will review recent literature that focuses on the technical aspects, system design, and performance analysis of coupled systems [32–34]. Firstly, an introduction to the development of the geothermal heating system, including the classification, development, and theoretical studies about the prediction methods, will be carried out. Then a thorough investigation will be conducted on the geothermal energy hybrid system using solar energy, wind energy and air source heat pump. Finally, summaries will be given after each section and at the end of the study. A comprehensive examination of system configuration, operating principle, investigation methods and system efficiency is crucial for advancing the integration of geothermal energy with other renewable energy sources, which will help promote the development of renewable energy applications.

2. Geothermal Heating System

2.1. Development of Geothermal Heating System

Geothermal energy is a type of clean and widely distributed renewable energy that has been utilized for decades. Swiss scientists first introduced the notion of a “ground source heat pump” through patents in the early 20th century, which led to a global study on shallow geothermal energy [35]. By 1999, ground-source heat pumps have been widely adopted in developed countries like Europe and Japan, dominating residential heating systems. By the end of 2019, the global installed capacity for direct geothermal energy reached 107,727 MWt, marking a 52.0% increase from 2015 [36]. Standards guiding geothermal energy applications have been implemented in Canada, Europe, and other regions. By the end of 2017, China has the largest utilization area in terms of shallow geothermal energy for heating and cooling [37]. These demonstrate the significant global expansion and international focus on geothermal energy.

One of the main ways to use geothermal energy is to extract the heat contained in the underground rock and soil bodies or underground water through certain means and then transfer it to the above-ground equipment for building heating [38]. According to different ways of heat extraction (as shown in Figure 1), geothermal energy utilization systems can be divided into water source heat pump (WSHP) and GSHP [39,40]. The WSHP extracts high-temperature groundwater for immediate use, and then reintroduces it back into the aquifer [41,42]. In contrast, the GSHPutilizes a BHE to exchange heat with the surrounding rock and soil. This allows the system to continuously transport the heat from the rock and soil to the above-ground equipment using a circulating fluid, typically water [43,44].

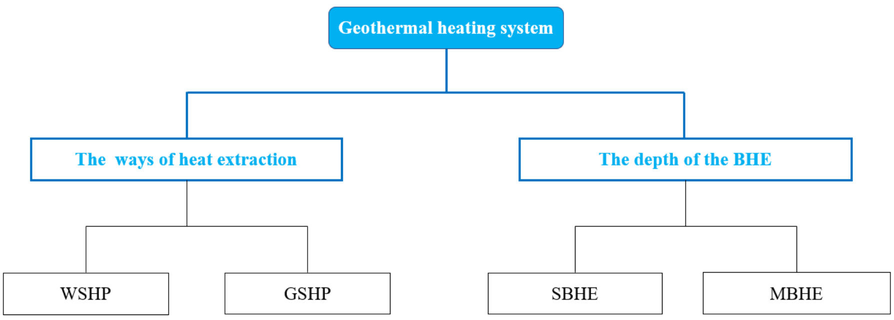

Figure 1. Geothermal heating system classification.

Further, according to the depth of the BHE, the geothermal heating systems can be further classified into shallow buried heat exchanger (SBHE) systems and medium-deep buried heat exchanger (MBHE) systems [45]. SBHE is notable for its ability to be used for both heating and cooling purposes [46,47]. MBHE stands out due to its superior thermal efficiency for heat supply and ability to maintain constant operating temperatures over a relatively long period of time. MBHE also has a longer lifespan, making it ideal for larger-scale applications [48]. The characteristics of these two categories, in terms of their suitability and effectiveness, highlight their substantial capacity for use in a wide range of energy applications.

2.2. Research Advancements

The BHE is the equipment responsible for directly exchanging heat with the exterior soil in the use of geothermal energy. It is also the key component that significantly impacts the overall performance of the geothermal system. Due to the high costs associated with drilling, logging, and pipe burial in the early stages, the evaluation of the BHE performance is particularly important [49,50]. On this basis, various evaluation methods have been established to guide the design and operation of the BHE system for project application (as shown in Figure 2). These methods can be theoretically divided into analytical approaches, numerical approaches utilizing software, and other self-developed numerical calculation methods such as finite element and finite difference methods [51–53].

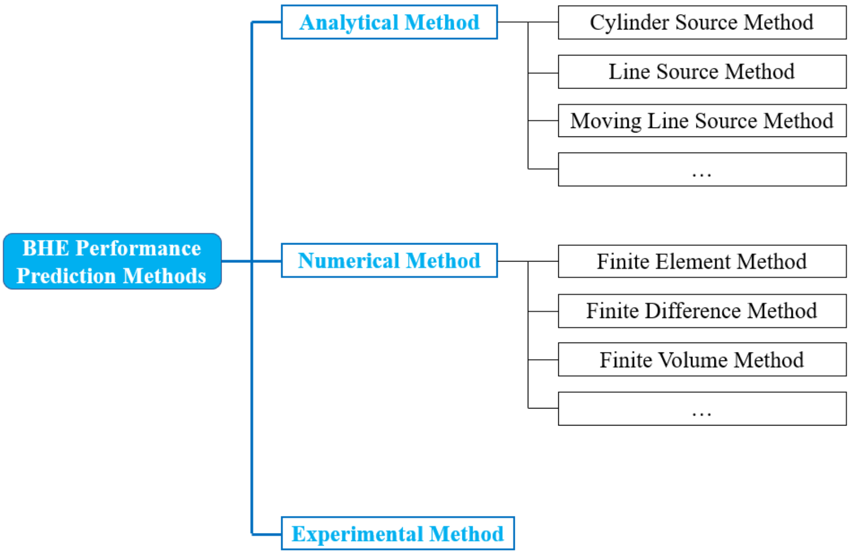

Figure 2. Different methods for BHE performance prediction.

Analytical methods solve the governing equations directly and have the benefit of fact computation speed, rendering them appropriate for quick design with appropriate simplifications. Contrarily, numerical methods contain detailed boundary conditions, including complex geological conditions and BHE configurations. This enables the attainment of more precise outcomes considering real geological and BHE structural parameters. Experimental approaches yield tangible data and empirical proof, which is necessary for verifying the simulation methods and bolstering the dependability of the design. By integrating these approaches the design and operation of BHE systems can be optimized. This ultimately leads to more efficient utilization of geothermal energy.

3. Geothermal Energy Coupled Hybrid Heating System

As previously mentioned, the research focusing on geothermal energy applications has become well-developed. The performance of the system depends on many factors. For example, in horizontal BHE, system efficiency generally enhances with an increase in pipe diameter, length, and flow rate. In the case of medium-deep coaxial BHE, increasing the thermal conductivity of the outer pipe or diminishing the thermal conductivity of the inner pipe can enhance system efficiency.

For long-period operations, when the building heat load and BHE inlet temperature are consistent, the heat extraction rate will exceed the ground temperature recovery rate. This results in a decrease in the geothermal temperature, which in turn reduces the thermal efficiency of the BHE year after year. For example, by conducting a 20-year simulation on a closed MBHE system with a depth of 2000 m, Luo et al. [54] found that the soil temperature decreased by approximately 6 °C at a depth of 1600 m. Liu et al. [55] found that after 30 years operation of a 2500-m closed MBHE system, the output temperature was reduced by almost 15% and the system performance decreased by 7.5% due to ground temperature reduction. Thus, it is necessary to find ways to allow the ground temperature to recover and maintain the BHE performance at a higher level. One of the feasible ways is to couple geothermal energy with other energy sources to jointly provide heat to the building. The following part will give a detailed introduction to three types of commonly investigated hybrid systems, including solar-geothermal energy hybrid systems, wind-geothermal energy hybrid systems and air source-geothermal energy hybrid systems (as shown in Figure 3).

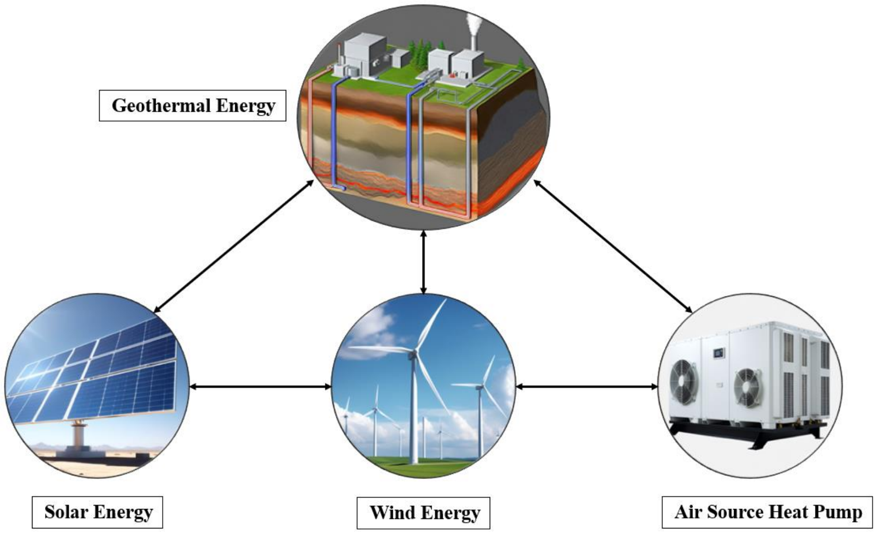

Figure 3. Multi-Energy Hybrid Systems.

3.1. Solar-Geothermal Energy Hybrid Systems

The integration of solar and geothermal energy sources offers a promising approach to enhancing the sustainability and reliability of heat supply systems. The classification of two typical types of solar-geothermal energy hybrid systems is based on their functions and configurations: (1) hybrid solar-assisted ground source heat pump (SAGSHP) system for heating, (2) hybrid ground source heat pump-photovoltaic thermal (GSHP-PVT) system for both heating and power generation. Integrating the benefits of these two sustainable energy sources improves system efficiency, enhances economic viability, and diminishes environmental impact.

The GSHP-PVT system is an integrated energy system of GSHP with photovoltaic thermal (PV/T) systems. The PV/T system is used for two purposes, i.e., providing electrical power for the GSHP and offering heat to the heat exchange medium in the system. During periods of low heat demand, the system alternates between utilizing geothermal energy or solar energy separately. During periods of higher heat demand, solar and geothermal energy are used simultaneously. In the non-heating season, solar energy can be utilized for thermal recharging to address the problem of soil temperature attenuation and overcome the BHE performance deterioration. Existing research concentrates on optimizing the design of the GSHP-PVT system by utilizing numerical simulations and experimental validation. These studies include not only the technical performance investigation but also the economic study of the system. The objective of utilizing these research methodologies is to attain solutions that are more efficient, cost-effective, and environmentally sustainable.

As shown in Figure 4, a typical GSHP-PVT system usually contains the PV/T component, heat storage tank, BHEs, and heat pump, utilizing solar and geothermal energy to achieve efficient heating. The system leverages the PV/T components for dual solar energy conversion. The photovoltaic portion converts solar energy into electrical power, which is then converted to alternating current via an inverter to power internal devices such as circulating pumps and valves. Any excess electricity is stored in a battery. The thermal portion absorbs solar radiation and transfers the generated heat to a fluid, which is then directed to the heat storage tank. The heat storage tank can store excess heat during periods of ample sunlight and release it when needed to supply to the heat pump. The BHE extracts heat from the ground for heating during winter or injecting excess heat into the ground during summer to balance the system’s thermal load. The heat pump extracts heat from either the heat storage tank or the BHE, raises it to the appropriate temperature, and delivers it to the user end for heating purposes.

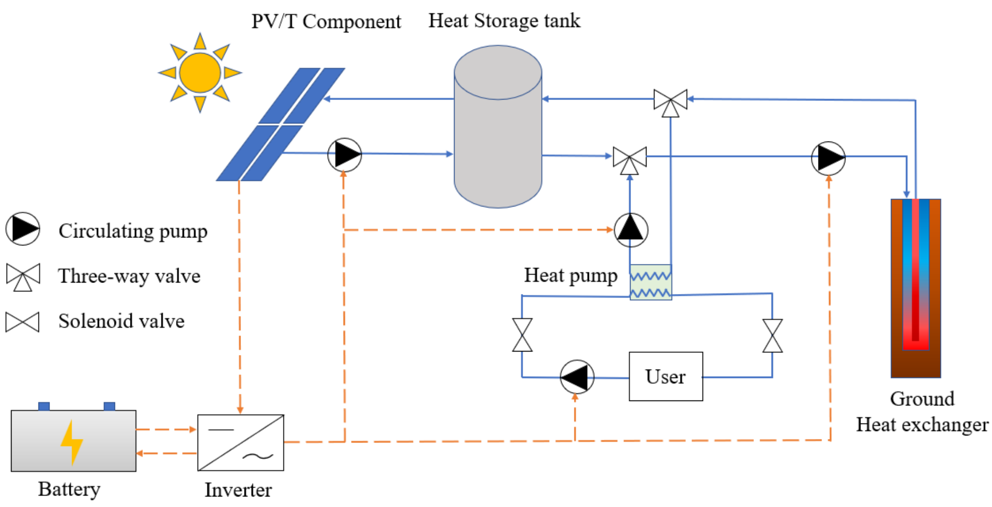

Figure 4. Schematic diagram of solar-geothermal energy hybrid systems.

3.1.1. Hybrid SAGSHP System for Heating

Rad et al. [56] investigated the application and feasibility of a SAGSHP system located in Milton, Canada. The BHE part consisted of four vertical closed-loop circuits, each 55 m in length (as shown in Figure 5). The BHE circuits were connected in parallel with the solar collectors. In cooling mode, the desuperheater absorbed a portion of the high-temperature waste heat from the compressor's discharge and transferred it to a secondary water stream, typically connected to the domestic hot water tank. In heating mode, the desuperheater released the energy absorbed by the liquid stream, which was then used not only for space heating but also for domestic hot water heating. By integrating solar thermal energy storage, the BHE length was reduced by approximately 30 m. Cost analysis indicates that the proposed system is 3.7–7.6% more cost-effective compared to a conventional GSHP system. By focusing on the heat pump's coefficient of performance (COP) and average entering fluid temperature (EFT), it is shown that, in heating mode, the SAGSHP system has an 18.26% higher EFT and a 2.84% higher COP than the GSHP system, indicating that a hybrid GSHP system with a solar thermal collector is a feasible choice for heating load is much larger than cooling load.

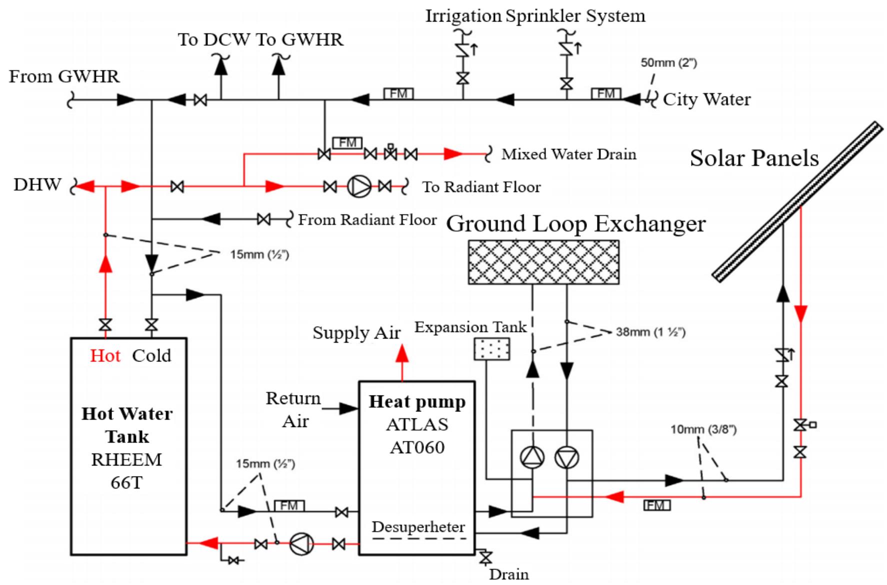

Figure 5. Schematic diagram of SAGSHP system configuration by Rad et al. [56].

Eslami-nejad et al. [57] presented a novel double U-tube borehole system with two independent loops (as shown in Figure 6), one circuit was connected to a GSHP operating in heating mode, while the other was linked to thermal solar collectors. The BHE system was a closed-loop system with a length of 142 m. The system could operate in three different modes: heat pump only, solar charging only, or simultaneous operation. Solar thermal energy was stored underground in the summer and extracted in the winter for use by the GSHP. This reduced the operating hours of the GSHP, leading to lower energy consumption. A 20-year energy simulation comparison between the double-U-tube well system and the single ground-source heat pump system reveals a 3.5% reduction in energy consumption. Additionally, the well depth can be reduced to 117 m, which represents a 17.6% decrease in length. The average temperature of the heat pump fluid in the dual U-tube borehole system can be maintained without decreasing.

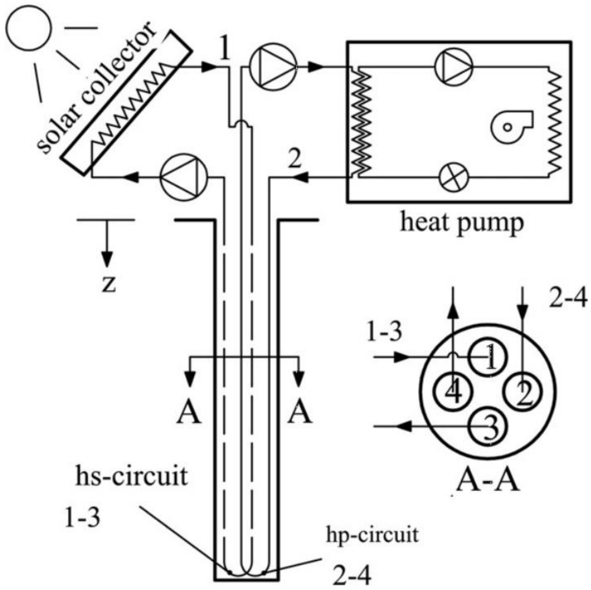

Figure 6. Schematic diagram of a novel double U-tube borehole system configuration by Eslami-nejad et al. [57].

Chen et al. [58] investigated a building located in Tongzhou, Beijing, which used a parallel operation mode of solar energy and a hybrid GSHP system. The test field encompassed a total area of 2600 m^2. An experimental study was conducted on a BHE array that included double U-tube BHEs with lengths of 150 m and 300 m, single U-tube BHEs with a length of 300 m, and enhanced coaxial BHEs with lengths of 150 m and 300 m (as shown in Figure 7). The parallel operation mode integrating solar energy with a hybrid ground-source heat pump (HGSHP) system was implemented to fulfill the building's heating requirements in winter and/or cooling needs in summer. When the temperature of the solar water tank reached the cooling or heating standard, solar energy was directly used to supply energy to the building. Otherwise, the GSHP was used for heating or cooling. During a heating period, the SAGSHP system has a 2.3% lower outlet temperature drop than the HGSHP system. When operating in a single season, the temperature drop rate of the soil and rock is reduced by 0.78%.

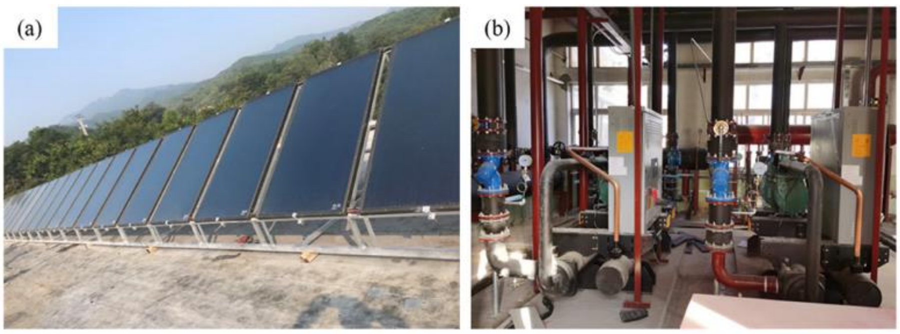

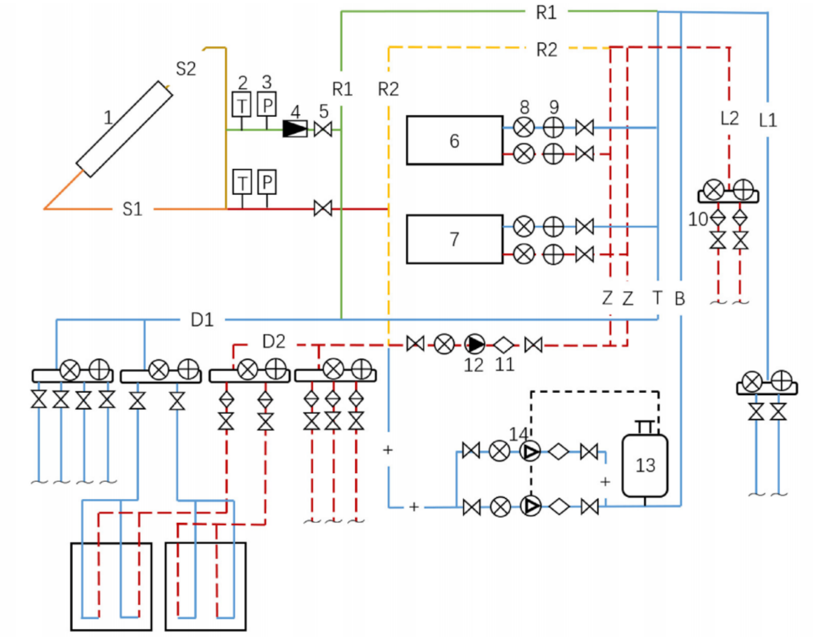

(**c**)

Figure 7. (**a**) Solar collector; (**b**) plant room system; (**c**) Design diagram of SAHGSHP system by Chen et al. [58].

Liu et al. [59] studied an experimental platform located in Tianjin, which belongs to a cold region. The BHE system was a closed-loop system with a burial depth of 120 m (as shown in Figure 8). The system was divided into two parts: the first part was the heat storage system, which operated in the non-heating season to transfer water heated by solar radiation to the BHE, where it exchanged heat with the soil and the heat was thereby stored in the soil. The second part was the GSHP heating system, which operated in winter to extract the stored heat through buried pipes for building heating. The solar energy utilization efficiency achieved 50.2% and soil temperature was raised by 0.21 C. The study focused on solar radiation and soil heat storage. The total solar radiation was 265,830.92 kWh and the soil heat storage was 133,416.41 kWh. It was 2.03 times the average heat extraction, indicating that the soil heat balance can be achieved through the coupling of solar energy storage and GSHP technology.

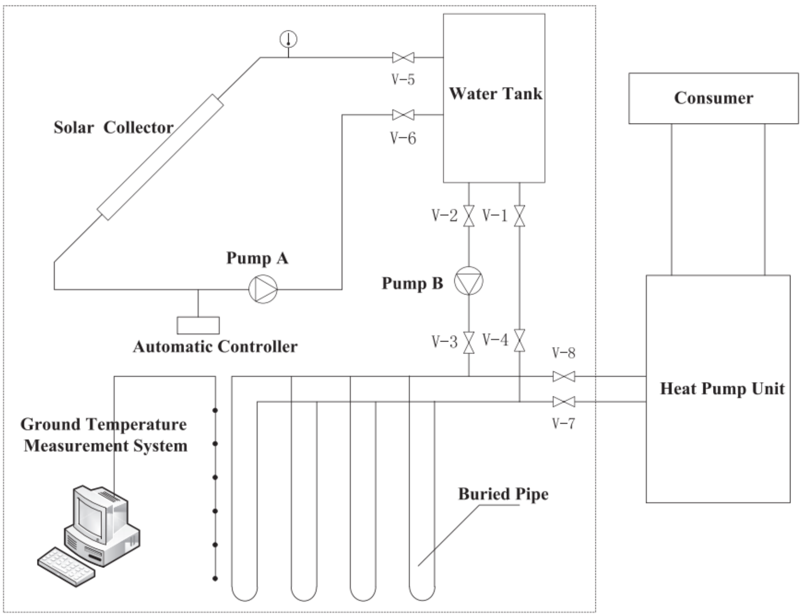

Figure 8. A central solar seasonal storage system based on GSHP by Liu et al. [59].

Yang et al. [60] studied a set of SAGSHP experimental devices located at Yangzhou University, which were used for air-conditioning for laboratories and office buildings. The BHE system was a closed-loop system with a length of 80 m. The system consisted of the following parts: a solar water storage circulation system (the heat absorbed by the solar collector was stored in the water tank), a storage water tank, and a plate heat exchanger water circulation system (heat exchange between the BHE system and the storage water tank). As shown in Figure 9, the solar collection and storage water cycle, the heat storage tank plate heat exchanger water cycle, the GHE water cycle, and the inner terminal water cycle could each be activated by operating the water pumps P1, P2, P3, and P4, respectively. The operation of the combined operation mode, the GSHP daytime operation mode, the GSHP daytime stop mode, the ground intermittent storage mode, and the ground continuous storage mode were analyzed and compared. The SAGSHP system operated in combination mode, where the ground and solar heat sources were dynamically coupled through a flat plate heat exchanger and a water tank. In this configuration, the ground served as an energy storage medium to retain excess solar energy. Under the experimental conditions described in this paper, the average unit COP and collection efficiency for the combination operation mode were 3.61 and 51.5%, respectively.

(**a**)

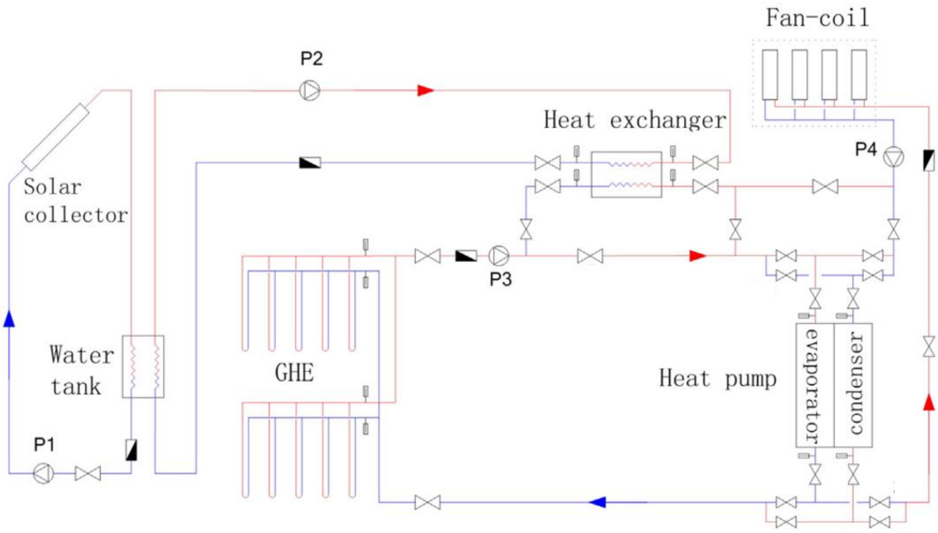

(**b**)

Figure 9. The experimental set-up of solar-ground source heat pump system investigated here by Yang et al. [60]. (**a**) Experimental system and (**b**) Schematic diagram of the experimental system.

Si et al. [61] studied a building located in Beijing, which used a new SAGSHP to provide heating, cooling and domestic hot water for the building (as shown in Figure 10). Two operation modes were compared: the first is SAGSHP, in which the working fluid first flowed through the solar collector and then entered the BHE. When there was sufficient heat in the solar collector, the excess solar heat could be stored in the soil to maintain the soil temperature. The second was SAGSHP, in which the heat collected by the solar collector during the day was stored in a storage tank and released to the BHE at night to restore the soil temperature. The BHE system was a closed-loop system with a length of 160 m. After 10 years of operation, the soil temperature of the former was only 0.8 °C lower, while that of the latter was 1.6 °C lower. A new operational strategy was proposed in which the heat pump was turned off during transitional seasons and the GHE was directly connected to the fan coil unit heat exchanger. This approach can reduce annual electricity consumption by 20.86%.

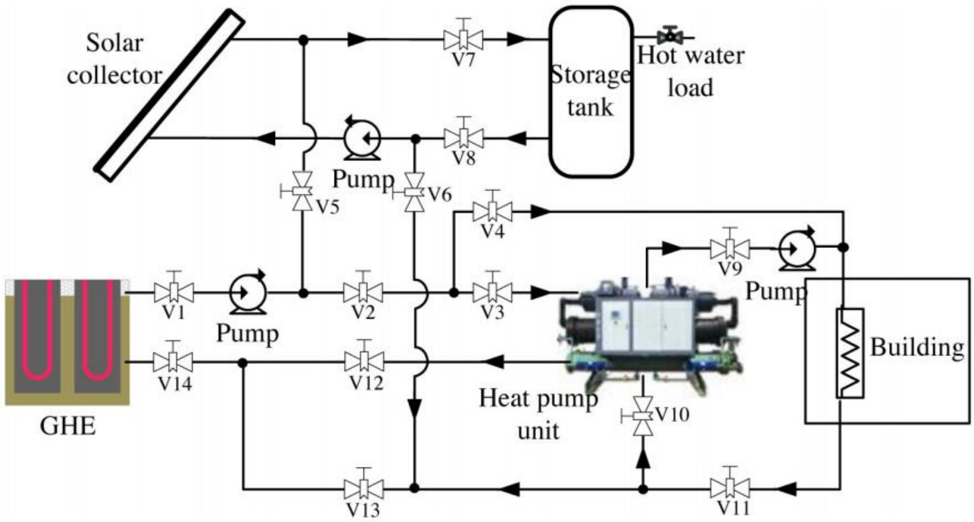

Figure 10. Schematic of SGSHPS(s) and SGSHPS(r) by Si et al. [61].

Yang et al. [62] investigated a SAGSHP installed in Nanjing, China. The system comprised five main components: BHE, heat pump unit, indoor terminal fan-coil system, solar collecting and storage system, and circulating water pump (as shown in Figure 11). The experimental system consisted of two U-tube vertical closed-loop boreholes, each with a depth of 30 m. The boreholes had a diameter of 110 mm and were spaced 4 m apart. The study analyzed four different operational modes: sole use of the GSHP mode, combined operation mode of solar collectors and GSHP, daytime operation with solar collectors and nighttime operation with GSHP, and nighttime operation with GSHP supplemented by solar thermal recovery. Comparison of the hybrid mode, day-night alternating mode, solar-powered U-tube heat exchanger mode, and GSHP mode, experimental and simulation results showed that the hybrid mode achieves COP values of 2.69 and 3.67 respectively, indicating superior comprehensive efficiency.

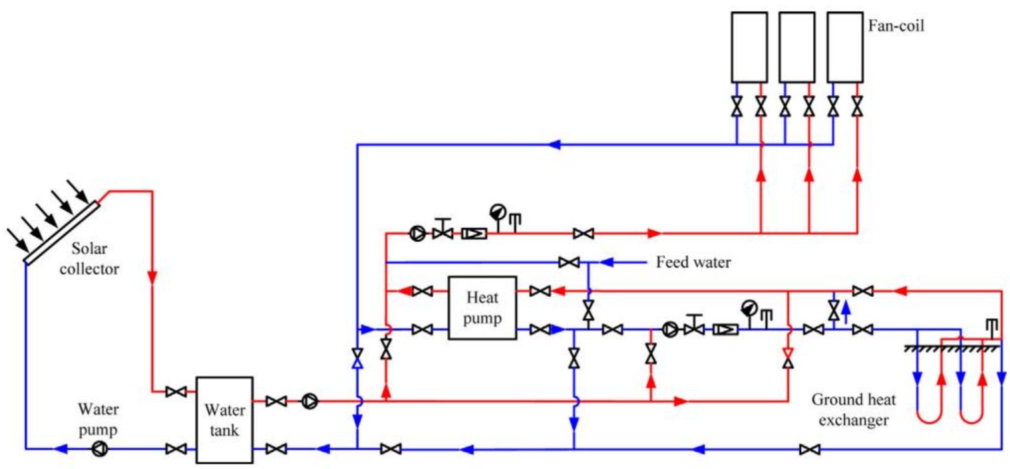

Figure 11. Schematic diagram of SAGSHP experimental system by Yang et al. [62].

Wang et al. [63] presented experimental research on a solar-assisted ground source heat pump system in Harbin. The GHE consisted of two sets of a total of 12 vertical single U-tubes. They were installed below the house with an individual depth of 50 m. The GSHP system functioned for both summer cooling and winter heating. However, during the winter heating season, the heat extracted from the ground significantly exceeded the heat injected into the soil during summer, leading to a potential deficit in thermal energy. Therefore, during non-heating seasons, solar collectors were employed to store heat in the soil, which could be utilized by the GSHP system during the heating season. After a year of operation, the solar system stored 70.76 GJ of thermal energy, while the GSHP system extracted 54.45 GJ of thermal energy. This storage strategy contributes to the stability of the GSHP system over extended periods and enhances the system's COP.

3.1.2. Hybrid GSHP-PVT for Both Heating and Power Generation

Li et al. [64] selected a residential area in Handan, China as the research object and proposed a GSHP-PVT system, to solve the problem of medium-deep ground temperature decay during long-term operation. The BHE system was a closed-loop system with a length of 1500 m. The system included three operating modes: (1) the GSHP extracted heat from geothermal wells to supply the user side; (2) the PV/T module heated the geothermal well water via the thermal storage tank, while simultaneously generating electricity; (3) the water from the PV/T module's thermal storage tank released heat into the soil through the geothermal well heat exchanger. Compared with the traditional GSHP system, the average soil temperature decreased by 1.4 °C after 20 years of operation, while the average soil temperature of the GSHP-PVT system increased by 0.09 °C, effectively solving the problem of ground temperature decay during long-term operation. An analysis of the first-year power balance shows that the system can generate 196,850 kWh of electricity, meeting a demand of 121,920 kWh, with the surplus available for sale to the grid.

Yan et al. [65] studied the GSHP-PVT system located in Tikanlik, China (40.63° N, 87.70° E). The principle of the system (as shown in Figure 12) was that when the temperature of the solar panel exceeded 50 °C, water was used to transfer the heat from the solar panel to the soil. When the solar panel temperature fell below 48 °C, the water pump was turned off. This approach reduced the temperature of the solar panel and improved the efficiency of the PV system. The BHE system was a closed-loop system with a length of 100 m. By cooling the system, the typical daily panel temperature was reduced by 26.8%, and compared with the traditional PV system, its PVT efficiency and annual power generation were increased by 4.1–11.1% and 7.9%, respectively. After ten years of simulated operation, the ground temperature increased by approximately 6.7 °C.

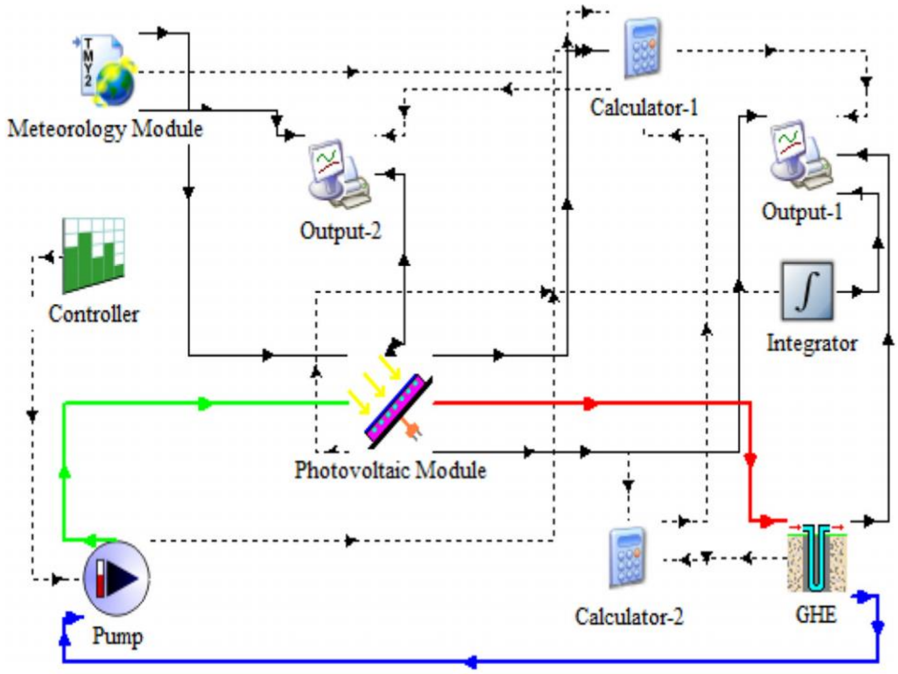

Figure 12. Schematic diagram of a GSHP-PVT system model built using TRNSYS by Yan et al. [65].

Jeong et al. [66] proposed a GSHP-PVT system for a simulated standard residential building in Seoul, South Korea (as shown in Figure 13). The BHE system was a closed-loop system with a length of 150 m. The operation mode was classified into three distinct categories: heating and cooling mode, heat storage mode, and subsurface heat storage mode. The building heating load was predominantly satisfied by the GSHP system. The GSHP system alone was used for cooling during the summer, PVT and storage tanks were used for heating and hot water supply in winter. By using the PVT system, 19% of the total heat supply can be provided, and the operating time of the GSHP system can be reduced by 12%. The system has a 55.3% higher seasonal performance factor (SPF) than the

GSHP system. Due to the power generation from the solar photovoltaic system, the average SPF during the heating period increased to 5.33, which is a 102% increase compared to the building's existing daytime system.

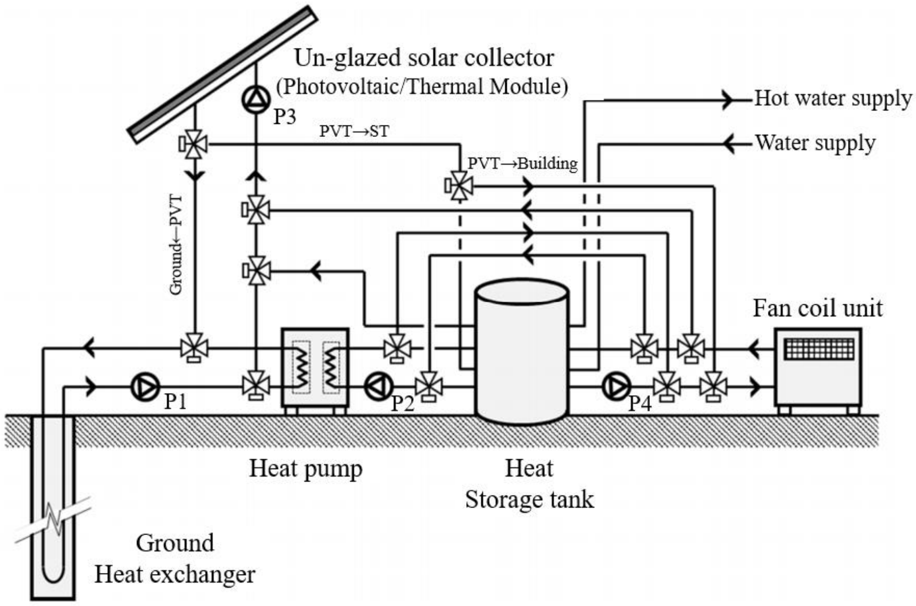

Figure 13. System concept of GSHP-PVT system by Jeong et al. [66].

Xia et al. [67] proposed a design optimization strategy for GSHP-PVT systems to address the design challenges of hybrid systems. A model based on Artificial Neural Network (ANN) was utilized to forecast performance, while a Genetic Algorithm (GA) was implemented as the optimization strategy. A total of 180 scenarios were designed and simulated. Based on a typical Australian residential building, the optimal design option is compared with two baseline design cases, and the annual CO_2 emissions are reduced by 29.5% and 31.4%, respectively. Under the 20-year operating conditions, the life cycle cost (LCC) of the GSHP-PVT system is reduced by 20.1% and 10.2%, respectively.

Pourier et al. [68] studied a building located in Stockholm, Sweden, and analyzed the technical and economic feasibility of integrating free cooling and PVT collectors into a residential GSHP system. With 4 boreholes, 5 m borehole spacing, and 300 m borehole depth, the system compared with GSHP system can improve the SPF by 1.3% over a 20-year system operation.

Lazzarin et al. [69] presented the refurbishment of a school building in northern Italy, where PVTs were coupled with a GSHP system. Solar radiation was used to generate electricity, power the heat pump, provide domestic hot water, and store heat in the ground. The system extracted 14,695 kWh of heat from the ground annually, while 19,722 kWh of heat were injected. The design of the plant, modeled through dynamic simulation, evaluated five alternatives by expanding the solar field (20–40–60 m²) and reduced the ground field (500–400–300 m), in comparison to a conventional system utilized a natural gas boiler and an air/water chiller. A solution with 60 m^2 of PVTs and 300 m of borehole was identified through dynamic simulations as the one with the best performance and lowest cost. A comparison between the proposed scheme and the conventional approach in terms of operation shows that the system yields a net annual savings of €3470.

Jakhar et al. [70] investigated the hybrid system integrating a PV/T solar system with an earth-water heat exchanger. The experimental apparatus was situated in Rajasthan, India. The earth-water heat exchanger system consisted of pipes with a diameter of 0.02 m, each 80 m in length, buried in flat, dry soil at a depth of 3 m. The system enhanced the electrical generation efficiency of photovoltaic panels by cooling them with water and transferring the heat through water to the ground for cooling. Different experiments were conducted to determine the optimal flow rate for the system. Compared to a system without cooling, the electrical generation efficiency of the system increased by approximately 1%.

Kastner et al. [71] studied the application of seasonal solar heat storage in aquifers under typical basin geology in Germany. The wells are connected to the formations over a vertical distance of 200 m with lengths ranging from 150 to 350 m. During loading mode, thermal solar energy is harvested and stored in a subsurface aquifer by means of hot water bodies (as shown in Figure 14). In unloading mode, the injected water bodies are produced form aquifer and reinjected into the water supply well after heat extraction at surface. The annual schedule includes a thermal storage period from April to September and a thermal supply period from November to February. During the thermal storage period, the total amount of solar energy stored can reach 4,580,000 kWh. After five years of system operation, the fluid temperature increased by at least 13 °C during low and medium flow conditions.

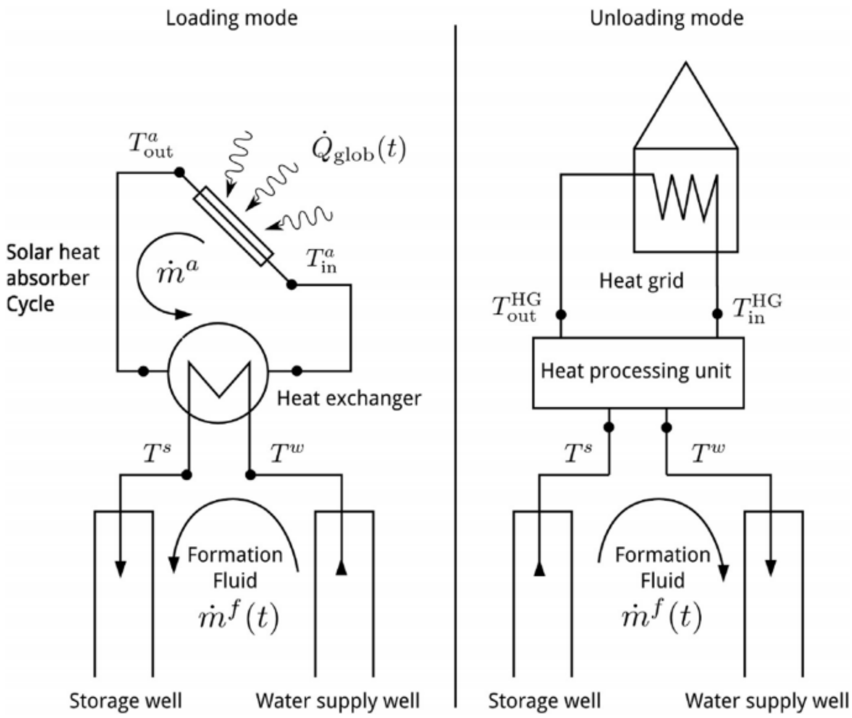

Figure 14. Schematic diagram of an ATES-equipped solar energy supply system by Kastner et al. [71].

3.1.3. Geothermal System Coupled with a Solar Chimney

The solar chimney is another way to improve the effectiveness and functionality of the geothermal system. By establishing a connection between the solar chimney and the geothermal system using ducts, the overall performance of the system can be improved. The design can be customized according to the specific climate and building layout in order to optimize system flexibility and efficiency in various seasons and weather conditions.

Noorollahi et al. [72] proposed a novel configuration that integrated a solar chimney with a waste geothermal spring, taking advantage of Iran's abundant geothermal spring resources. This integration aimed to generate stable and clean electricity by combining solar and geothermal resources, thereby improving electricity generation efficiency. The system consisted of a solar chimney at the center, surrounded by transparent collectors and a geothermal spring at the bottom (as shown in Figure 15). Solar radiation and heat released from the spring heated the air, increasing its velocity through the heating process and the chimney effect. The accelerated air drove a turbine inside the chimney to generate electricity. The system could utilize low-temperature geothermal energy for nighttime power generation, significantly reducing the storage costs of the solar chimney system. By comparing full geothermal mode (FGM), full solar mode (FSM) and geothermal solar mode (GSM), the heat transfer rate under GSM was 585.12% greater than that under FGM and 17.1% greater than that under FSM. Due to the combined effects of solar radiation, hot geothermal water, and ambient air temperature variations, the power generation under GSM exceeded the sum of that under FSM and geothermal heat exchange power generation. By comparing the power generation of the system, the combined solar chimney and geothermal spring system generated 21.06% more electricity than the solar chimney system alone.

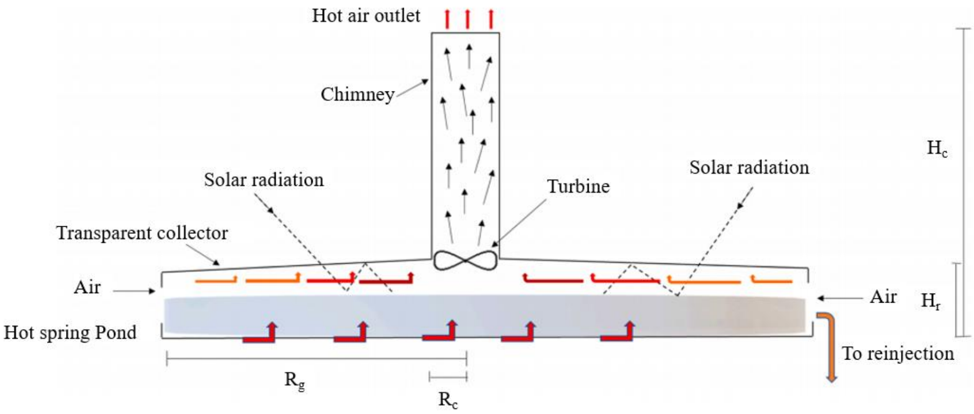

Figure 15. Schematic diagram of the cooling process by the coupled geothermal system by Noorollahi et al. [72].

Yu et al. [73] constructed an EAHE-solar chimney coupled geothermal system in Omaha, Nebraska, USA. The purpose of the system was to provide ventilation and cooling for an experimental building. The principle of the system was that the air in the solar collector was continuously heated by solar radiation, creating a temperature difference with the air in the solar chimney, which caused indoor air to be drawn into the solar chimney, and the indoor space became negatively pressurized, continuously drawing in outdoor air into the EAHE. After entering the EAHE, the air was heat-regulated through pipes and soil, providing cooling capacity for the indoor space. Analysis of experimental data on outdoor air environment, indoor air environment, and soil temperature showed that in most cases, the EAHE-solar chimney coupled geothermal system met indoor environmental requirements. From Figure 16, the variation of soil temperature closer to the EAHE tube was more pronounced compared to locations further from the tube. For instance, the underground soil temperature at 0.3 m above the EAHE remained at approximately 17.8 °C during the initial passive cooling period. However, it increased to 21.1 °C during the forced airflow test and even exceeded the temperature curve at 1.2 m above the tube. Subsequently, the temperature gradually stabilized at around 18 °C over the course of two weeks. Passive cooling methods are more stable than active cooling methods, and excessive heat extraction from the soil in forced air mode may lead to soil saturation around the pipes, requiring a significant amount of time for recovery.

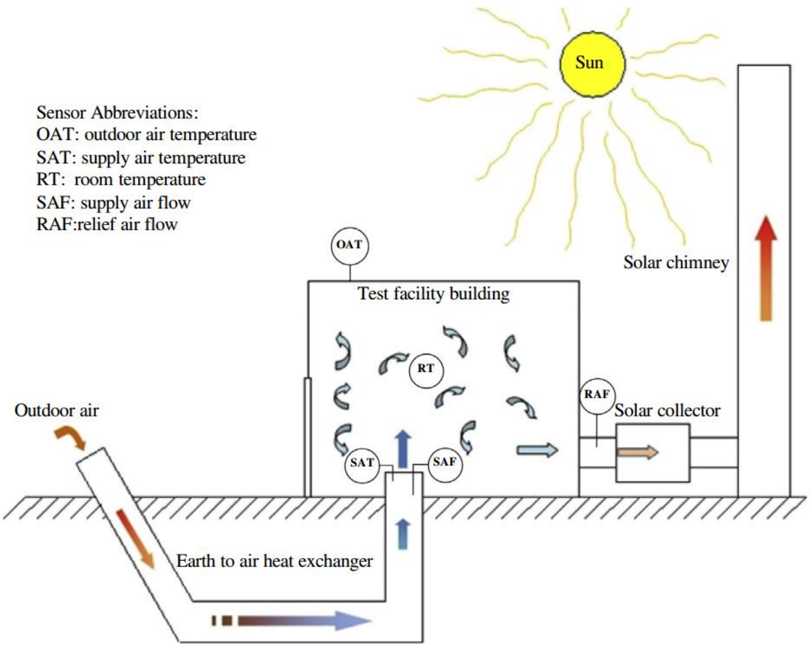

(a)

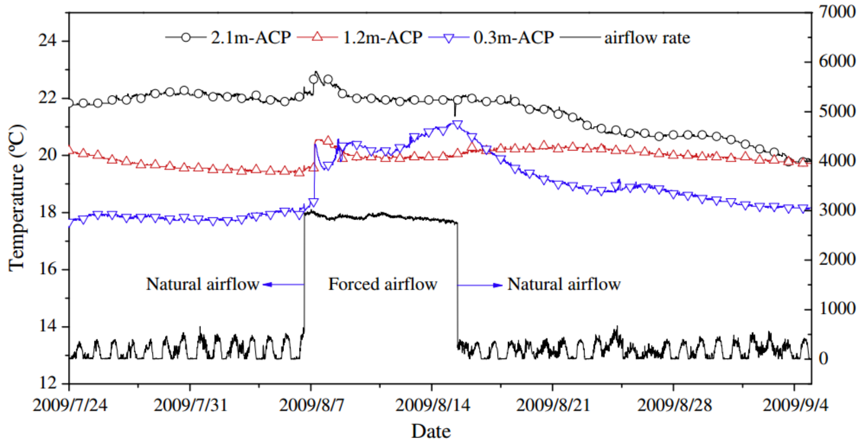

(**b**)

Figure 16. The coupled geothermal system by Yu et al. [73] (**a**) Layout of the system and (**b**) The underground soil temperature at three different heights above EAHE.

Elghamry et al. [74] presented an experimental investigation of a combined solar chimney and geothermal air duct for indoor heating and ventilation of buildings in the hot semi-arid climate conditions of New Borg El Arab city, Alexandria, Egypt. The geothermal air duct was used to provide fresh and preheated air to the building, and the solar chimney effect was utilized to draw the air from the duct into the building. Additionally, photovoltaic (PV) panels were installed at the back of the solar chimney, which both reduced heat loss from the chimney, enhanced the chimney effect, and generated some of the electricity required by the building. By comparing the indoor temperature and ventilation rate with and without the PV system in the chimney, it was shown that the proposed system could meet the heating and ventilation requirements of the building, while also generating electricity to power the building. The maximum temperature increases inside the room were 7.2 °C, 6.4 °C, 5.1 °C, and 4.3 °C for the forced convection system, natural convection system without PV, natural convection system with PV at 45°, and natural convection system with PV at 30°, respectively. The daily ventilated air volumes for the natural geothermal system coupled with the solar chimney were 374.2 m^3, 289.17 m^3, and 232.47 m^3 for the solar chimney without PV, the solar chimney with PV at 45°, and the solar chimney with PV at 30°, respectively.

3.1.4. Summary of Solar-Geothermal Hybrid Heating Systems

Solar-geothermal hybrid heating systems can utilize solar energy to assist geothermal heating in cold regions during winter. The solar thermal storage in a hybrid system can reduce the length of the BHE required by a traditional GSHP. This reduces the construction costs of the system.

The research on geothermal and solar energy coupled systems primarily encompasses system optimization and efficiency improvement, technical applications, economic evaluations, as well as control strategy. Key areas of investigation include: optimizing system design through algorithms, analyzing the dynamic performance of the coupled system under various operational strategies (such as utilizing solar thermal storage to release heat into the BHE to restore soil temperature or using the solar energy system to assist in heating and reduce the operational time of the GSHP), evaluating the economic viability of the coupled system (such as reducing BHE length by using solar thermal storage) and integrating emerging research technologies. Some important points, including the region, research methodology, system characteristics and conclusions of the reviewed studies have been summarized in Table 1.

Table 1. Summary of the solar-geothermal hybrid heating systems.

Reference	Region	Research Methodology	System	System Characteristics	Main Conclusions	Remark
[56]	Milton, Canada (43.52° N, 79.88° W)	Simulation	SAGSHP	Desuperheater-equipped liquid source heat pump	BHE length was reduced by 30 m. An 18.26% higher EFT and a 2.84% higher COP than the GSHP system.	Heating-dominated regions
[57]	Montréal, Canada (45.50°N, 73.57°W)	Simulation	HGSHP	Double U-tube BHE	In energy savings of 3.5% and 6.5%. BHE depth was reduced by 17.6%.	Well-insulated buildings with heating demand only
[58]	Tongzhou, Beijing (39.90° N, 116.65° E)	Experiment and simulation	SAGSHP	An array of BHEs with multiple types and lengths	The temperature drop rate of the soil and rock was reduced by 0.78%.	Constant temperature of rock and soil and sufficient solar energy
[59]	Tianjin, China (39.34° N, 117.36° E)	Experiment and simulation	SAGSHP	Thermal equilibrium research for solar seasonal storage system coupling with GSHP	Total solar radiation was 2.03 times the average heat extraction. Soil heat balance can be achieved by coupling the solar energy storage	Heating-dominated regions
[60]	Yangzhou, China (32.39° N, 119.43° E)	Experiment and simulation	SAGSHP	Different heat source coupling modes	Combined operation mode has the highest collection efficiency of 51.5%.	Heating-dominated regions
[61]	Beijing, China (39.90° N, 116.40° E)	Simulation	SAGSHP	Solar heat is released to the BHE at night to restore the soil temperature.	Annual electricity consumption was reduced by 20.86%. Soil temperature was only 0.8 °C lower after 10 years of operation.	In transition seasons, keeping the heat pump off
[62]	Nanjing, China (32.06° N, 118.79° E)	Experiment and simulation	SAGSHP	Multi-mode operational SGSHPS experimental system	The combined operation mode achieved COP values of 3.67.	Heating-dominated regions
[63]	Harbin, China (45.80° N, 126.53° E)	Experiment	GSHP-PVT	Seasonal thermal storage, 12 vertical U-tube BHEs	After a year of operation, the system stored 70.76 GJ thermal energy, while the GSHP system extracted 54.45 GJ.	Severe cold regions
[64]	Handan, China (36.62° N, 114.48° E)	Simulation	GSHP-PVT	1500 m MBHE	Average soil temperature increased by only 0.09 °C, effectively solving the problem of ground temperature decay. The system can generate 196,850 kWhof electricity.	Cold regions
[65]	Tikanlik, China (40.63° N, 87.70° E)	Simulation	GSHP-PVT	Solar panel temperature is controlled between 48 °C and 50 °C	PV efficiency and annual power generation increased by 4.1–11.1% and 7.9%, respectively. Ground temperature increased by approximately 6.7 °C after 10 years.	The arid climate
[66]	Seoul, South Korea (37.56° N,	Simulation	GSHP-PVT	Use the PVT system to reduce the GSHP operating time	The system has a 55.3% higher SPF than GSHP system.	Temperate monsoon climate

	126.97° E)					
[67]	Australian (25.27° S, 133.77° E)	Simulation	GSHP-PVT	ANN model was used for performance prediction. GA was employed as the optimization technique	Annual CO_2 emissions were reduced by 31.4%. LCC of the GSHP-PVT system was reduced by 20.1%.	Temperate marine climate
[68]	Stockholm, Sweden (59.32° N, 18.06° E)	Simulation	Free cooling + GSHP	Integration of free cooling and PV/T into a GSHP system in a severe winter climate	Free cooling + GSHP system can improve the SPF of the GSHP system by 1.3% over a 20-year system operation.	Temperate marine climate
[69]	Belluno, Italy (46.20° N, 12.21° E)	Simulation	GSHP-PVT	Solar radiation for generating electricity, powering the heat pump, providing domestic hot water, and storing heat in the ground	The system extracts 14,695 kWh of heat from the ground annually, while 19,722 kWh of heat are injected.	A rather severe climate in wintertime
[70]	Rajasthan, India (75.61° E, 28.38° N)	Experiment	PV/T solar system with earth-water heat exchanger	80 m horizontal BHE	Experimental electrical efficiency of IPVTS increased by 1.02–1.41% after cooling with EWHE.	The semi-arid regions
[71]	Berlin, Germany (52.52° N, 13.40° E)	Simulation	Solar ATES model	Enhancing the Energy and Economic Efficiency of ATES Systems by Solar Thermal Energy and Electricity	After five years of system operation, the fluid temperature increased by at least 13 °C during low and medium flow conditions.	A sedimentary setting typical
[72]	Iran (33.15° N, 58.78° E)	Simulation	Solar chimney with waste geothermal spring	Integration of abandoned geothermal springs with solar chimneys	The combined solar chimney and geothermal spring system generated 21.06% more electricity than the solar chimney system alone.	An abandoned hot spring
[73]	Omaha, Nebraska, USA (41.25° N, 95.94° W)	Simulation	EAHE-solar chimney coupled geothermal system	An EAHE-solar chimney coupled geothermal system in natural and forced airflow conditions	Excessive heat extraction from the soil in forced air mode may lead to soil saturation around the pipes, requiring a significant amount of time for recovery.	Free space cooling in summer
[74]	New Borg El Arab, Alexandria, Egypt (31.2° N, 29.91° E)	Simulation	Combined solar chimney and geothermal air duct	Study of air flow in the geothermal pipe environment influenced by solar chimneys	The maximum output PV power was 117 W, representing about 86.7% of the maximum PV power outside the chimney.	Mediterranean climate

3.2. Wind-Geothermal Energy Hybrid Systems

Wind and geothermal energy hybrid systems employ wind turbines to produce electricity, which is subsequently utilized to operate a geothermal heat pump. The generated electricity can be utilized to meet the electrical requirements of the building or be sold to the power grid. Geothermal energy addresses the base load demands of buildings, while photovoltaic and wind power supply electricity and supplement demand during peak periods. This approach is utilized simultaneously for both building heating and power generation.

3.2.1. Hybrid Wind and Geothermal Energy Systems

Aryanfar et al. [75] investigated a hybrid system in Shanghai, China, which consisted of a geothermal heat pump with a wind turbine (as shown in Figure 17). The wind turbine generated electricity to meet the power needs of the GSHP and the building, with any excess electricity fed back into the grid. The geothermal pump extracted heat from the ground. During cooling, the refrigerant absorbed heat before it was pressurized and heated by the compressors. Then it released heat through the condenser. In heating mode, the heat was transferred from the refrigerant to the indoor environment. By studying the effects of variations in condenser pressure, evaporator pressure, intermediate pressure, ambient temperature, and soil temperature on the net power output of the heat pump system, it was observed that increasing the condenser pressure from 350 kPa to 500 kPa resulted in an increase in the system's net power output from 21.98 kW to 22.14 kW. The total installed capacity of wind turbines in Shanghai was 49.33 kW, which could meet the electricity demand of the heat pump system. The wind turbine can provide stable and clean electricity for the system when the grid electricity consumption reaches its peak.

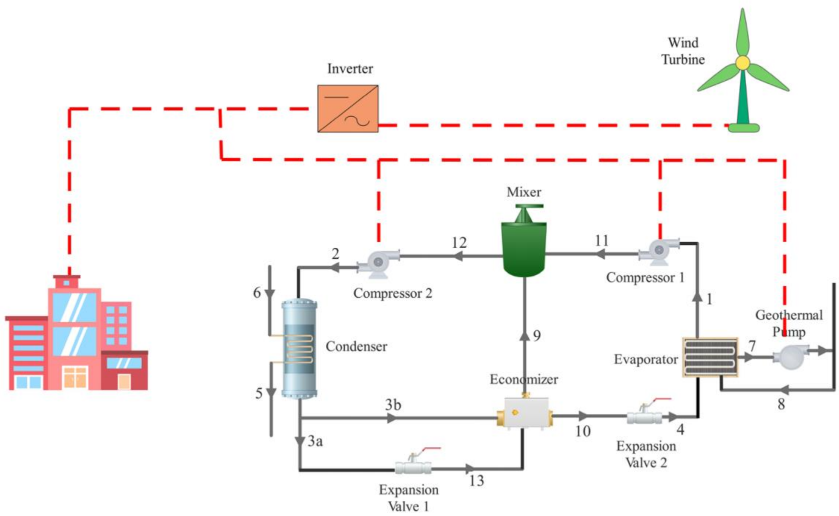

Figure 17. Schematic of geothermal heat pump and wind turbine hybrid system by Aryanfar et al. [75].

Ciapala et al. [76] presented a model study of a system consisting of a geothermal heat source, thermal energy storage systems and a wind turbine in Warsaw (Poland). Wind energy was used to power electric heaters or heat pumps, which were connected to large, insulated tanks employed for thermal storage. The wind turbine was used to increase the peak performance of the GSHP system, which was used to compensate for the limitations of geothermal energy due to soil conditions and provide energy for the heating system. In the Warsaw climate, to provide electricity for a 1000 m^2 house, the system requires 4800 kWh of thermal storage, 45 kW of geothermal source and 5 kW of wind source. A system designed in this manner would minimize wind curtailment, optimize the utilization of geothermal resources, and enhance the reliability of the supply.

Bamisile et al. [77] presented a wind-geothermal hybrid multi-generation system designed to produce electricity, hydrogen, hot water, cooling, and seawater desalination (as shown in Figure 18). The wind turbine transformed incoming wind energy into mechanical energy, which was then converted into electrical energy. The produced electricity was initially directed to the control center before being distributed to the various subsystems. The majority (70%) of the generated power was supplied to the end users, while 15% of the total electricity was utilized in the power desalination system to produce fresh water. Additionally, 10% of the total power output was used by the cooling system to generate cooling effects, and the remaining 5% was allocated for hydrogen production. By integrating the Kalina cycle of geothermal energy with wind power generation, the system ensured stability. Under both electricity-only and multi-generation conditions, the system's energy and exergy efficiencies were significantly improved, from 17.73% and 22.45% to 81.01% and 52.52%, respectively. The total electricity generated by the geothermal-Kalina system and wind power system was 9,940,000 kWh/year and 2,540,000 kWh/year, respectively.

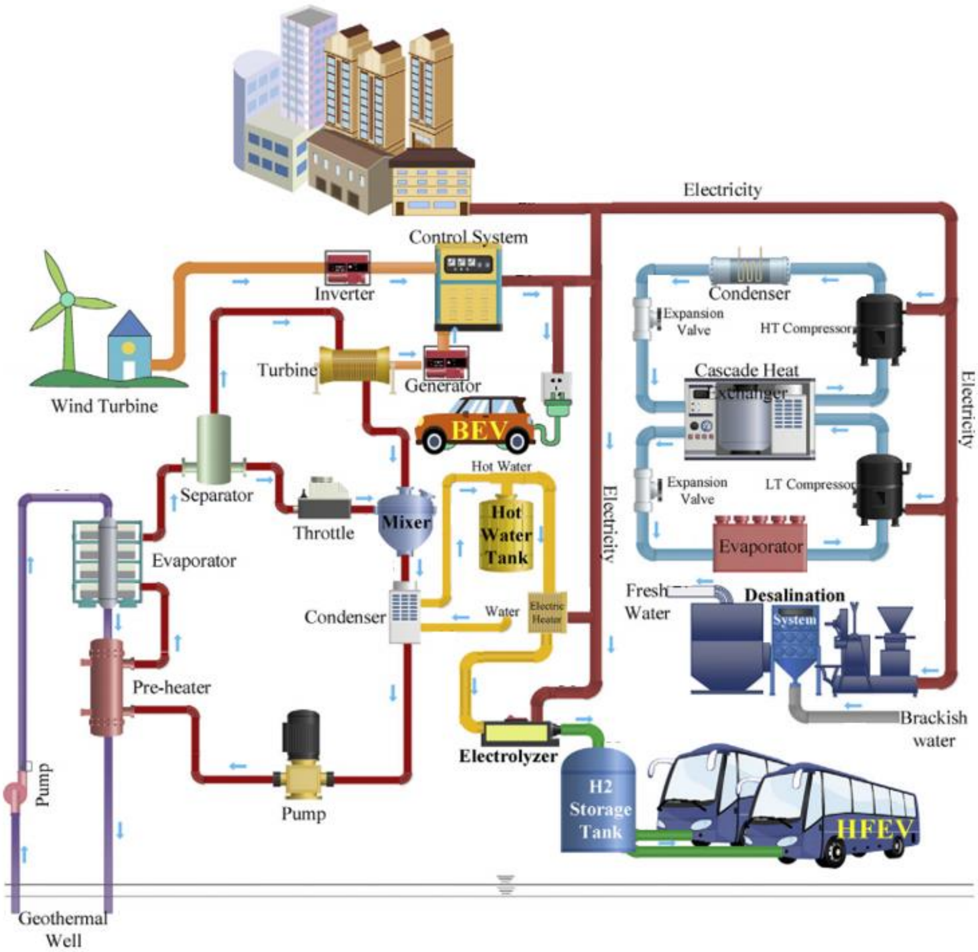

Figure 18. Schematic diagram of the proposed geothermal-wind multigeneration system by Bamisile et al. [77].

3.2.2. Hybrid Wind, Solar and Geothermal Energy Systems

Wind energy, solar energy and geothermal energy are also used simultaneously for building heating and power generation. Xu et al. [78] proposed a multi-energy supply coupling framework to construct a renewable energy system that can provide electricity, heating, and hydrogen for communities by utilizing the complementarity of geothermal energy, solar energy, and wind energy (as shown in Figure 19). The system comprised a solar thermal system, wind turbines, GSHPs, and an electrolyzer. In the framework of the energy hub, hybrid renewable energy was first converted into electrical energy, thermal energy, and hydrogen carriers through PV/T system, wind turbine, GSHP, and electrolyzers. Subsequently, it was transformed, regulated, and stored through BES systems, hydrogen tanks, and combined heat and power (CHP) units. At the output end, it was converted into community electricity, thermal energy, and hydrogen loads. This system reduced energy loss and efficiently coordinated multiple energy and energy storage systems. The accommodation of solar and wind energy can be enhanced by up to 1.59%.

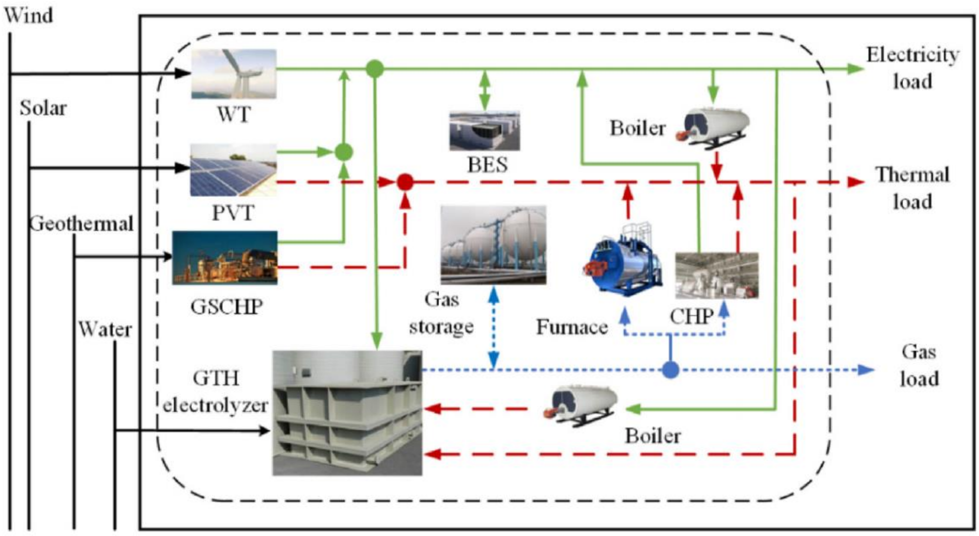

Figure 19. Geothermal-solar-wind renewable energy hub framework by Xu et al. [78].

Kazmi et al. [79] investigated a hybrid geothermal-photovoltaic-wind power system for a village in Pakistan. The system operated normally using geothermal energy to meet the community's basic load demand throughout the year, while the photovoltaic and wind power plants supplied electricity to the grid, and supplemented the demand during peak periods. Through an integrated simulation of the region's geothermal, solar, and wind resources, a hybrid system with capacities of 250 kW, 250 kW, and 100 kW for geothermal, photovoltaic, and wind power, respectively, was found to be a feasible design, with a Net Present Cost (NPC) of 234.11 million Pakistani Rupees and an interest rate of 5%. The system could meet an average daily load demand of 7350 kWh, with excess energy sold to the grid. The proposed system had a Cost of Energy (COE) of 7.50 Pakistani Rupees/kWh and was expected to avoid 1.8 million kilograms of CO_2 emissions and other air pollutants.

Geng et al. [80] proposed a multi-energy complementary heating system integrating solar energy, wind energy, and geothermal energy based on the meteorological conditions and geothermal resources in Zhengzhou, Henan Province. The system consisted of four subsystems: the solar collector subsystem, the geothermal subsystem, the wind energy subsystem, and the two-stage reheat subsystem. The solar collector subsystem heated the heat transfer fluid using solar collectors and stored energy in a thermal storage tank. The geothermal subsystem raised the temperature of the circulating water by applying work, predominantly through the operation of an inverse Carnot cycle. The wind energy subsystem generated electricity to drive compressors, and the geothermal subsystem enhanced the circulation of water. Finally, the two-stage reheat subsystem adjusted water temperature to meet user-side demands. The wind turbine system outputted power ranging from 0 to 3000 kW, ensuring the normal operation of the geothermal system. The average heat exchange efficiency during the heating season reached 90%, effectively meeting user requirements.

3.2.3. Summary of Wind-Geothermal Hybrid Heating Systems

In regions with abundant wind energy resources, utilizing wind power generation to meet electricity demands while simultaneously harnessing geothermal energy for heating is an effective approach.

Current research on wind-geothermal hybrid heating systems encompasses several key areas: the design of the coupling system (including determining the number of wind turbines and the borehole depth for ground-source heat pumps), the integration of the system and the design of control systems and energy management strategies (such as using wind power to meet the electrical needs of the ground-source heat pumps and buildings or for other industrial purposes), and the use of auxiliary systems (such as two-stage reheat subsystems). The main characteristics of the reviewed systems in this part have been summarized in Table 2.

Table 2. Summary of wind-geothermal hybrid heating systems.

Reference	Region	Research Methodology	System	System Characteristics	Main Conclusions	Remark
[75]	Shanghai, China (31.23° N, 121.47° E)	Simulation	A geothermal heat pump with an intermediate economizer and a wind turbine	The wind turbine generates electricity to meet the power needs of the GSHP and building, with excess electricity fed back into the grid	Increasing the condenser pressure from 350 kPa to 500 kPa resulted in an increase in the system's net power output from 21.98 kW to 22.14 kW.	To provide the heat and electricity required during the winter
[76]	Warsaw, Poland (52.22° N, 21.01° E)	Simulation	Geothermal heat source combined with thermal storage and a wind turbine	Wind power generation fulfills peak demand	Provide electricity for a 1000 m^2 house, the system requires 4800 kWh of thermal storage, 45 kW of geothermal source and 5 kW of wind source.	Cooler periods (winter)
[77]	Inner Mongolia Autonomous Region, China (40.80° N, 111.65° E)	Simulation	Wind-geothermal hybrid multi-generation system	Produce electricity, hydrogen, hot water, cooling, and seawater desalination	The total electricity generated is 9,940,000 kWh/year and 2,540,000 kWh/year, respectively.	Temperate continental monsoon climate
[78]	/	Simulation	A multi-energy supply coupling framework to construct a renewable energy system	A multi-energy supply coupling system that can provide electricity, heating, and hydrogen for communities	The solar-wind accommodation can be improved by at most 1.59%.	/
[79]	Pakistan (33.61° N, 73.94° E)	Simulation	A hybrid geothermal-photovoltaic-wind power system	Using geothermal energy to meet the community's basic load demand, while photovoltaic and wind power plants supply electricity to the grid, and supplement the demand during peak periods	The system COE is 7.50 Pakistani Rupees/kWh and is expected to avoid 1.8 million kilograms of CO_2 emissions and other air pollutants.	Abundant resources of geothermal, solar, and wind energy
[80]	Henan, China (34.75° N, 113.66° E)	Simulation	An integrated heating system technology that combines solar energy, wind energy, and geothermal energy	Two-stage reheat subsystem	Wind turbine system outputs power ranging from 0 to 3000 kW. Average heat exchange efficiency during the heating season reaches 90%.	/

3.3. Air Source-Geothermal Energy Hybrid Systems

The geothermal energy is also combined with the air source heat pumps (ASHP) for building heating. The BHEs possess the advantage of high efficiency and the initial cost of ASHP is relatively low. The coupled system involves the simultaneous operation of the geothermal heat pump and the air source heat pump, where the geothermal heat pump is responsible for meeting the primary heating and cooling needs. The ASHP serves as an additional source of assistance during periods of high demand or when external air temperatures are more advantageous. This strategy can maximize energy efficiency, save operational expenses, and improve the overall dependability of the heating and cooling system.

3.3.1. Air Source-Geothermal Energy Hybrid Systems

Grossi et al. [81] studied the energy performance of a dual-source heat pump system (DSHP). The yearly simulation results were carried out based on a residential building in Bologna, Italy (as shown in Figure 20). The building's heating loads were much larger than the cooling loads. The ASHP was used to reduce the ground temperature attenuation after BHE's long-term operation. The DSHPs were conducive to overcoming the thermal unbalance of the ground caused by unbalanced heating and cooling loads. A reduction of the BHE length of 30% to 50% could be achieved with larger energy performance in the presence of strongly unbalanced loads. The investment cost was reduced concerning a GSHP of a percentage variable from 6% to 32%.

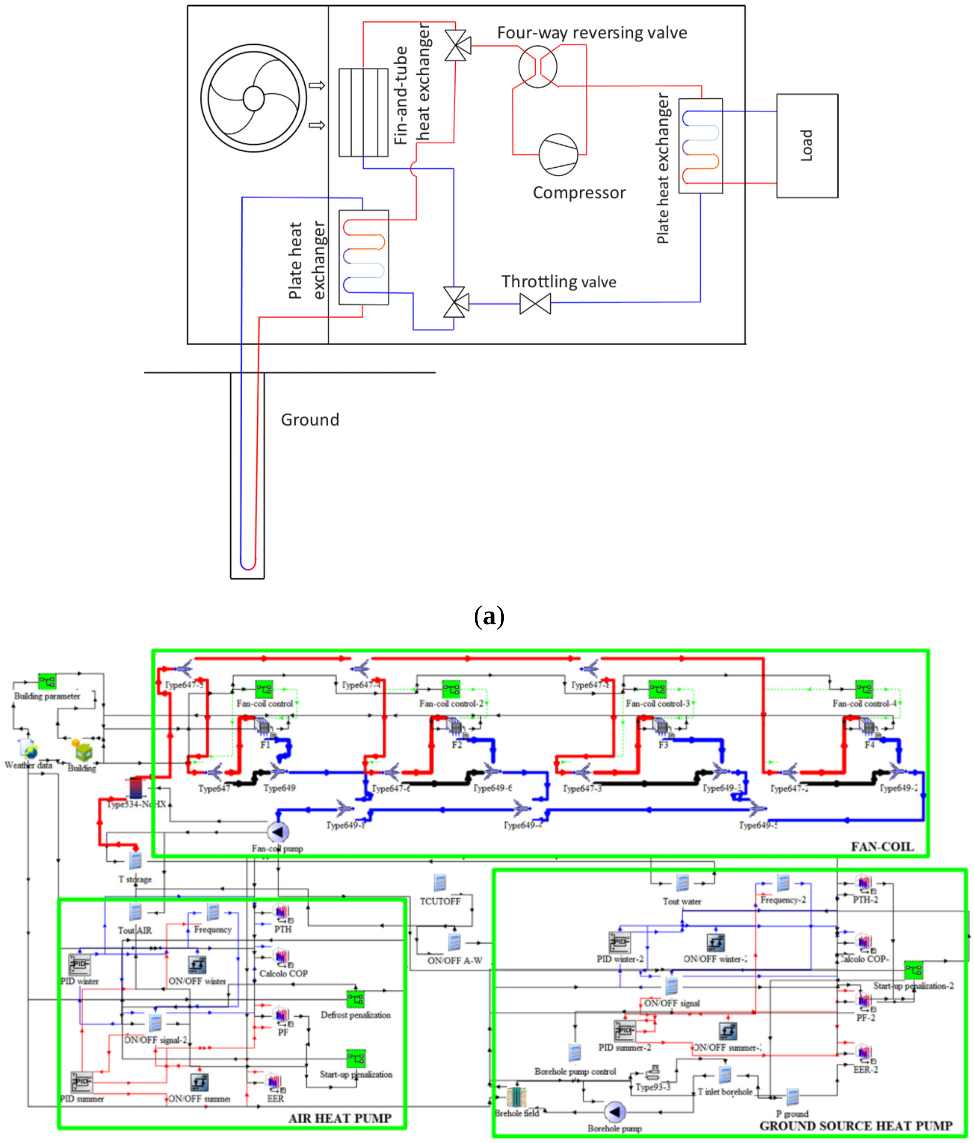

(**a**)

(**b**)

Figure 20. DSHP system by Grossi et al. [81] (**a**) Layout of the system and (**b**) DSHP system constructed in TRNSYS.

You et al. [82] also proposed a multi-mode air-source heat compensator (AHC) integrated GCHP to eliminate the thermal imbalance in cold regions. A hotel in Harbin, China with an 8700 m^2 air-conditioning area was selected for simulation. The AHC served as the auxiliary unit, which could inject heat into the soil, and supply heat directly for space heating simultaneously (as shown in Figure 21). It was found that the ASHP can inject the heat into the ground with the average COP ranging from 4.49 to 15.09. Compared to the conventional "boiler + split air conditioner" system, the coupled system achieves an energy savings rate of up to 23.86%.

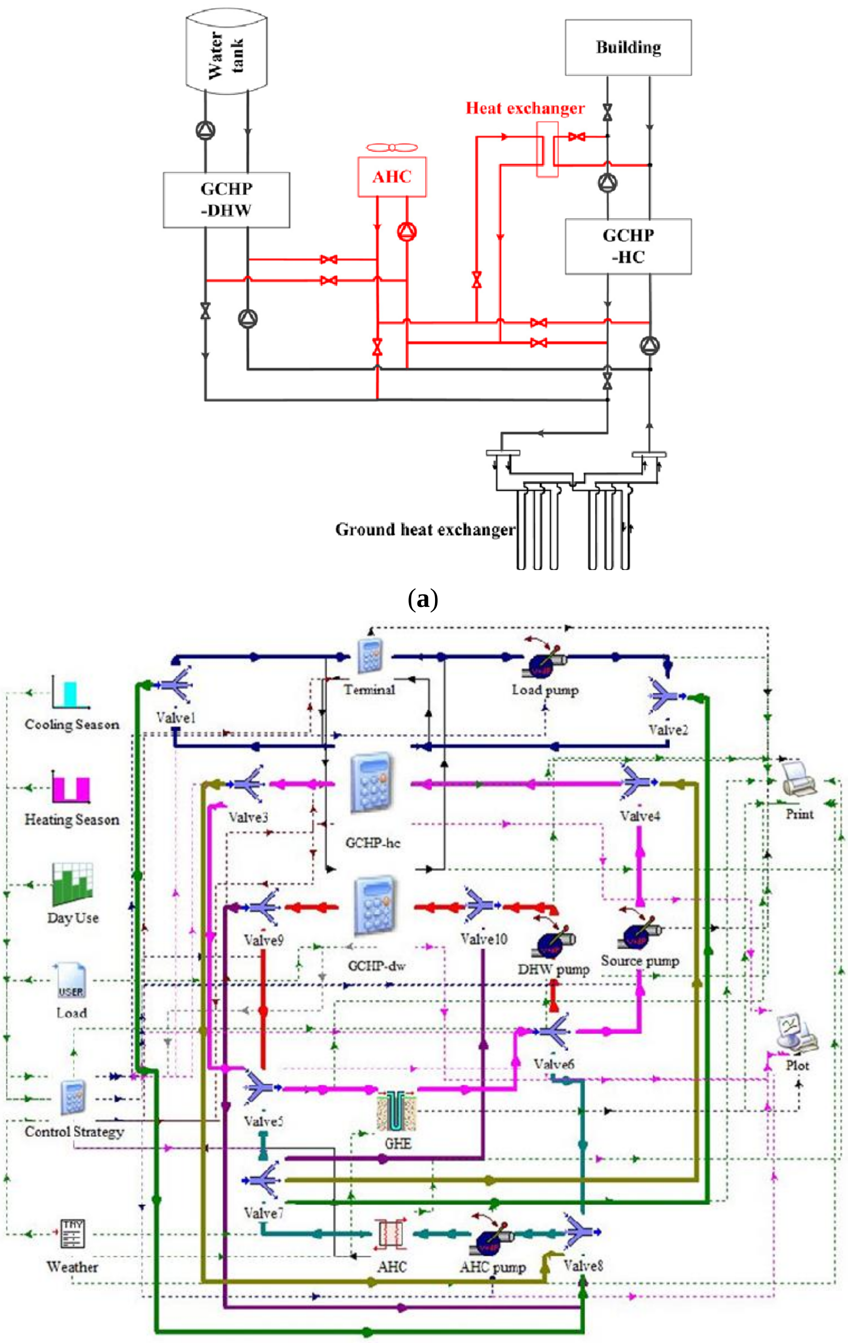

(**a**)

(**b**)

Figure 21. DSHP system [82] (**a**) Layout of the system and (**b**) DSHP system constructed in TRNSYS.

A hotel building energy supply system in northern China was taken as the research object to study the feasibility of a coupled air and GSHP system with energy storage [83]. An ASHP and a WSHP were utilized as supplementary heat sources for a portion of the heat provision (as shown in Figure 22). At a temperature of −6 ℃, the average COP of the system approached 2.3. The integration of energy storage equipment enabled the power grid to shift peak loads and minimized system running costs. The findings demonstrated that using an optimal defrosting control system could enhance the heating capacity of the ASHP by 13.9%. The proposed system has the capability to not only maintain the soil heat imbalance rate at 2.6%, but also to decrease the running cost. The unique system has an annual operation cost that is just 58% of the typical GSHP system, and it can minimize carbon emissions by 7.14%. The CAGHP system with energy storage offers a 42% reduction in operation costs compared to the typical GSHP system. Additionally, it results in a 7.14% decrease in carbon emissions and has an investment payback period of 3.16 years.

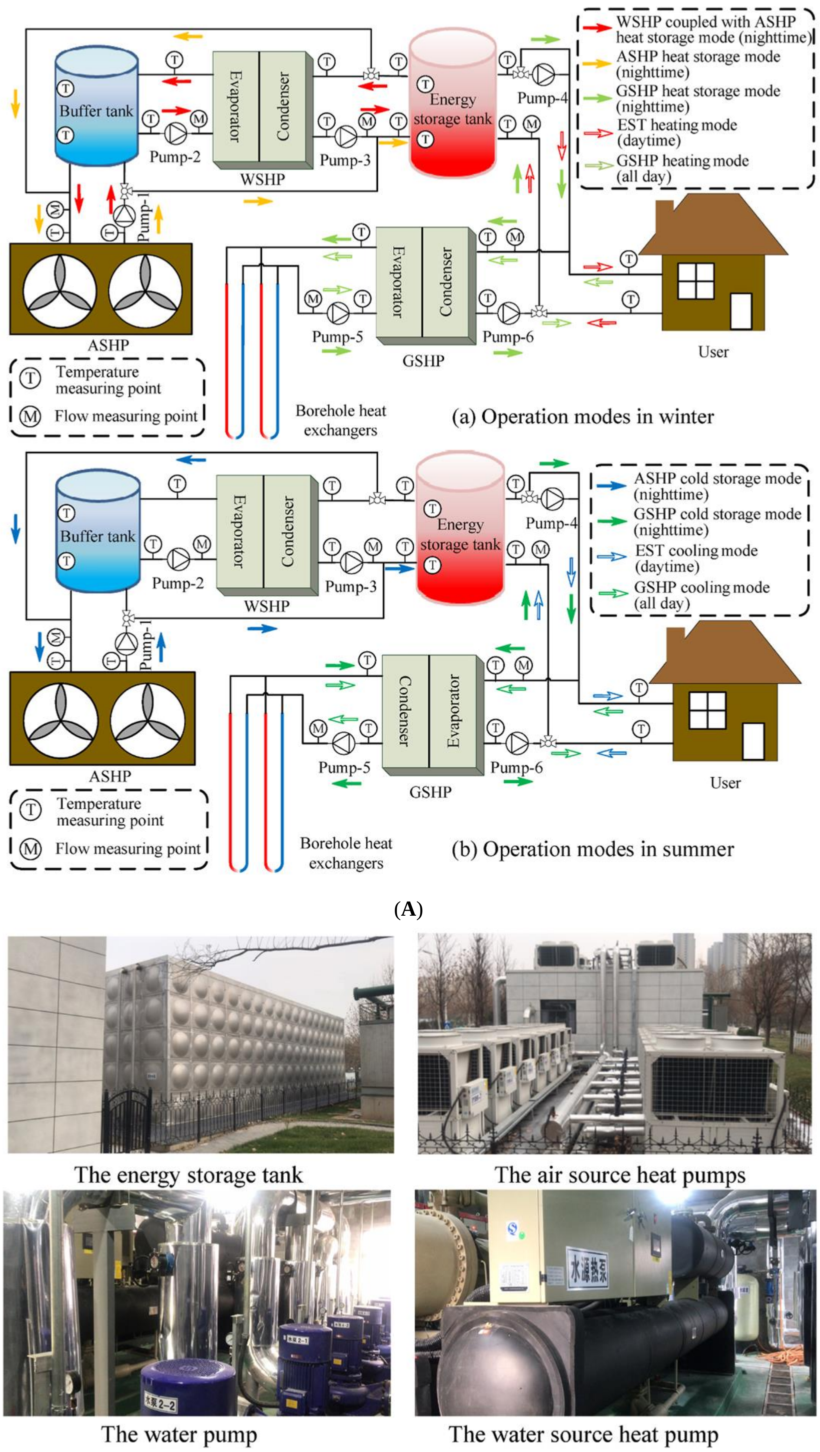

Figure 22. DSHP system [83] (**A**) Layout of the system and (**B**) Actual project photo.

Zheng et al. [84] investigated the performance of a photovoltaic-assisted GSHP and PVGSHP-ASHP for a campus building in Changsha, China. Three kinds of hybrid systems, i.e., the PVGSHP-ASHP system, photovoltaic assisted ground source heat pump and electric heater (PVGSHP-EH) system and photovoltaic assisted ground source heat pump system (PVGSHP) were simulated for performance and economy comparison (as shown in Figure 23). The number of the BHEs was 86 and the rated power was assumed to be 69 kW. The TRNSYS simulation results showed that the soil temperature decreased from 18.1 °C to 11.8 °C after 15 years of operation for the traditional PVGSHP-EH system. This led to a decrease in the annual COPGSHP from 3.2 kW/kW to 2.9 kW/kW and an increase in the annual electricity consumption from 77,468 kWh to 85,384 kWh. The PVGSHP-ASHP system effectively addressed the issue with its high annual COPGSHP and COP values of 3.49 kW/kW and 4.69 kW/kW, respectively. Additionally, it consumed just 71,700 kWh of power annually. In terms of cost, its annual lifespan cost was the lowest at 99,223 CNY, which is 8.1% lower than the PV-aided GSHP system. Following optimization, the PV-assisted GSHP-ASHP system achieved an annual lifecycle cost of 91,158 CNY, which represented an 8.1% reduction.

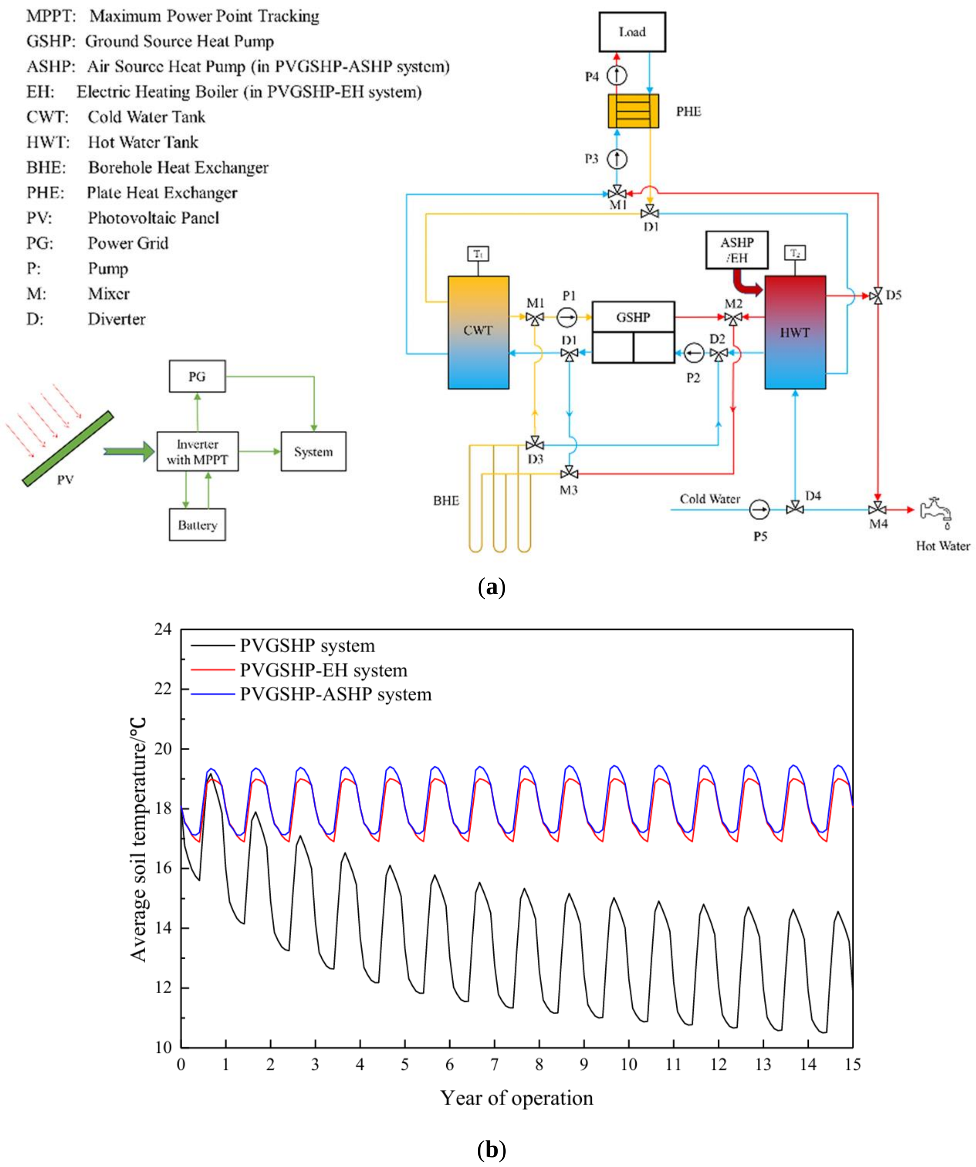

Figure 23. PV-assisted GSHP system by Zheng et al. [84] (**a**) Schematics of the PV-assisted GSHP system and (**b**) Average soil temperature changes for different systems.

Bottarelli et al. [85] numerically studied the DSHP system coupled with a flat-panel as a horizontal ground heat exchanger (HGHE) using COMSOL Multiphysics (as shown in Figure 24). The EnergyPlus software was used to simulate the TekneHub laboratory in Ferrara, Italy as a reference. A 2D computational domain was established, consisting of a flat-panel HGHE (2.5 m deep with a consistent heat flux) cross-section and a 6 m wide × 10 m deep soil domain, for soil temperature simulation. At flat-panel volume-to-length ratio r = 30, which represented around 17% of the standard r = 5, the ground heat extraction per meter of Flat-Panel was roughly 78 kWh/m for a temperature difference of 0 K and 33 kWh/m for a temperature difference of 10 K. The mean thermal dissipation rate was approximately 130 W/m for a temperature gradient of 0 K and 150 W/m for a temperature gradient of 10 K. Utilizing a DSHP might result in a substantial decrease in the size of the Flat-Panel HGHE, leading to a reduced cost for installation.

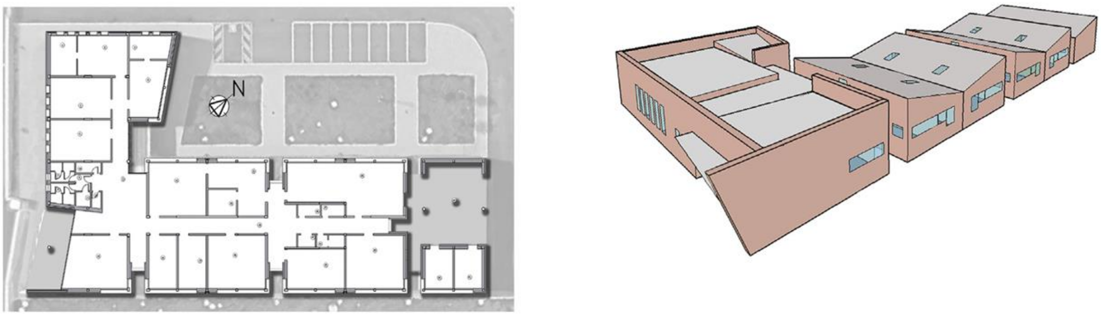

(**a**)

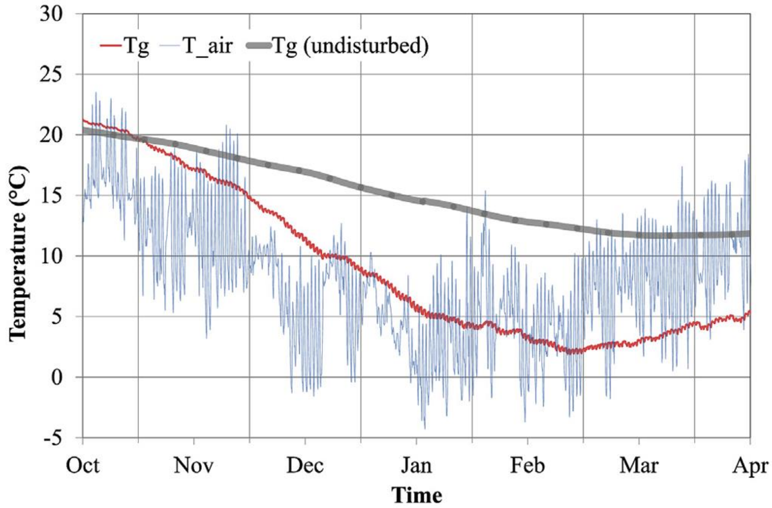

(**b**)

Figure 24. DSHP system with HGHE [85] (**a**) 3D model of TekneHub laboratory in Energy Plus and (**b**) Temperatures of air, undisturbed ground and Flat-Panel surface in the of GCHP.

3.3.2. Summary of Air Source-Geothermal Hybrid Heating Systems

In the hot summer and cold winter regions, air source-geothermal hybrid heating systems can effectively reduce the drilling length of BHE, thereby lowering the overall cost of the system.

Current research on GSHP-ASHP systems primarily focuses on two aspects. One aspect involves evaluating the performance of these systems. For example, how much heat can air source heat compensators inject into the soil to mitigate the decrease in system efficiency caused by soil temperature decay, or how much heat can ASHPs and water source heat pumps supply as auxiliary heat sources. The other aspect involves developing and evaluating methods designed to optimize performance, reduce energy consumption, and enhance stability, such as integrating BHE arrays or HGHE to improve system efficiency. The main characteristics of the reviewed systems have been summarized in Table 3.

Table 3. Summary of air source-geothermal hybrid heating systems.

Reference	Region	Research Methodology	System	System Characteristics	Main Conclusions	Remark
[81]	Bologna, Northern Italy (44.49° N, 11.34° E)	Simulation	GSHP-ASHP	ASHP is used to reduce the ground temperature attenuation	BHE length can be reduced by 30% to 50%.	A typical climate of Northern Italy
[82]	/	Simulation	AHC-GCHP	AHC can inject heat into the soil	The AHC-GCHP system effectively keeps the soil thermal balance and saves 23.86% energy compared with a traditional "boiler + split air conditioner" system.	/
[83]	Zibo City, China (36.81° N, 118.04° E)	Experiment and simulation	GSHP-ASHP	ASHP and WSHP were used as auxiliary heat sources for part of the heat supply	The proposed system can maintain the soil heat imbalance rate to 2.6%. Compared with traditional GSHP system, the annual operation cost of the novel system is only 58%. Carbon emission was by 7.14%.	Cold regions
[84]	Changsha, China (28.22° N, 112.93° E)	Simulation	PVGSHP-ASHP	86 shallow BHEs	The PVGSHP-ASHP system could solve load imbalance problem with high annual COP-GSHP and COP-sys values of 3.49 kW/kW and 4.69 kW/kW, respectively with only 71,700 kWh of the annual electricity consumption.	Hot summer and cold winter regions
[85]	Ferrara, northern Italy (44.83° N, 11.61° E)	Experiment and simulation	GSHP-ASHP	Coupled with a Flat-Panel HGHE	The use of a DSHP can offer a significant size reduction of the Flat-Panel HGHE and therefore a lower installation cost.	Humid continental climate, with a harsh and humid winter

4. Conclusions

As geothermal energy utilization has become widespread, it has emerged as a highly advantageous renewable energy source. In order to overcome the performance degradation during the utilization process and improve the efficiency of the renewable energy system, the ground-source heat pumps are combined with various kinds of renewable energy sources to mitigate the decline of utilization efficiency over the long-term operation. This paper provides a comprehensive review of the research on the integration of geothermal energy, solar energy, wind energy, and air-source energy into a coupled system. The main conclusions are as follows,

(1) There is rapid progress in the investigation of geothermal energy, particularly in the areas of collecting, utilizing, storing, and optimizing of the geothermal energy system design. An essential problem of geothermal energy systems is accurately forecasting and maximizing their performance. Traditionally, predictive methods consisted of three primary classifications: analytical methods, simulation methods, and experimental methods. Combining these methods can enhance the efficiency of GSHP systems. However, there are still several ongoing issues, including the decrease in the system long-term performance caused by ground temperature reduction. There has been a growing interest in the implementation of multi-source coupling systems.

(2) Solar-geothermal energy hybrid systems can be utilized for heating and cooling buildings. By combining solar thermal collectors to accumulate heat during the day and storing it underground, these systems address the issue of reduced COP due to soil temperature decline during long-term operation. Geothermal heat pump systems can compensate for the instability of solar systems and provide cooling for solar photovoltaic components, thereby enhancing the overall system efficiency. Current research focuses on several key areas: optimizing the design of the dual heat source coupling methods, investigating the ground temperature drop during long-term operation, analyzing the dynamic performance under different operational strategies, and evaluating the economic impact of the coupling system.

(3) Wind-geothermal energy hybrid systems utilize wind turbines to generate electricity, which is then used to operate a geothermal heat pump, meet the building's electrical needs or be sold to the power grid. Hybrid wind, solar and geothermal energy systems utilize geothermal energy to meet the base load of buildings, while photovoltaic and wind power systems provide electricity and supplement demand during peak periods. Additionally, energy storage devices can be integrated to address peak demand. Current research focuses on several key areas: the design of coupled systems, the impact of variations in system parameters, the optimization of energy management and the generation cost, and the production of multiple types of energy (electricity, heating, and hydrogen, etc.).

(4) Air source-geothermal energy hybrid systems are widely employed for building heating. During periods of increased demand, air-source heat pumps are usually selected as supplementary sources to provide additional energy. By combining these two systems, we may improve the energy efficiency and effectively address the long-term temperature decline problems of geothermal systems. Current research focuses on several key areas: system energy consumption analysis, BHE size reduction, soil thermal imbalance, and carbon emission.

Current research on multi-energy coupled systems indicates their potential to significantly improve overall efficiency and reliability, while reducing cost, environmental impact and energy consumption. However, the coupled system also faces challenges such as high system complexity, difficulties in selecting appropriate operating methods, and reliability. Future research directions may focus on developing more intelligent coupling methods and control strategies, improving system reliability, reducing more costs and carbon emissions, and expanding the system's range of applications.

Author Contributions: J.H.: Writing, Original draft, Conceptualization. G.J.: Data curation, Visualization, Supervision. Z.M.: Methodology, Investigation. Z.Z.: Visualization, Writing. C.M.: Data curation, Writing. C.C.: Validation. L.J.: Supervision, Methodology. All authors have read and agreed to the published version of the manuscript.

Funding: The authors are grateful for the support by the Key Research and Development Projects of Shaanxi Province (2023-GHZD-54), Shaanxi Qinchuangyuan Scientist + Engineer Team Construction Project (2022KXJ-049), China Postdoctoral Science Foundation (2023M742802, 2024T170721) and Fundamental Research Funds for the Central Universities (xzy012024069).

Institutional Review Board Statement: Not applicable.

Informed Consent Statement: Not applicable.

Data Availability Statement: All relevant data are within the paper.

Conflicts of Interest: The authors declare no conflict of interest.

Nomenclature

ASHP	Air Source Heat Pump
BHE	Buried Heat Exchanger
COE	Cost of Energy
COP	Coefficient of Performance
EFT	Entering Fluid Temperature
EAHE	Earth-Air Heat Exchanger
GSHP	Ground Source Heat Pump
WSHP	Water Source Heat Pump
GSHP-PVT	Ground Source Heat Pump-Photovoltaic Thermal
GSHP-ASHP	Ground Source Heat Pump-Air Source Heat Pump
HGSHP	Hybrid Ground Source Heat Pump
LCC	Life Cycle Cost
MBHE	Medium-deep Buried Heat Exchanger
NPC	Net Present Cost
PV/T	Photovoltaic Thermal
PVGSHP-ASHP	Photovoltaic Ground Source Heat Pump - Air Source Heat Pump
SPF	Seasonal Performance Factor
SBHE	Shallow Buried Heat Exchanger
SAGSHP	Solar-Assisted Ground Source Heat Pump

References

1. Bakhyt, B.; Aimankul, Y.; Biken, N.; et al. Current state and problems of alternative energy development in the world. *E3S Web Conf.* **2020**, *159*, 07004.
2. Cao, X.; Dai, X.; Liu, J. Building energy-consumption status worldwide and the state-of-the-art technologies for zero-energy buildings during the past decade. *Energy Build.* **2016**, *128*, 198–213.
3. Mohammadi, M.; Noorollahi, Y.; Mohammadi-ivatloo, B.; et al. Energy hub: From a model to a concept–A review. *Renew. Sustain. Energy Rev.* **2017**, *80*, 1512–1527.
4. Jia, Y.; Alva, G.; Fang, G. Development and applications of photovoltaic–thermal systems: A review. *Renew. Sustain. Energy Rev.* **2019**, *102*, 249–265.
5. Chow, T. A review on photovoltaic/thermal hybrid solar technology. *Appl. Energy* **2009**, *87*, 365–379.
6. Zhang, L.; Jiang, Y.; Dong, J.; et al. Advances in vapor compression air source heat pump system in cold regions: A review. *Renew. Sustain. Energy Rev.* **2018**, *81*, 353–365.
7. Kbodi, A.H.B.; Rajeh, T.; Zayed, E.M.; et al. Transient heat transfer simulation, sensitivity analysis, and design optimization of shallow ground heat exchangers with hollow-finned structures for enhanced performance of ground-coupled heat pumps. *Energy Build.* **2024**, *305*, 113870.
8. Alina, W.; Xiang, L.; Jonathan, C.; et al. Shallow geothermal energy potential for heating and cooling of buildings with regeneration under climate change scenarios. *Energy* **2022,** *244*, 123086.
9. He, Y.; Jia, M.; Li, X.; et al. Performance analysis of coaxial heat exchanger and heat-carrier fluid in medium-deep geothermal energy development. *Renew. Energy* **2021**, *168*, 938–959.
10. Jia, G.S.; Ma, Z.D.; Xia, Z.H.; et al. Influence of groundwater flow on the ground heat exchanger performance and ground temperature distributions: A comprehensive review of analytical, numerical and experimental studies. *Geothermics* **2022**, *100*, 102342.
11. Wu, W.; Li, X.; You, T.; et al. Hybrid ground source absorption heat pump in cold regions: Thermal balance keeping and borehole number reduction. *Appl. Therm. Eng.* **2015**, *90*, 322–334.
12. Davide, M.; Giulia, L.; Sergio, B.; et al. State of the Art, Perspective and Obstacles of Ground-Source Heat Pump Technology in the European Building Sector: A Review. *Energies* **2022**, *15*, 2685.
13. Miocic, J.M.; Schleichert, L.; Van de Ven, A.; et al. Fast calculation of the technical shallow geothermal energy potential of large areas with a steady-state solution of the finite line source. *Geothermics* **2024**, *116*, 102851.

14. Bao, L.; Wang, X.; Jin, P.; et al. An analytical heat transfer model for the mid-deep U-shaped borehole heat exchanger considering groundwater seepage. *J. Build. Eng.* **2023**, *64*, 105612.
15. Noorollahi, Y.; Saeidi, R.; Mohammadi, M.; et al. The effects of ground heat exchanger parameters changes on geothermal heat pump performance—A review. *Appl. Therm. Eng.* **2018**, *129*, 1645–1658.
16. Deng, F.; Pei, P.; Ren, Y.; et al. Investigation and evaluation methods of shallow geothermal energy considering the influences of fracture water flow. *Geotherm. Energy* **2023**, *11*, 25.
17. Lu, Y.; Cortes, D.D.; Yu, X.; et al. Numerical investigations of enhanced shallow geothermal energy recovery using microencapsulated phase change materials and metal fins. *Acta Geotech.* **2022**, *18*, 2869–2882.
18. Yousefi, H.; Ehara, S.; Noorollahi, Y. Progress of Geothermal Development in Iran. *J. Geotherm. Res. Soc. Jpn.* **2008**, *30*, 181–192.
19. Qian, H.; Wang, Y. Modeling the interactions between the performance of ground source heat pumps and soil temperature variations. *Energy Sustain. Dev.* **2014**, *23*, 115–121.
20. Qi, D.; Pu, L.; Sun, F.; et al. Numerical investigation on thermal performance of ground heat exchangers using phase change materials as grout for ground source heat pump system. *Appl. Therm. Eng.* **2016**, *106*, 1023–1032.
21. Dehghan, B.; Wang, L.; Motta, M.; et al. Modelling of waste heat recovery of a biomass combustion plant through ground source heat pumps- development of an efficient numerical framework. *Appl. Therm. Eng.* **2019**, *166*, 114625.
22. Kurevija, T.; Macenić, M.; Tuschl, M. Drilling Deeper in Shallow Geoexchange Heat Pump Systems—Thermogeological, Energy and Hydraulic Benefits and Restraints. *Energies* **2023**, *16*, 6577.
23. Lazzarin, R. Heat pumps and solar energy: A review with some insights in the future. *Int. J. Refrig.* **2020**, *116*, 146–160.
24. Kamel, S.R.; Fung, S.A.; Dash, R.P. Solar systems and their integration with heat pumps: A review. *Energy Build.* **2015**, *87*, 395–412.
25. Abbas, A.A.; Mohsen, A.; Adib, K.; et al. A Critical Review on the Use of Shallow Geothermal Energy Systems for Heating and Cooling Purposes. *Energies* **2022**, *15*, 4281.
26. Serageldin, A.A.; Abdelrahman, K.A.; Ookawara, S. Earth-Air Heat Exchanger thermal performance in Egyptian conditions: Experimental results, mathematical model, and Computational Fluid Dynamics simulation. *Energy Convers. Manag.* **2016**, *122*, 25–38.
27. You, T.; Wang, B.; Wu, W.; et al. Performance analysis of hybrid ground-coupled heat pump system with multi-functions. *Energy Convers. Manag.* **2015**, *92*, 47–59.
28. Kitsopoulou, A.; Zacharis, A.; Ziozas, N.; et al. Dynamic Energy Analysis of Different Heat Pump Heating Systems Exploiting Renewable Energy Sources. *Sustainability* **2023**, *15*, 11054.
29. You, T.; Wu, W.; Yang, H.; et al. Hybrid photovoltaic/thermal and ground source heat pump: Review and perspective. *Renew. Sustain. Energy Rev.* **2021**, *151*, 111569.
30. Nouri, G.; Noorollahi, Y.; Yousefi, H. Designing and optimization of solar assisted ground source heat pump system to supply heating, cooling and hot water demands. *Geothermics* **2019**, *82*, 212–231.
31. Ren, X.; Wang, J.; Hu, X.; et al. A novel demand response-based distributed multi-energy system optimal operation framework for data centers. *Energy Build.* **2024**, *305*, 113886.
32. Nouri, G.; Noorollahi, Y.; Yousefi, H. Solar assisted ground source heat pump systems—A review. *Appl. Therm. Eng.* **2019**, *163*, 114351.
33. Wang, E.; Fung, S.A.; Qi, C.; et al. Performance prediction of a hybrid solar ground-source heat pump system. *Energy Build.* **2012**, *47*, 600–611.
34. Thygesen, R.; Karlsson, B. Economic and energy analysis of three solar assisted heat pump systems in near zero energy buildings. *Energy Build.* **2013**, *66*, 77–87.
35. Sadeghi, H.; Ijaz, A.; Singh, R.M. Current status of heat pumps in Norway and analysis of their performance and payback time. *Sustain. Energy Technol. Assess.* **2022**, *54*, 102829.
36. Lund, J.W.; Toth, A.N. Direct utilization of geothermal energy 2020 worldwide review. *Geothermics* **2020**, *90*, 101915.

37. Jiang, J. *China's Energy Policy 2012*; Information Office of the State Council: Beijing, China, 2012.
38. Rivera, J.A.; Blum, P.; Bayer, P. Increased ground temperatures in urban areas: Estimation of the technical geothermal potential. *Renew. Energy* **2017**, *103*, 388–400.
39. Yu, X.; Li, H.; Yao, S.; et al. Development of an efficient numerical model and analysis of heat transfer performance for borehole heat exchanger. *Renew. Energy* **2020**, *152*, 189–197.
40. Moritani, S.; Saito, H.; Win, P.W.; et al. Assessment of potential groundwater contamination by ground source heat pump operation using solute transport models. *Int. J. Energy Environ. Eng.* **2020**, *12*, 1–10.
41. Li, Y.; Shu, L.; Xiao, R.; et al. How groundwater flow field change affects heat transfer in groundwater heat pumps based on physical experiments. *Energy Build.* **2023**, *282*, 112804.
42. Bina, S.M.; Fujii, H.; Kosukegawa, H.; et al. Evaluation of groundwater pumping impact on the thermal conductivity of neighboring ground source heat exchangers. *Geothermics* **2023**, *108*, 102618.
43. Arghand, T.; Javed, S.; Trüschel, A.; et al. Cooling of office buildings in cold climates using direct ground-coupled active chilled beams. *Renew. Energy* **2020**, *164*, 122–132.
44. Huang, Y.; Zhang, Y.; Xie, Y.; et al. Field test and numerical investigation on deep coaxial borehole heat exchanger based on distributed optical fiber temperature sensor. *Energy* **2020**, *210*, 118643.
45. Zhao, Z.; Lin, Y.F.; Stumpf, A.; et al. Assessing impacts of groundwater on geothermal heat exchangers: A review of methodology and modeling. *Renew. Energy* **2022**, *190*, 121–147.
46. Li, J.; Xu, W.; Li, J.; et al. Heat extraction model and characteristics of coaxial deep borehole heat exchanger. *Renew. Energy* **2021**, *169*, 738–751.
47. Pastore, N.; Cherubini, C.; Giasi, C.I. Analysis of gravel back-filled borehole heat exchanger in karst fractured limestone aquifer at local scale. *Geothermics* **2021**, *89*, 101971.
48. He, Y.; Bu, X. A novel enhanced deep borehole heat exchanger for building heating. *Appl. Therm. Eng.* **2020**, *178*, 115643.
49. Guo, Y.; Hu, X.; Banks, J.; et al. Considering buried depth for vertical borehole heat exchangers in a borehole field with groundwater flow—An extended solution. *Energy Build.* **2021**, *235*, 110722.
50. Karabetoglu, S.; Ozturk, Z.F.; Kaslilar, A.; et al. Effect of layered geological structures on borehole heat transfer. *Geothermics* **2021**, *91*, 102043.
51. Bourhis, P.; Cousin, B.; Loria, A.F.R.; et al. Machine learning enhancement of thermal response tests for geothermal potential evaluations at site and regional scales. *Geothermics* **2021**, *95*, 102132.
52. Hart, D.P.; Couvillion, R. *Earth-Coupled Heat Transfer: Offers Engineers and Other Practitioners of Applied Physics the Information to Solve Heat Transfer Problems as They Apply to Earth-Coupling*; National Water Well Association: Westerville, OH, USA, 1986.
53. Jaeger, J.C.; Carslaw, H.S. *Conduction of Heat in Solids*; Clarendon Press: Oxford, UK, 1959.
54. Luo, Y.; Xu, G.; Zhang, S.; et al. Heat extraction and recover of deep borehole heat exchanger: Negotiating with intermittent operation mode under complex geological conditions. *Energy* **2022**, *241*, 122510.
55. Liu, J.; Wang, F.; Gao, Y.; et al. Influencing factors analysis and operation optimization for the long-term performance of medium-deep borehole heat exchanger coupled ground source heat pump system. *Energy Build.* **2020**, *226*, 110385.
56. Rad, M.F.; Fung, S.A.; Leong, H.W. Feasibility of combined solar thermal and ground source heat pump systems in cold climate, Canada. *Energy Build.* **2013**, *61*, 224–232.
57. Eslami-nejad, P.; Bernier, M. Coupling of geothermal heat pumps with thermal solar collectors using double U-tube boreholes with two independent circuits. *Appl. Therm. Eng.* **2011**, *31*, 3066–3077.
58. Ke, C.; Jia, Z.; Aihua, L.; et al. Numerical study on seasonal operation of solar assisted hybrid borehole heat exchange array. *Energy Build.* **2022**, *276*, 112487.
59. Liu, L.; Zhu, N.; Zhao, J. Thermal equilibrium research of solar seasonal storage system coupling with ground-source heat pump. *Energy* **2016**, *99*, 83–90.

60. Yang, W.; Zhang, H.; Liang, X. Experimental performance evaluation and parametric study of a solar-ground source heat pump system operated in heating modes. *Energy* **2018**, *149*, 173–189.
61. Si, Q.; Okumiya, M.; Zhang, X. Performance evaluation and optimization of a novel solar-ground source heat pump system. *Energy Build.* **2014**, *70*, 237–245.
62. Yang, W.; Sun, L.; Chen, Y. Experimental investigations of the performance of a solar-ground source heat pump system operated in heating modes. *Energy Build.* **2015**, *89*, 97–111.
63. Wang, X.; Zheng, M.; Zhang, W.; et al. Experimental study of a solar-assisted ground-coupled heat pump system with solar seasonal thermal storage in severe cold areas. *Energy Build.* **2010**, *42*, 2104–2110.
64. Li, J.; Bao, L.; Niu, G.; et al. Research on renewable energy coupling system based on medium-deep ground temperature attenuation. *Appl. Energy* **2024**, *353*, 122187.
65. Yan, R.; Yu, X.; Lu, F.; et al. Study of operation performance for a solar photovoltaic system assisted cooling by ground heat exchangers in arid climate, China. *Renew. Energy* **2020**, *155*, 102–110.
66. Jeong Y D, Yu M G, Nam Y. Feasibility study of a heating, cooling and domestic hot water system combining a photovoltaic-thermal system and a ground source heat pump[J]. Energies, 2017, 10(8): 1243.
67. Xia, L.; Ma, Z.; Kokogiannakis, G.; et al. A model-based design optimization strategy for ground source heat pump systems with integrated photovoltaic thermal collectors. *Appl. Energy* **2018**, *214*, 178–190.
68. Pourier, C.; Beltrán, F.; Sommerfeldt, N. Solar photovoltaic/thermal (PVT) technology collectors and free cooling in ground source heat pump systems. *Sol. Energy Adv.* **2024**, *4*, 100050.
69. Lazzarin, R.; Noro, M. Photovoltaic/Thermal (PV/T)/ground dual source heat pump: Optimum energy and economic sizing based on performance analysis. *Energy Build.* **2020**, *211*, 109800.
70. Jakhar, S.; Soni, S.M.; Gakkhar, N. An integrated photovoltaic thermal solar (IPVTS) system with earth water heat exchanger cooling: Energy and exergy analysis. *Sol. Energy* **2017**, *157*, 81–93.
71. Kastner, O.; Norden, B.; Klapperer, S.; et al. Thermal solar energy storage in Jurassic aquifers in Northeastern Germany: A simulation study. *Renew. Energy* **2017**, *104*, 290–306.
72. Younes, N.; Mina, P.; Alireza, K.; et al. Reliable renewable power production by modeling of geothermal assisted solar chimney power plant. *Geothermics* **2023**, *111*, 102701.
73. Yu, Y.; Li, H.; Niu, F.; et al. Investigation of a coupled geothermal cooling system with earth tube and solar chimney. *Appl. Energy* **2014**, *114*, 209–217.
74. Elghamry, R.; Hassan, H. Impact a combination of geothermal and solar energy systems on building ventilation, heating and output power: Experimental study. *Renew. Energy* **2020**, *152*, 1403–1413.
75. Yashar, A.; García, L.J.A. Exergy and exergoenvironmental assessment of a geothermal heat pump and a wind power turbine hybrid system in Shanghai, China. *Geotherm. Energy* **2023**, *11*, 9.
76. Ciapała, B.; Jurasz, J.; Kies, A. The Potential of Wind Power-Supported Geothermal District Heating Systems—Model Results for a Location in Warsaw (Poland). *Energies* **2019**, *12*, 3706.
77. Bamisile, O.; Dongsheng, C.; Li, J.; et al. An innovative approach for geothermal-wind hybrid comprehensive energy system and hydrogen production modeling/process analysis. *Int. J. Hydrog. Energy* **2022**, *47*, 13261–13288.
78. Da, X.; Zhe-Li, Y.; Ziyi, B.; et al. Optimal operation of geothermal-solar-wind renewables for community multi-energy supplies. *Energy* **2022**, *249*, 123672.
79. Kazmi, S.W.S.; Sheikh, I.M. Hybrid geothermal–PV–wind system for a village in Pakistan. *SN Appl. Sci.* **2019**, *1*, 1–15.
80. Geng, Z.; Chen, K.; Li, J.; et al. Analysis of coupling characteristics of clean heating systems based on complementary solar, geothermal, and wind energy. *J. Renew. Sustain. Energy* **2024**, *16*, 024701.
81. Grossi, I.; Dongellini, M.; Piazzi, A.; et al. Dynamic modelling and energy performance analysis of an innovative dual-source heat pump system. *Appl. Therm. Eng.* **2018**, *142*, 745–759.
82. You, T.; Shi, W.; Wang, B.; et al. A new ground-coupled heat pump system integrated with a multi-mode air-source heat compensator to eliminate thermal imbalance in cold regions. *Energy Build.* **2015**, *107*, 103–112.

83. Yubo, W.; Zhenhua, Q.; Yaohua, Z.; et al. Operation mode performance and optimization of a novel coupled air and ground source heat pump system with energy storage: Case study of a hotel building. *Renew. Energy* **2022**, *201*, 889–903.
84. Zheng, Z.; Zhou, J.; Xu, F.; et al. Integrated operation of PV assisted ground source heat pump and air source heat pump system: Performance analysis and economic optimization. *Energy Convers. Manag.* **2022**, *269*, 116091.
85. Bottarelli, M.; Bortoloni, M.; Su, Y. On the sizing of a novel Flat-Panel ground heat exchanger in coupling with a dual-source heat pump. *Renew. Energy* **2019**, *142*, 552–560.